Beyond the limits of noise seismology: past and future

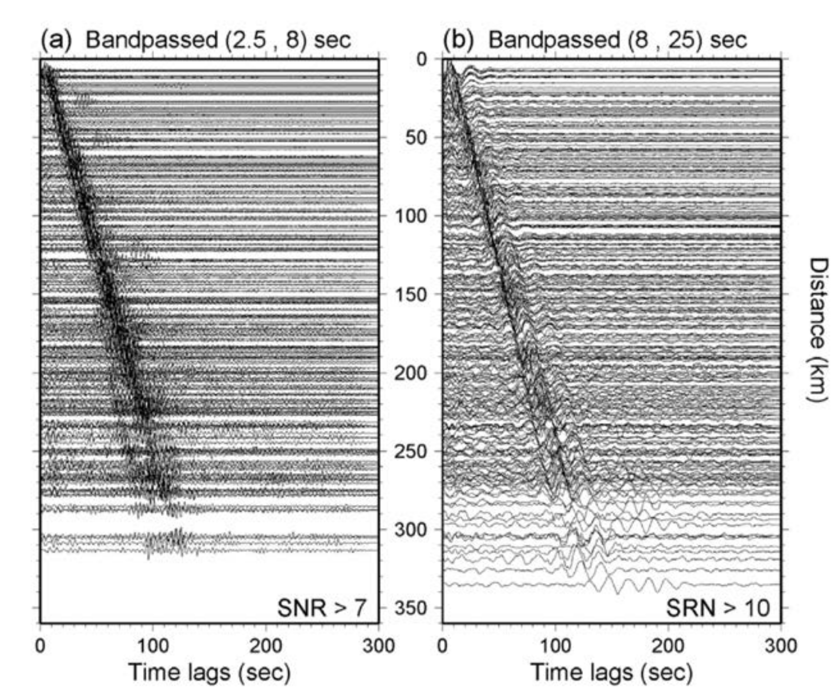

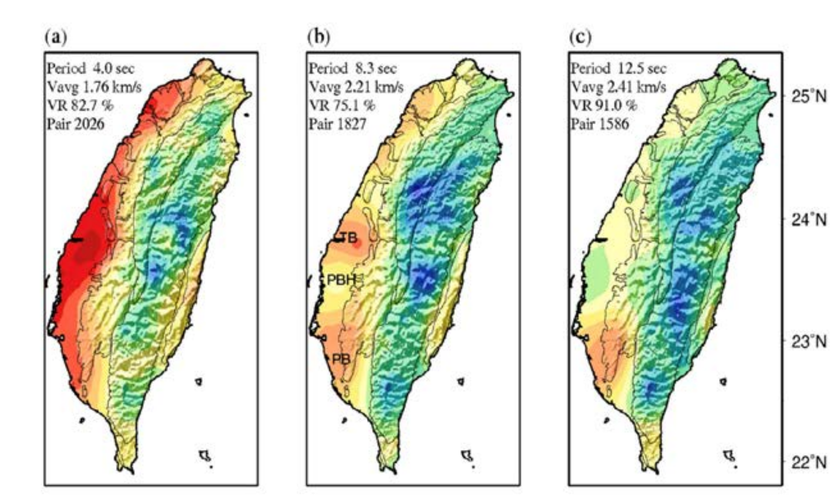

Three Topics

1. ***Dispersion measurement***
2. ***Using the “Noise” of noise cross-correlation Function (NCF)***
3. ***Investigating microseism PKIKP generated around Hawaii.***

Ying-Nien Chen

Introduction

Seismology
- *Signal: Earthquakes*
- *Noise : Coda & Microseism (Random wave fields)*

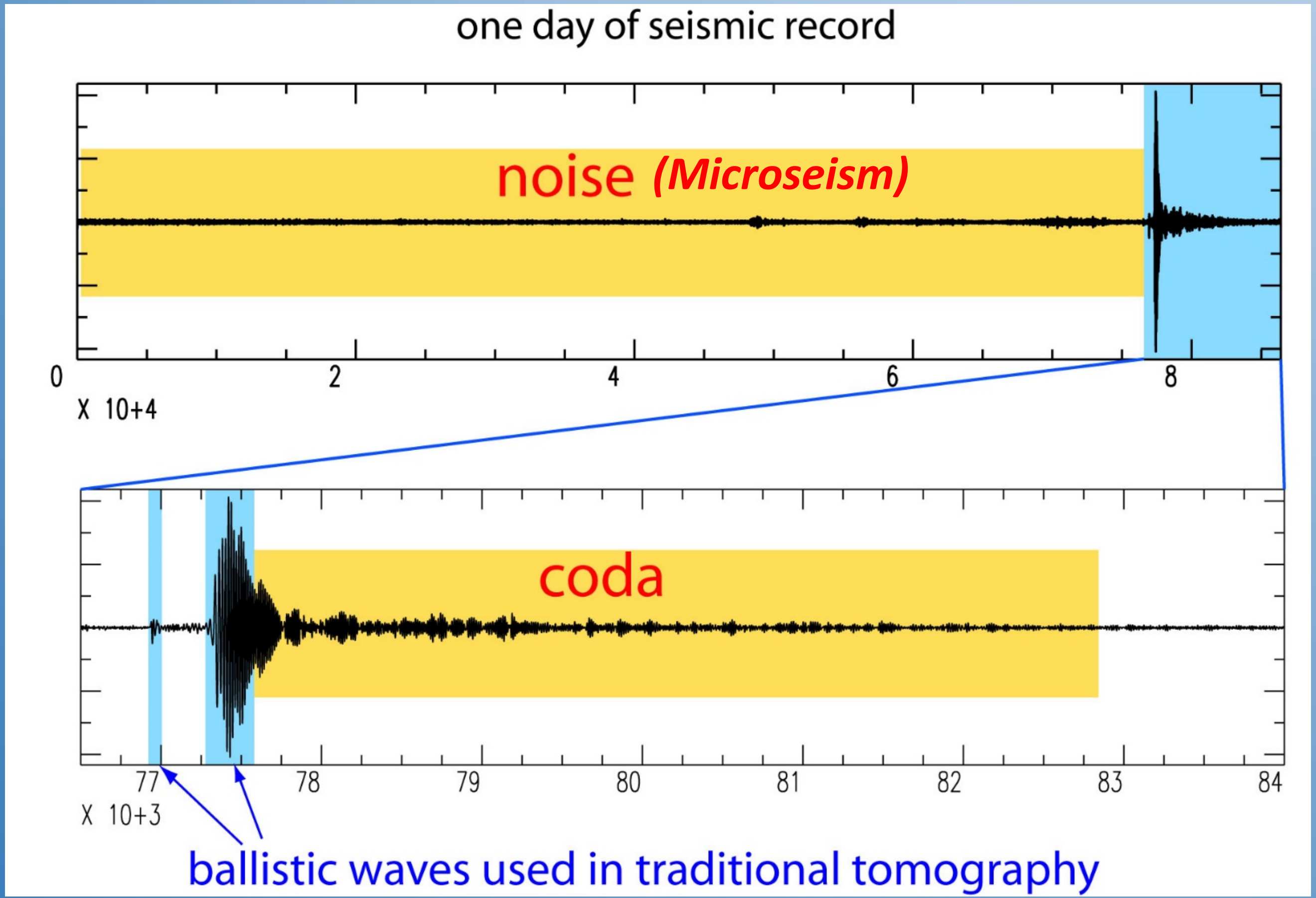

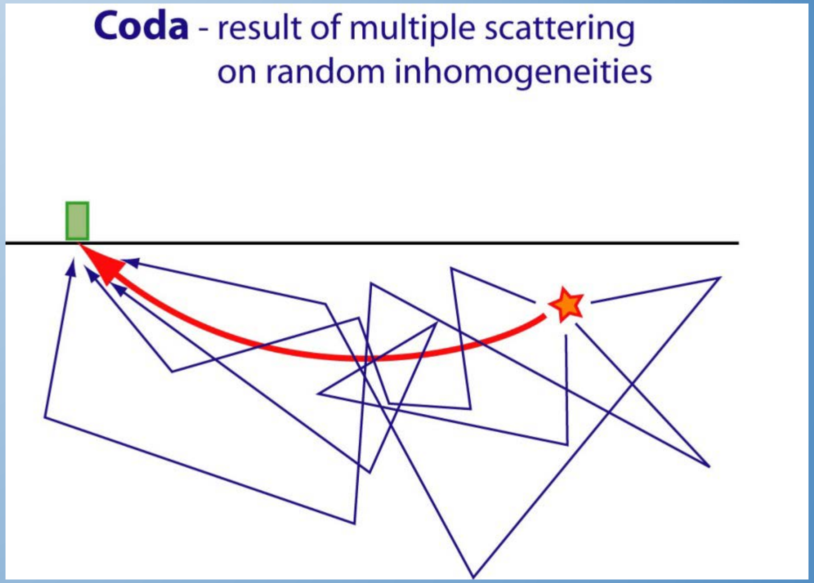

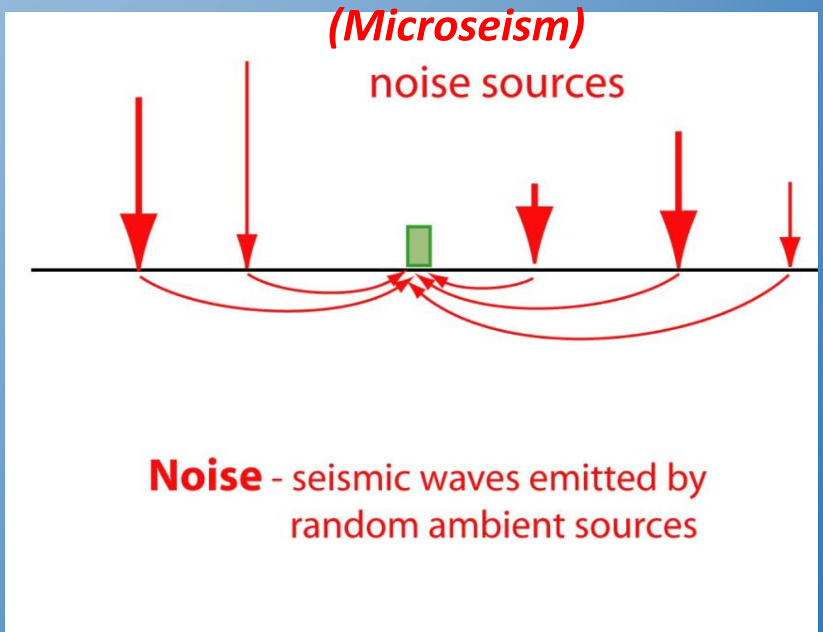

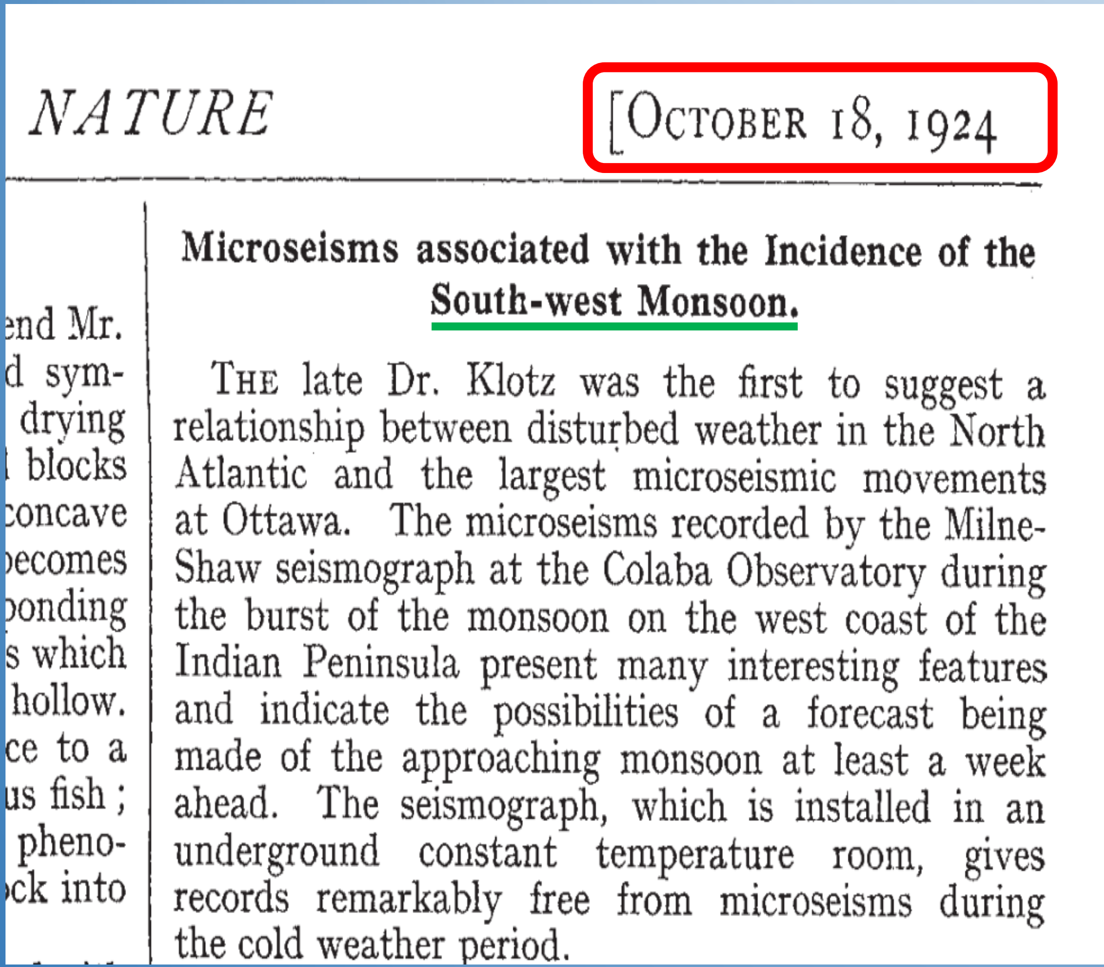

NATURE [OCTOBER 18, 1924

end Mr.
d sym-
drying
blocks
concave
becomes
ponding
s which
hollow.
ce to a
us fish ;
pheno-
ck into

Microseisms associated with the Incidence of the South-west Monsoon.

THE late Dr. Klotz was the first to suggest a relationship between disturbed weather in the North Atlantic and the largest microseismic movements at Ottawa. The microseisms recorded by the Milne-Shaw seismograph at the Colaba Observatory during the burst of the monsoon on the west coast of the Indian Peninsula present many interesting features and indicate the possibilities of a forecast being made of the approaching monsoon at least a week ahead. The seismograph, which is installed in an underground constant temperature room, gives records remarkably free from microseisms during the cold weather period.

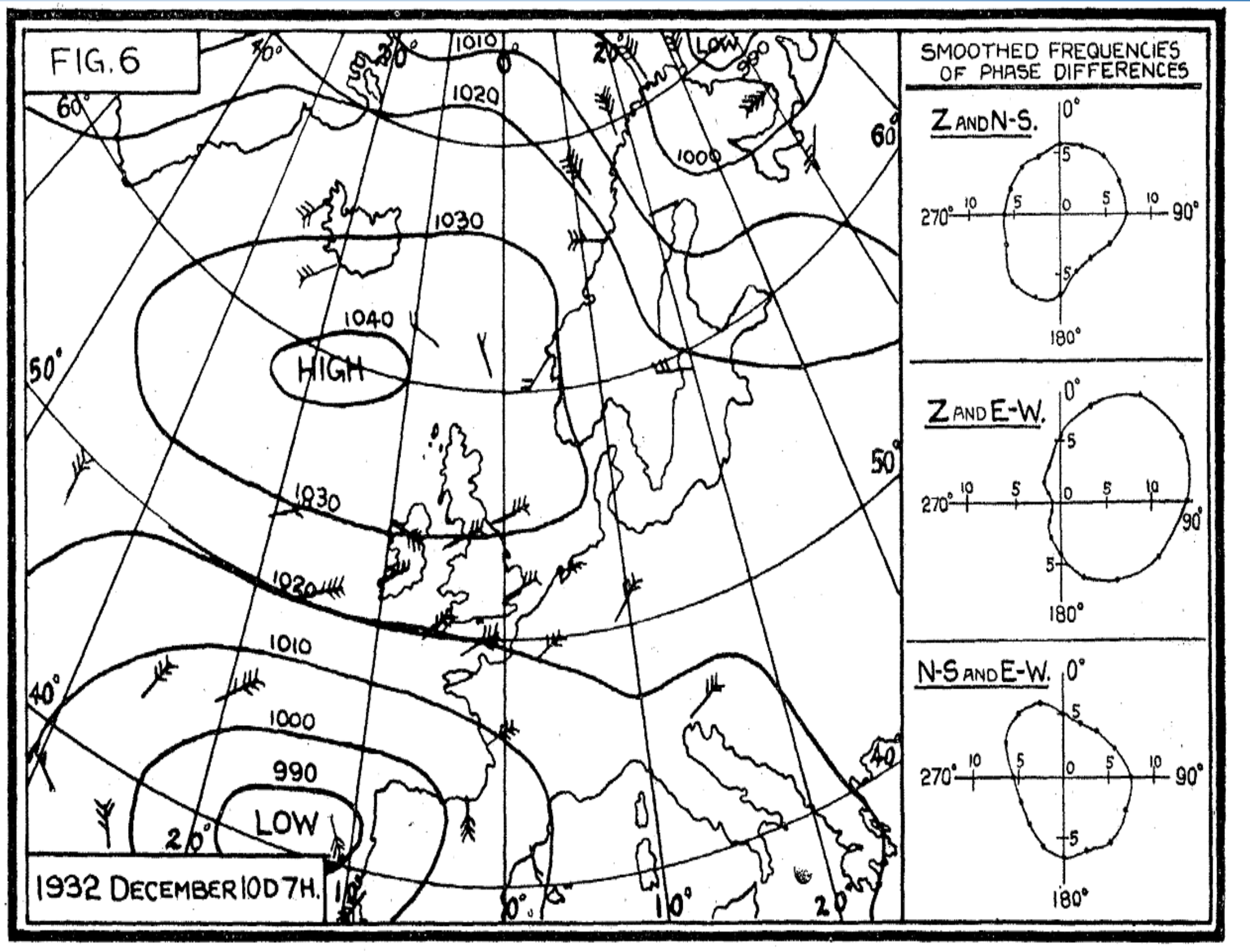

Lee. 1935 (particle motion analysis)

Origin: Energy Coupling between ocean wave & solid earth

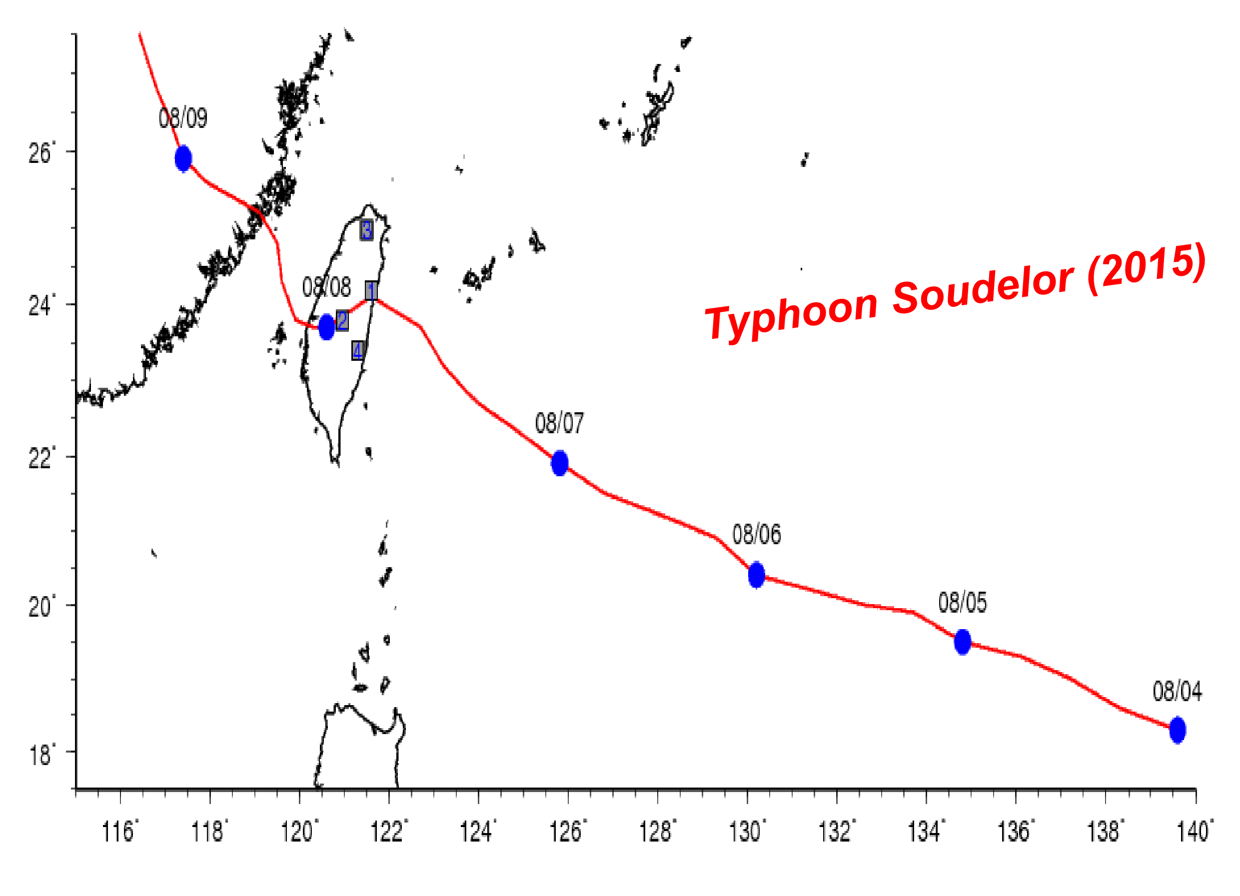

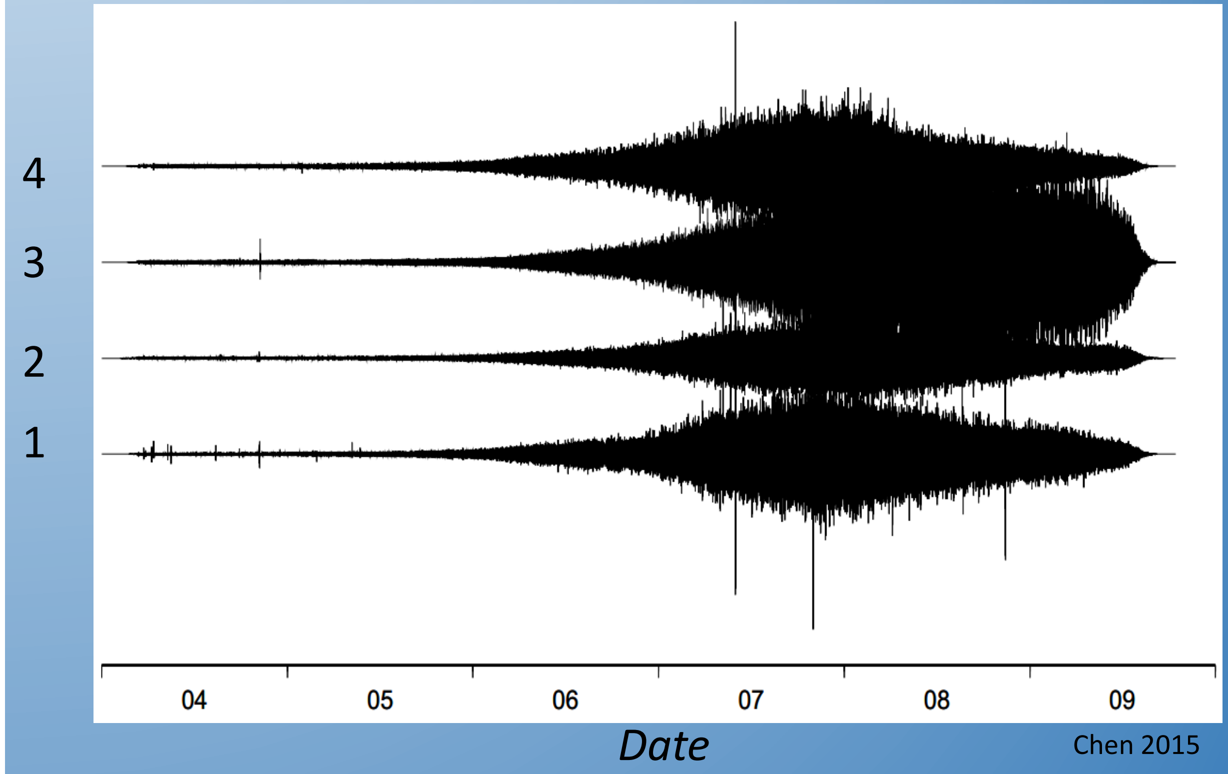

Primary microseisms (PM) *(Shallow water environment)*

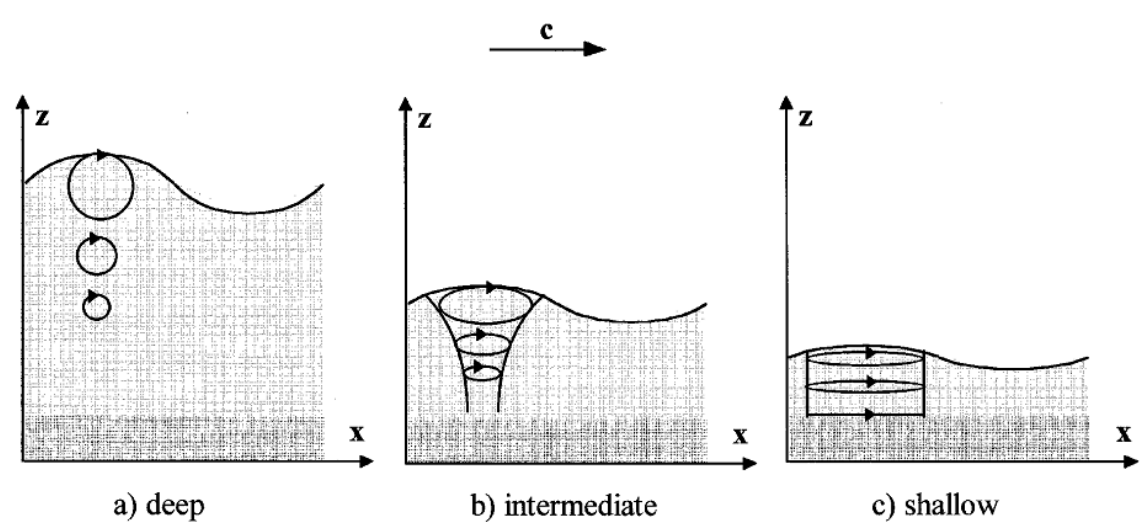

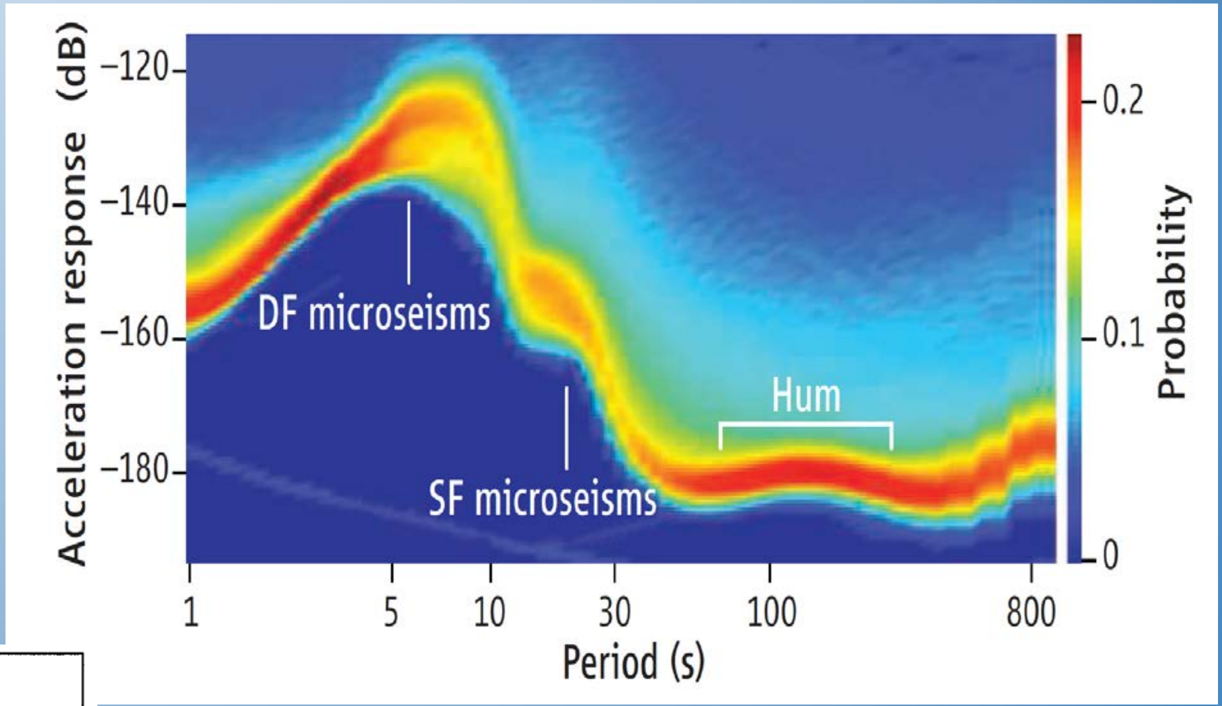

Bromirski 2009

Secondary microseisms (SM)

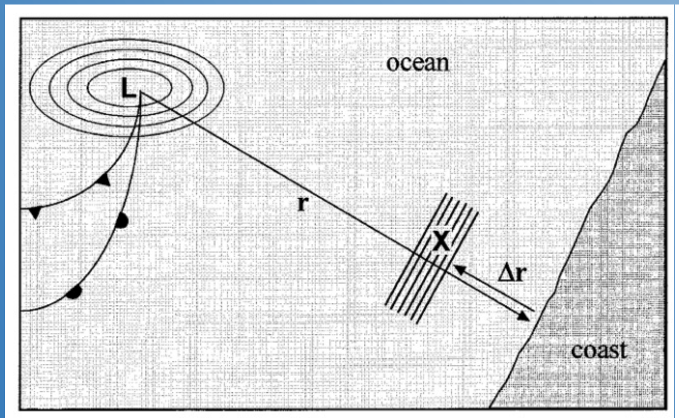

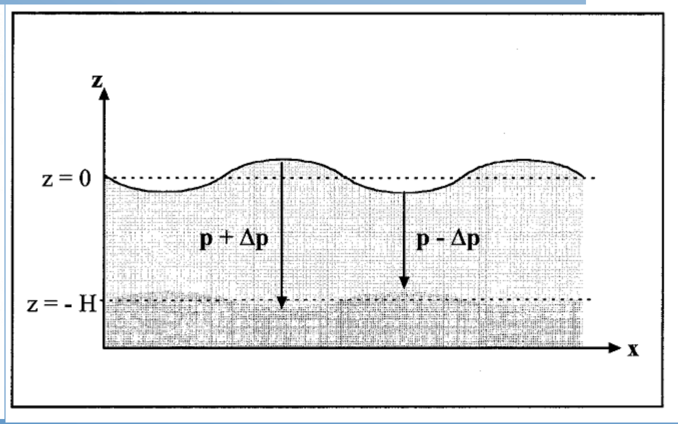

Friedrich et al., 1998

Turning noise into signal

Noise cross-correlation function (NCF) → Greens Function

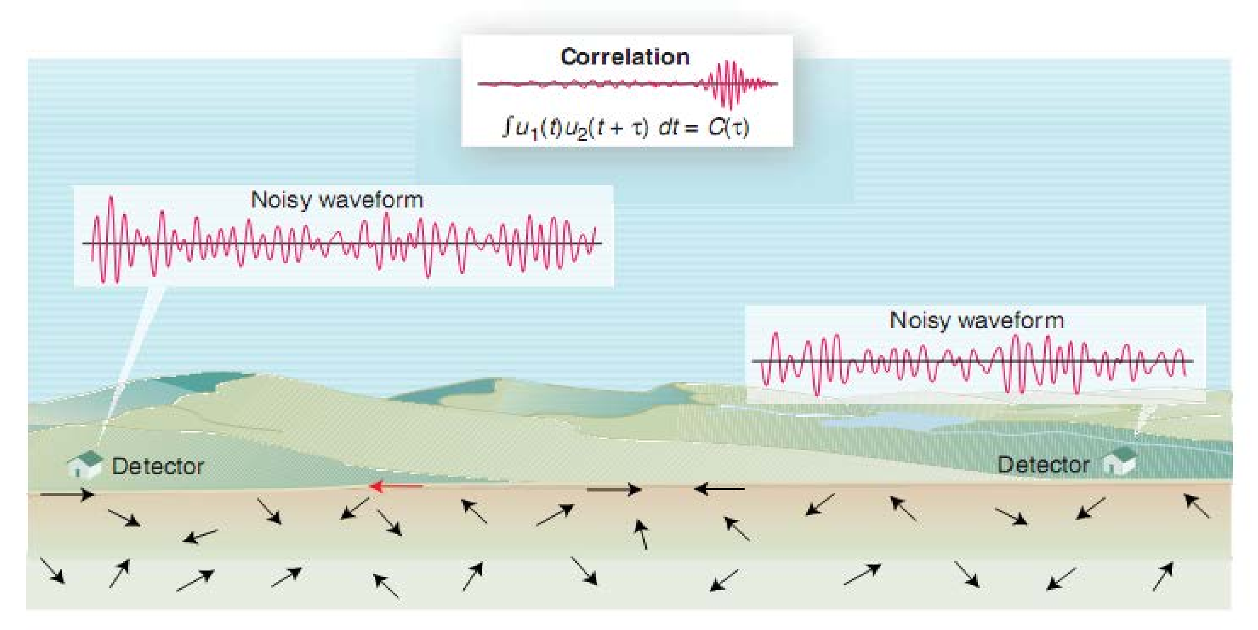

Weaver, 2005

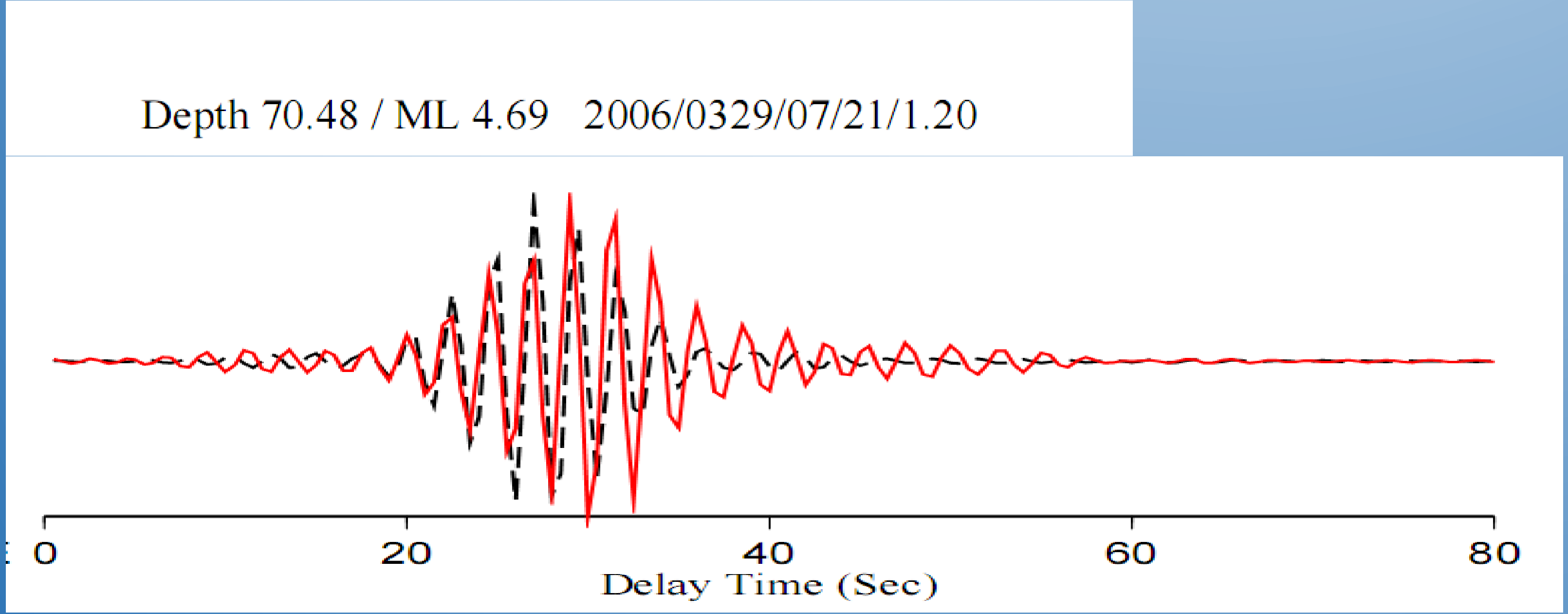

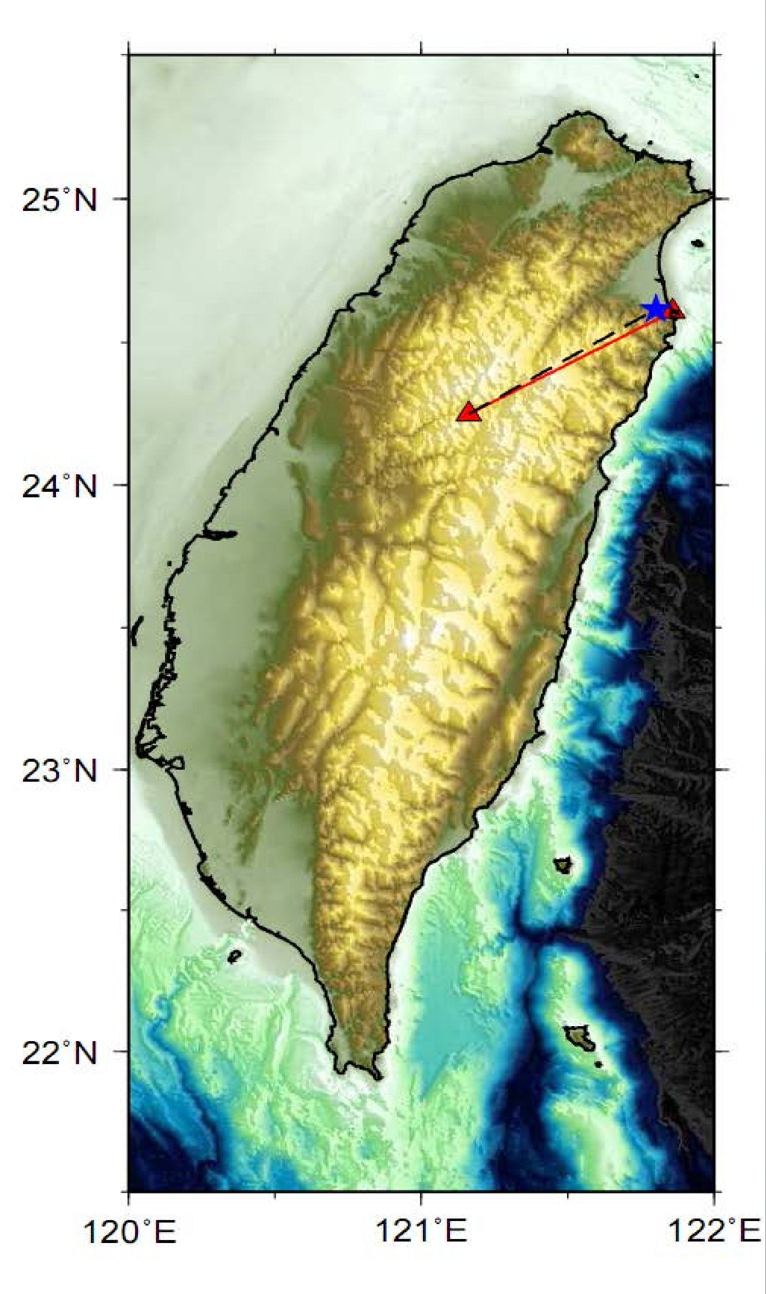

Advantages of ambient seismic noise tomography

1.No earthquakes required! (without source uncertainties).
2.Path coverage offered by station coverage.
3.Quality can be improved easily by increasing data length!

An example of NCF convergence within a day (2006,101)

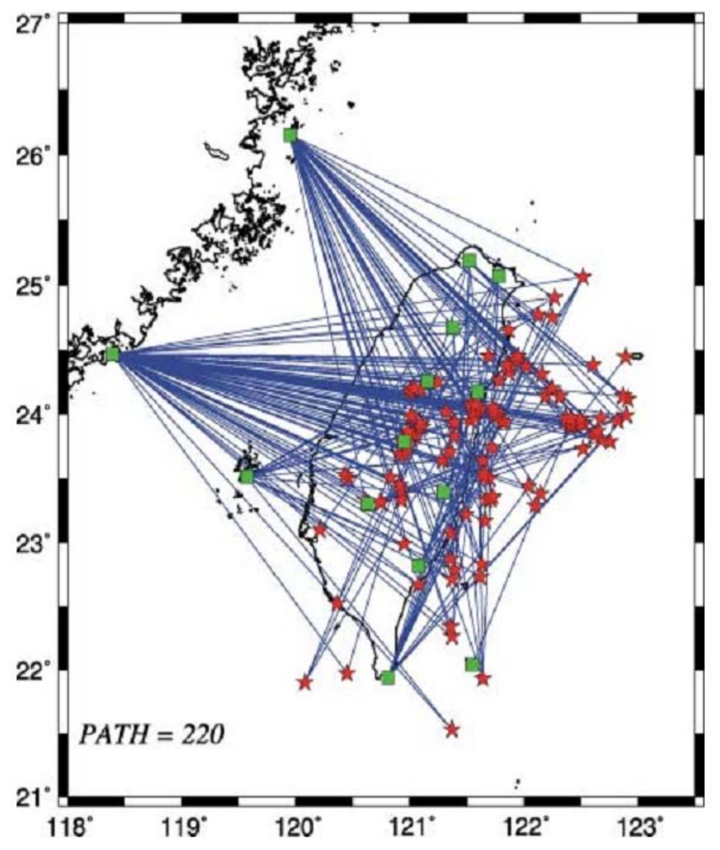

（翁偉哲，2006）

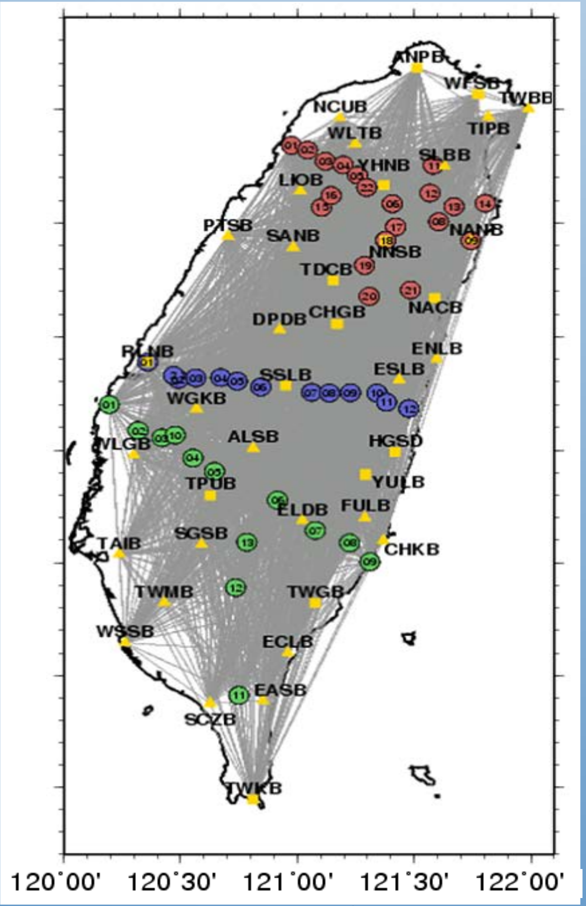

Huang et al., 2015

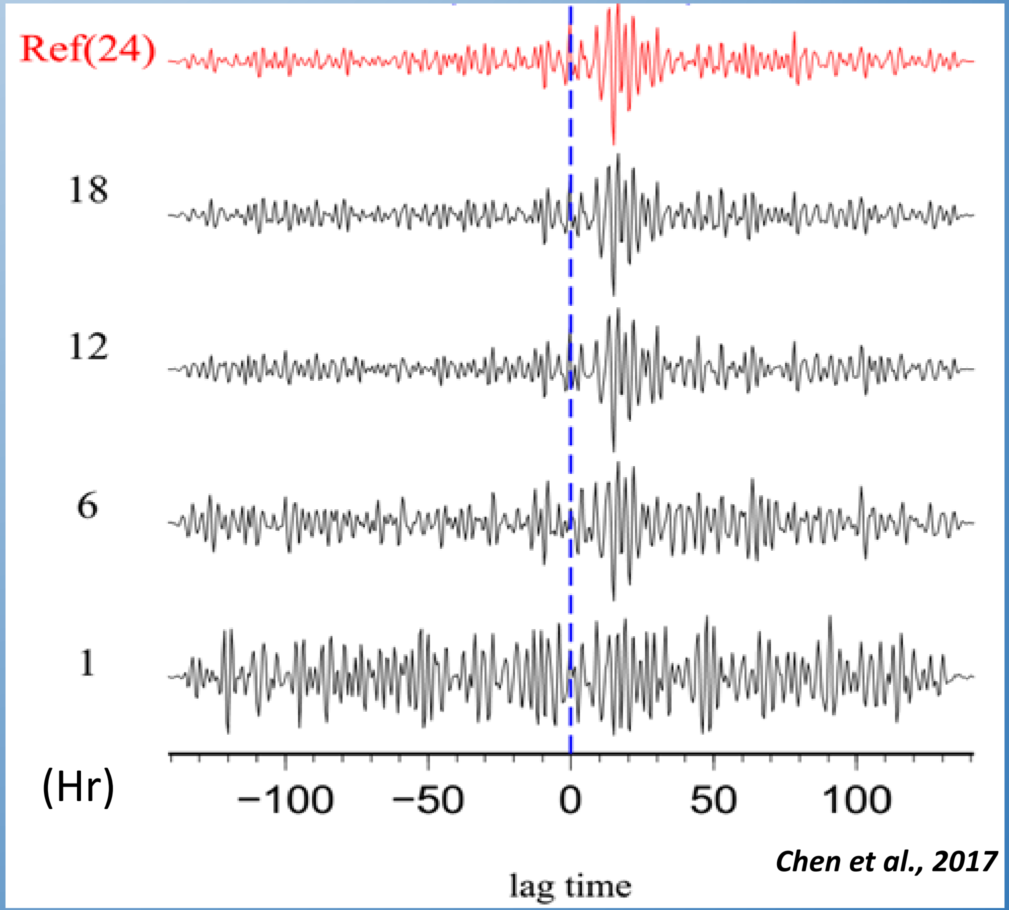

Chen et al., 2017

The mainstream of noise studies

Investigating structure using ambient noise

The Flow of noise studies :

Aki (1957)
seismology

Duvall et al., (1993)
Helioseismology

Acoustics (e.g., Oleg & Weaver. 2011)
Thermodynamics (e.g., Weaver et.al., 2002)

Seismology (e.g., Shapiro & Campillo, 2004)

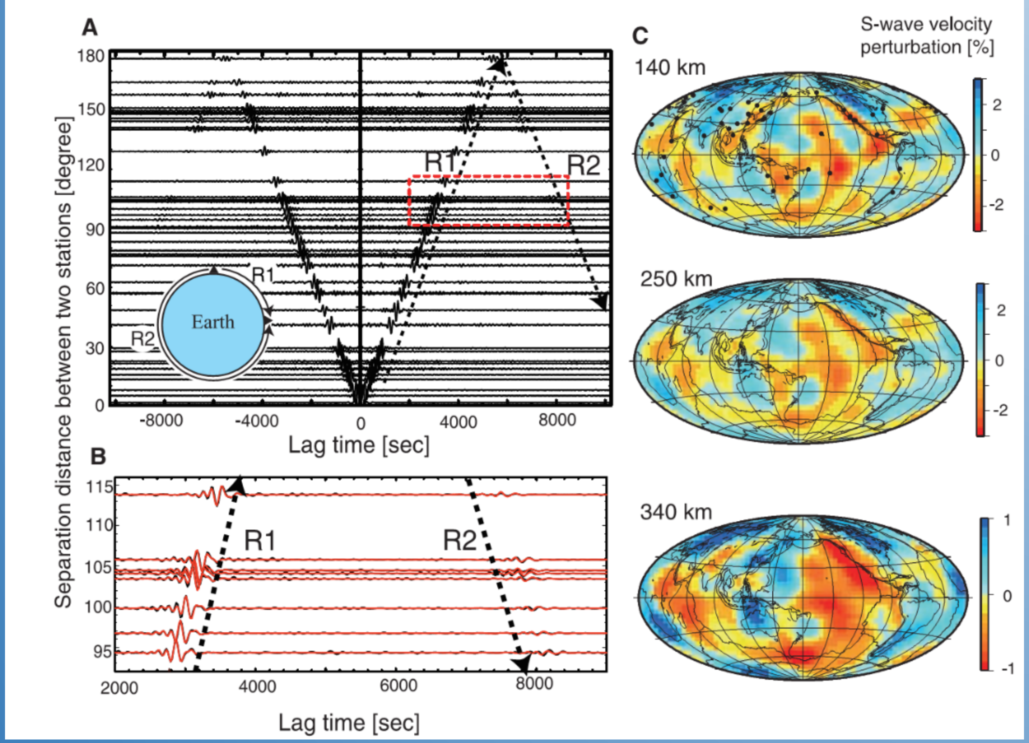

Nishida et al., 2010

...
Shapiro et al., 2005
...
Sabra et al., 2006
Yao et al., 2006
....
Draganov et al., 2007
...
Yang et al., 2008

Structure : 70%
Source : 10 %
Theory : 20%

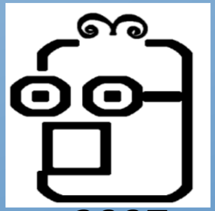

2007

2019

sunset industry?

Measuring NCF dispersion without the long interstation distance limitation – a new method based on hybrid peak time matching

Ying-Nien Chen[1], Yuancheng Gung[2], Ling-Yun Chiao[3]

1. Department of Earth and Environment Science, National Chung Cheng University, Chia-Yi, Taiwan.
2. Department of Geosciences, National Taiwan University, Taipei, Taiwan
3. Institute of Oceanography, National Taiwan University, Taipei, Taiwan.

Contents:

1. Motivation

High-Frequency Approximation
($r >> \lambda$)

Noise cross-correlation function (NCF)

Green's Function of the far-field surface waves

Table S1. The number of available paths for three wavelength criteria, and the selected paths used in the inversion.

Period	4.0	6.0	8.0	12.0	16.0	20.0
Number of paths (3λ criterion)	3309	3108	2880	2370	1867	1336
Qualified paths(U)	2487	2428	2287	1974	1628	1300

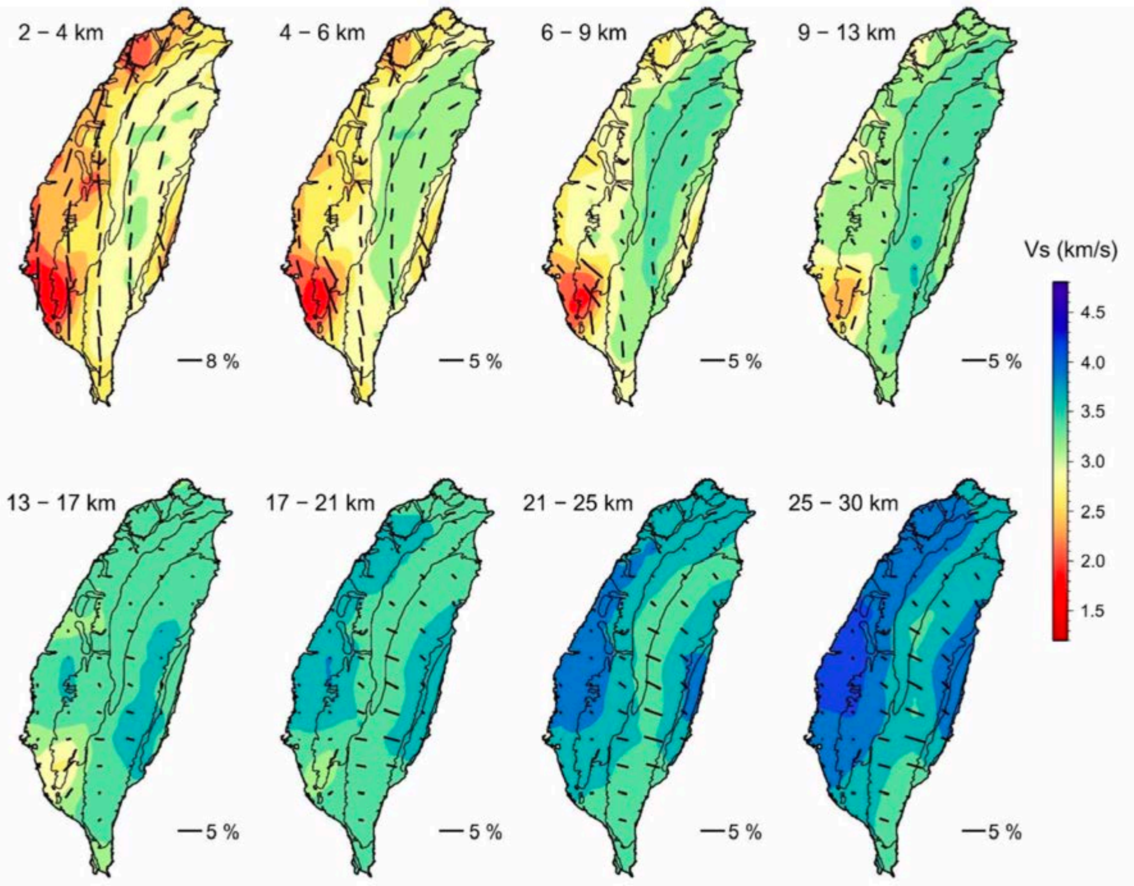

Huang et al., 2015

Hybrid peak time matching method

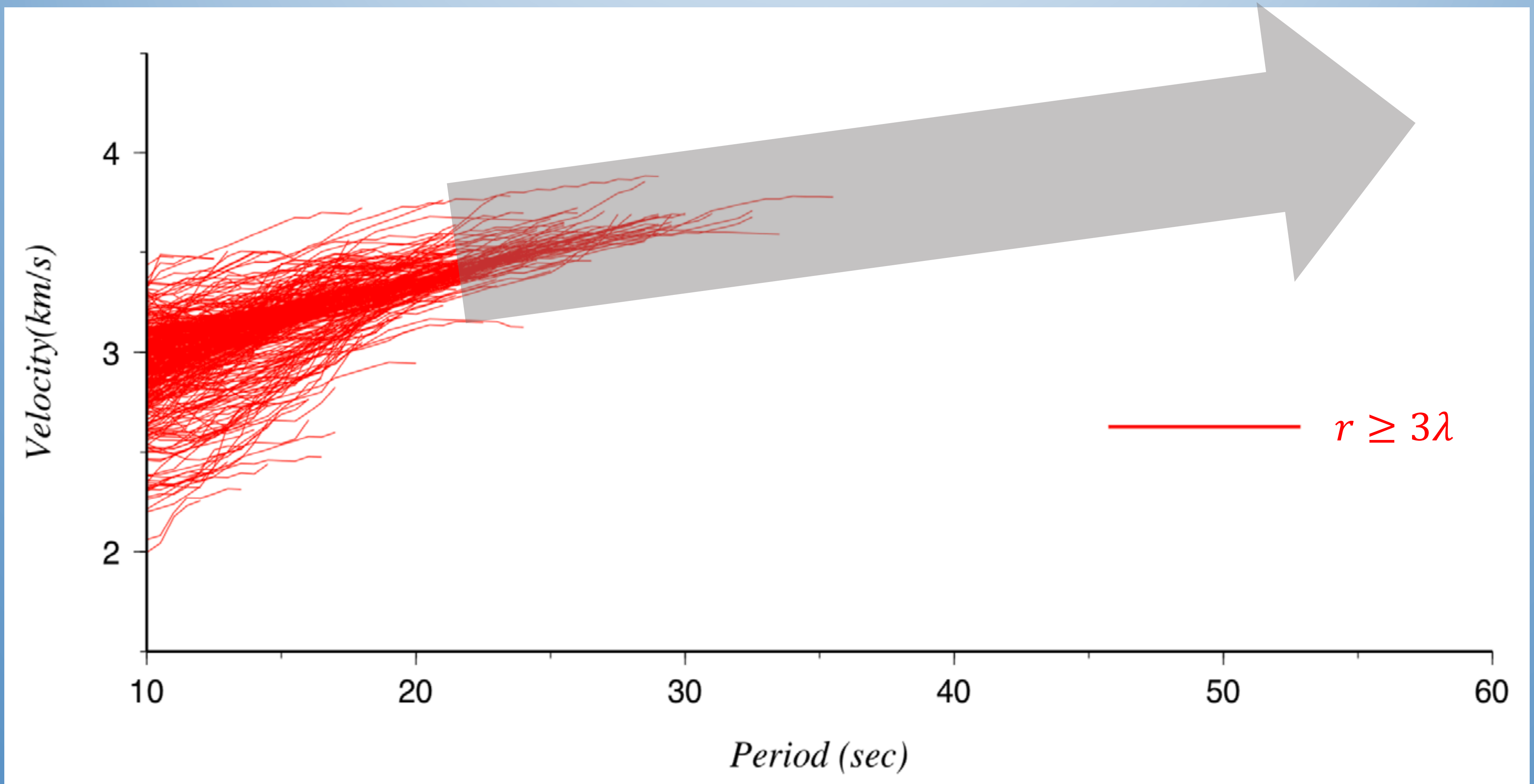

1. Extending the dispersion measurement to much longer periods.
2. Allowing the probing of deeper structures with the same NCF dataset.

2. Theoretical background

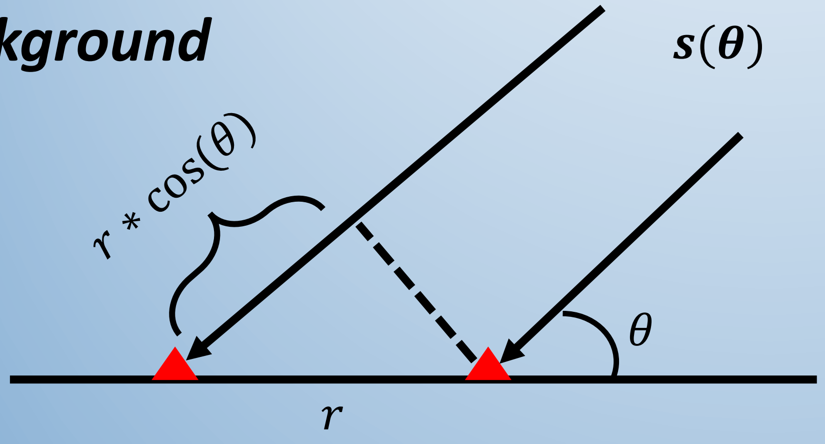

Using a **“Far field “** source condition, noise source can be considered as

1. a function of azimuth.
2. a function of the resulting delay time of a NCF.

$$NCF(\tau,\omega) \approx \sum_{\theta=0}^{\pi} A(\omega)^2 \cos\left[\omega\left(\tau - \Delta t(\theta)\right)\right] \qquad \Delta t(\theta) \equiv r * \cos(\theta)/\mathrm{c}$$

$$\approx \int_0^{\pi} A(\omega)^2 \cdot cos[\omega\tau - \Phi(\theta)]\, d\theta \qquad \Phi(\theta) \equiv r\omega\cos(\theta\,)/c$$

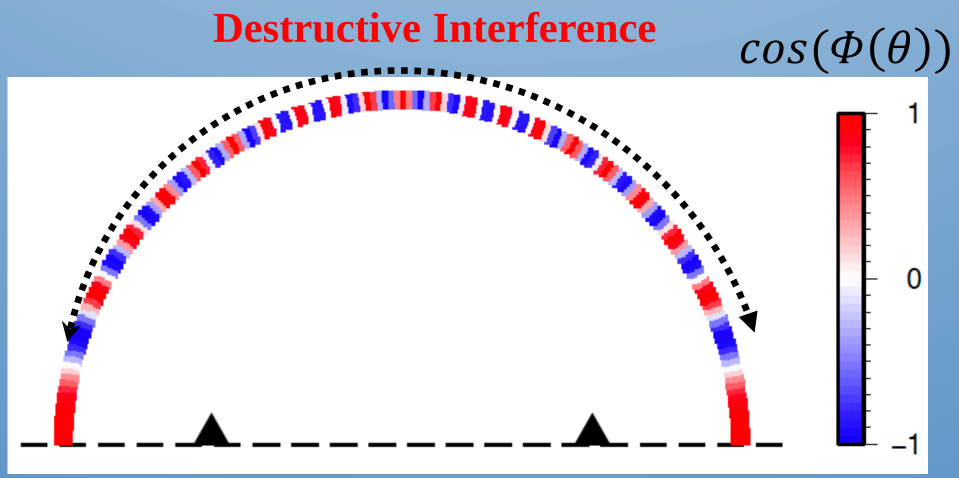

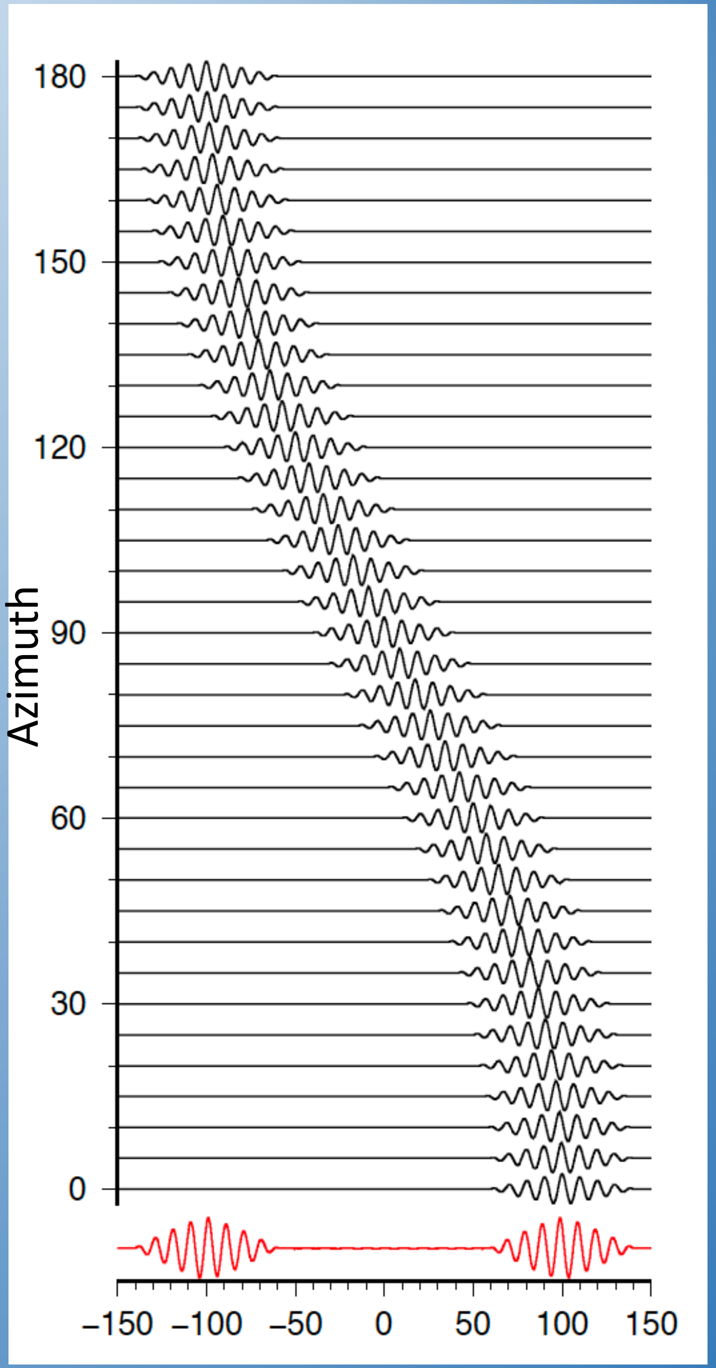

$$NCF(\tau,\omega) \sim \Re\left[e^{-i\omega\tau}\cdot\frac{\pi}{2}A(\omega)^2\cdot\left(J_0\left(\frac{r\omega}{c}\right)-iH_0\left(\frac{r\omega}{c}\right)\right)\right]$$

J_0 :zeroth order Bessel function of the first kind
H_0:zeroth order Struve function of the first kind

1. Peak delay time Measurement:

$$\omega\tau_{pk}(\omega)+2N\pi=\phi\left[J_0\left(\frac{r\omega}{c}\right)-iH_0\left(\frac{r\omega}{c}\right)\right]$$

$$Phase\ velocity\ c(T)=r/(\tau_{pk}(T))$$

T :period

2. *High-Frequency Approximation (r>>λ)*

$$\omega\tau_{HF}(\omega)+2N\pi\sim\phi\left[J_0\left(\frac{r\omega}{c}\right)-iY_0\left(\frac{r\omega}{c}\right)\right]=\frac{r\omega}{c}-\frac{\pi}{4}.$$

$$Phase\ velocity\ c(T)=r/(\tau_{HF}(T)+T/8)$$

Y_0 :zero-order Bessel function of the second kind

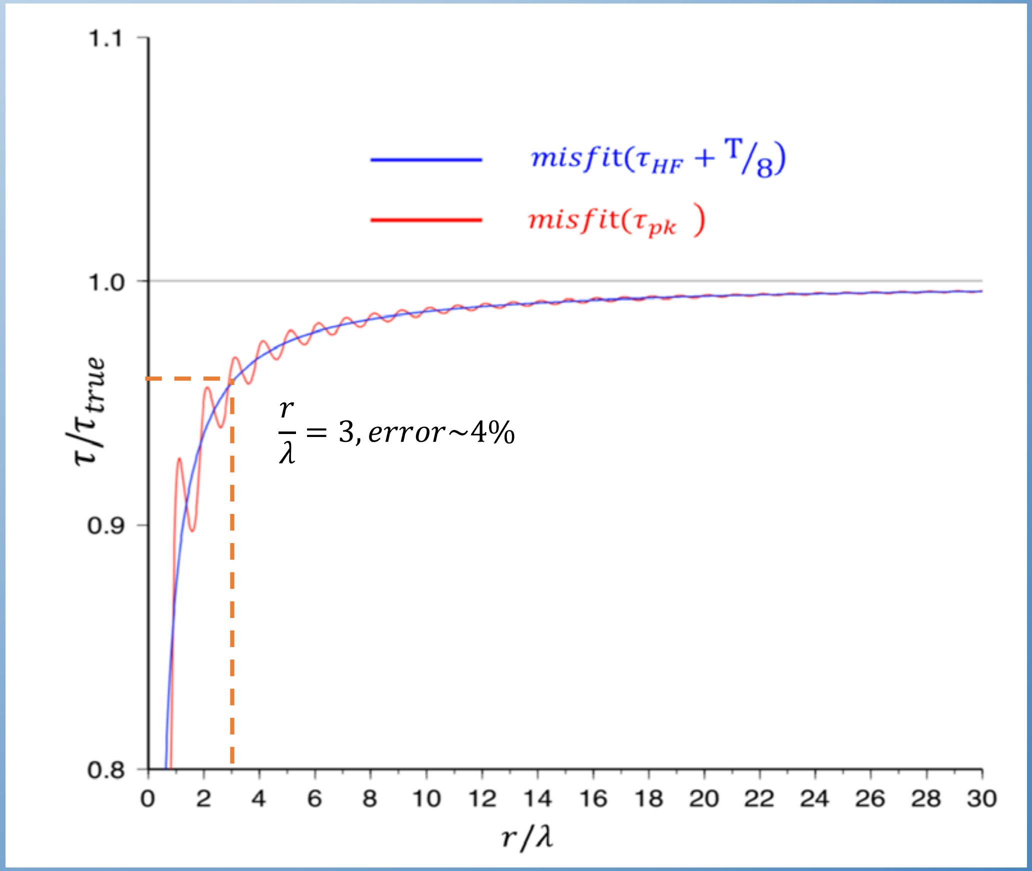

Comparisons of the delay time measurements predicted using different approaches. Following *Tsai* [2009], the estimated delay time is normalized by the true delay time (r/c) between stations.

3. Common measurement

If the high-frequency approximation is not valid for NCFs, the delay time measurement obtained from HF form should be

$$\omega\tau_{pk}(\omega) + 2N\pi = \phi[J_0\left(\frac{r\omega}{c}\right) - iH_0(\frac{r\omega}{c})]$$

$$\tau_{com} = \tau_{pk}(T) + T/8$$

$$Phase\ velocity\ c(T) = r/(\tau_{pk}(T) + T/8)$$

2. High-Frequency Approximation (r>>λ)

$$\omega\tau_{HF}(\omega) + 2N\pi \sim \phi\left[J_0\left(\frac{r\omega}{c}\right) - iY_0\left(\frac{r\omega}{c}\right)\right] = \frac{r\omega}{c} - \frac{\pi}{4}.$$

$$Phase\ velocity\ c(T) = r/(\tau_{HF}(T) + T/8)$$

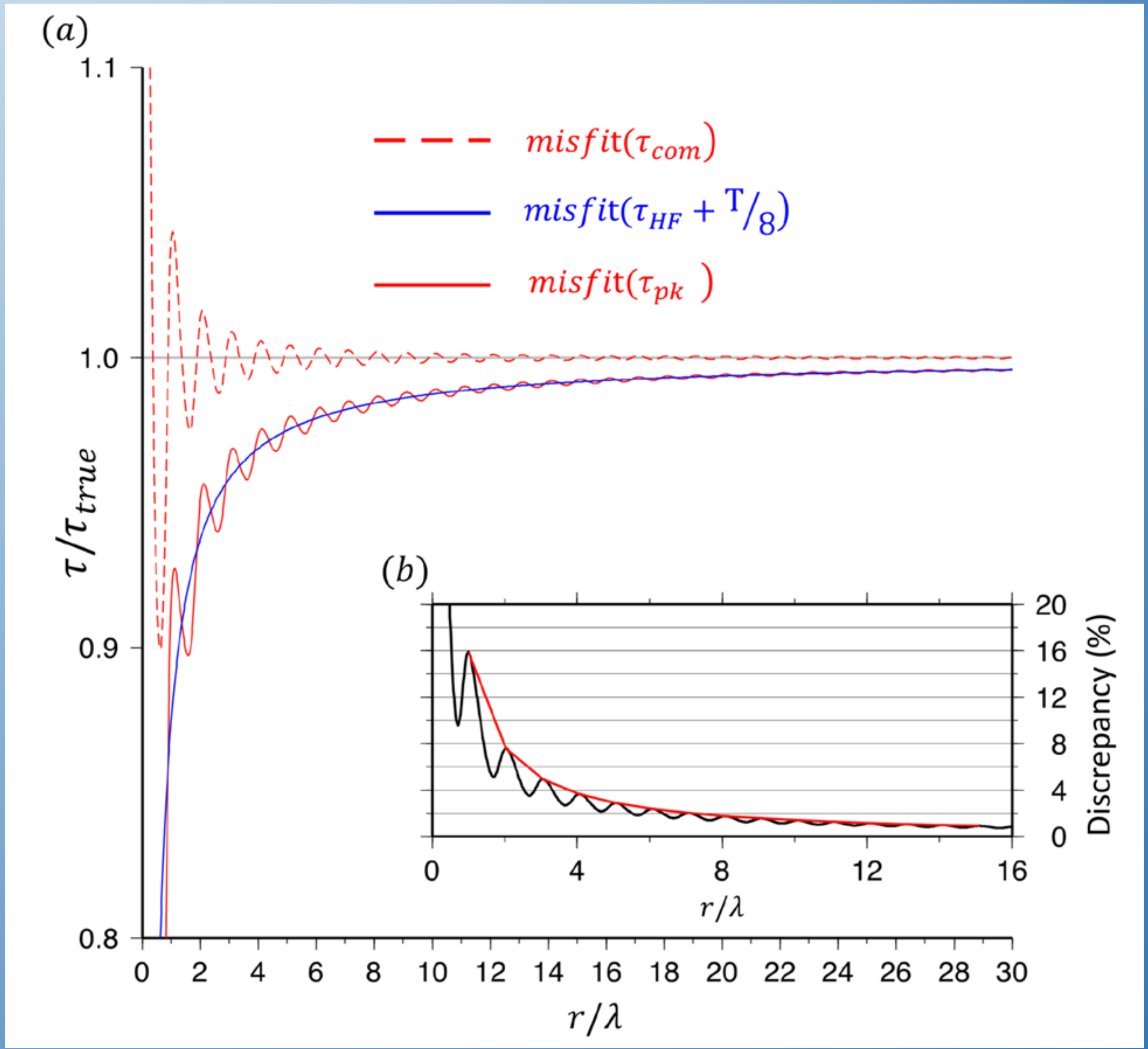

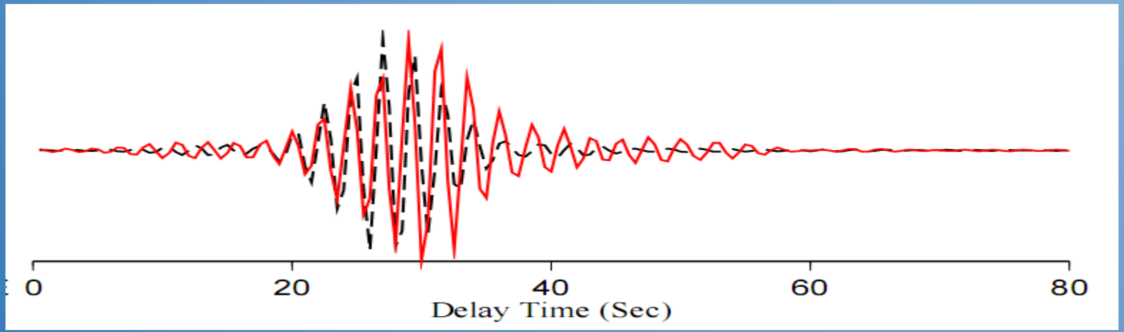

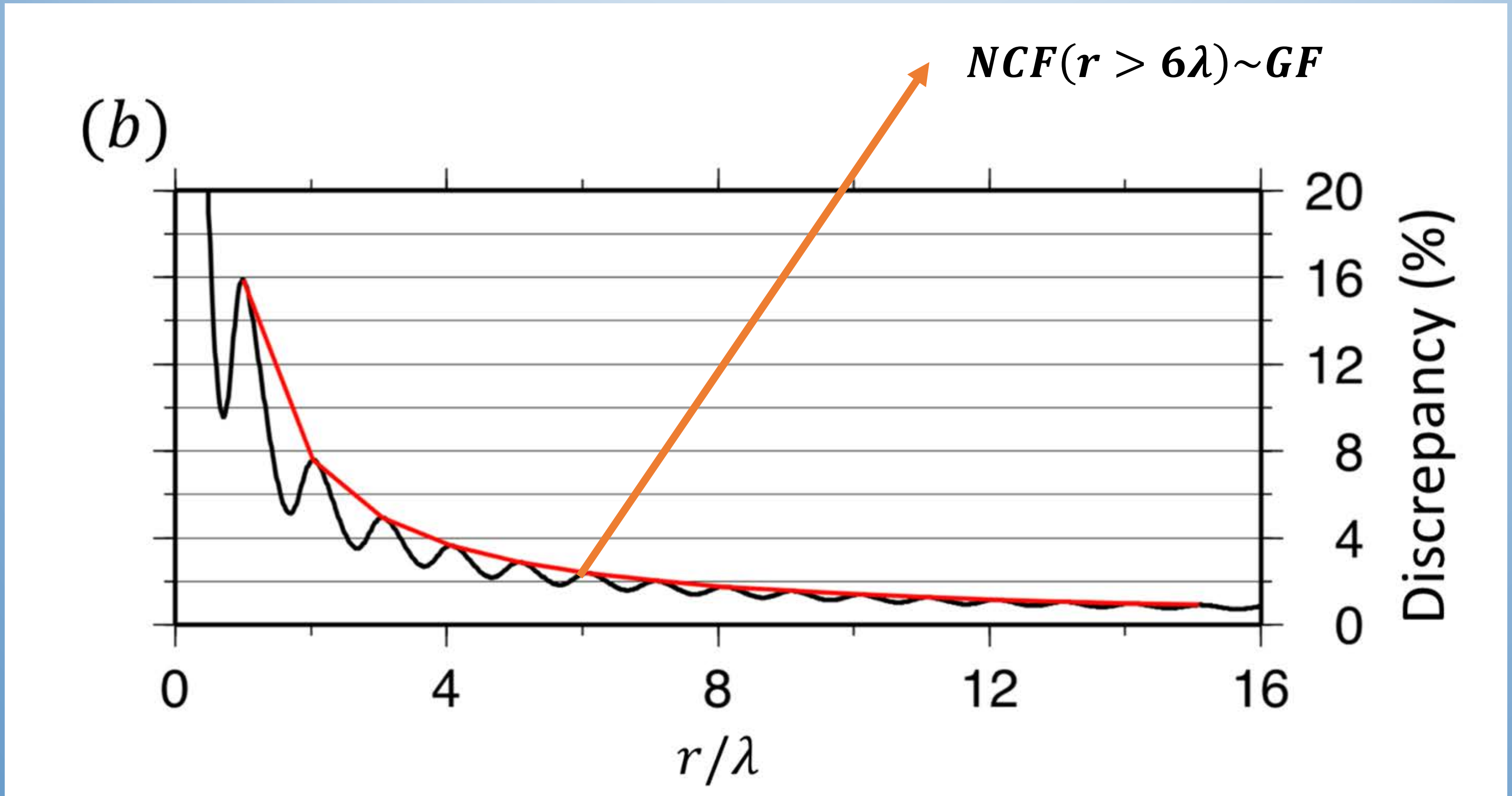

The discrepancy between the delay times given by the common and the *HF* approximation is defined as $\left(1-\frac{\tau_{HF}+T/8}{\tau_{com}}\right)\%$. The discrepancy between them is less than 2% only when $r > 6\lambda$ .Using the 2% misfit as a criterion, we argue that the *HF* approximation is only theoretically appropriate, i.e., $\tau_{HF}+\frac{T}{8}\approx\tau_{com}$, when the interstation distance between station pairs is longer than six wavelengths.

Common measurement **may not be a reasonable approach in the most noise studies. However, in practice, it does provide excellent velocity measurements.**

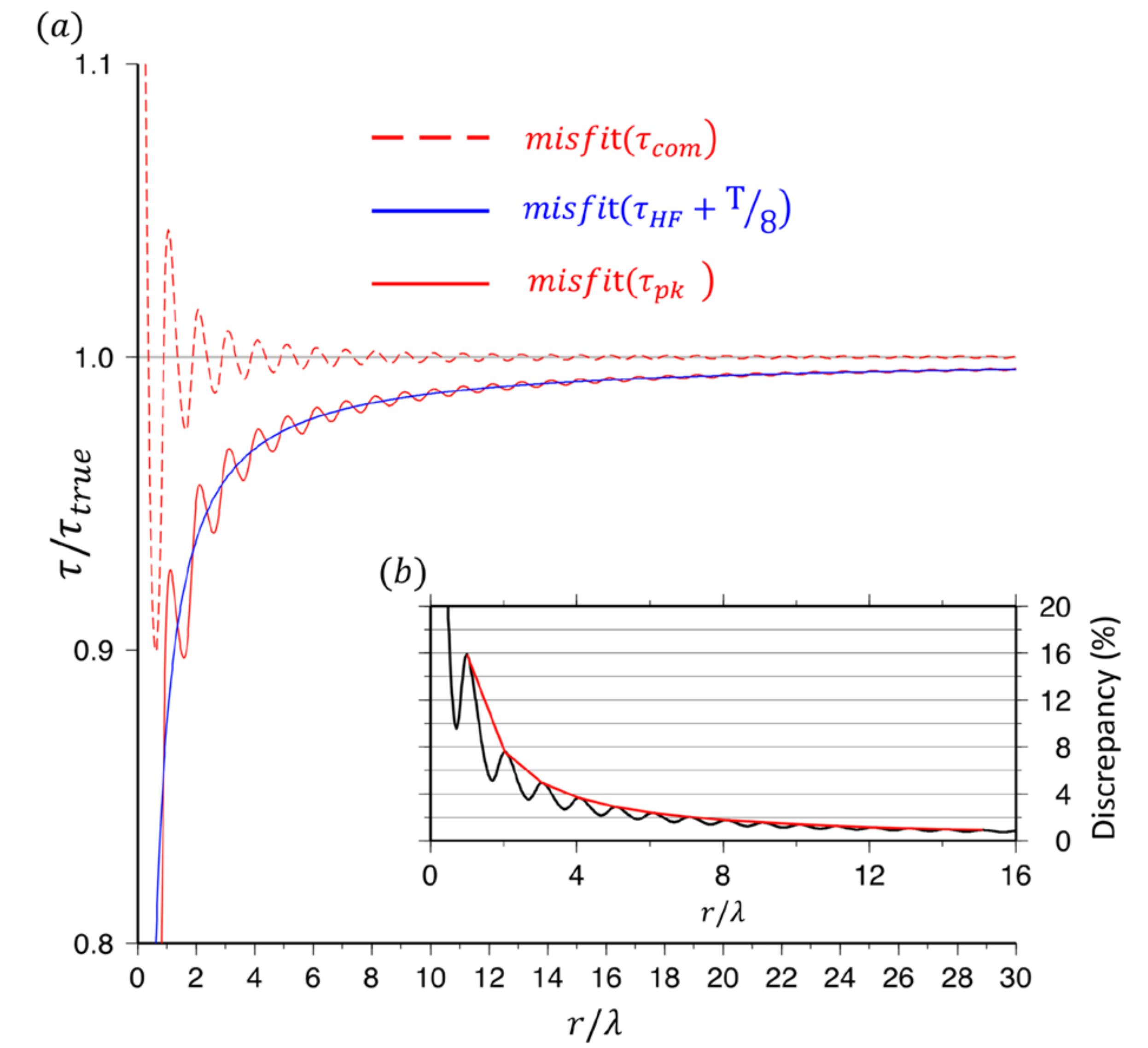

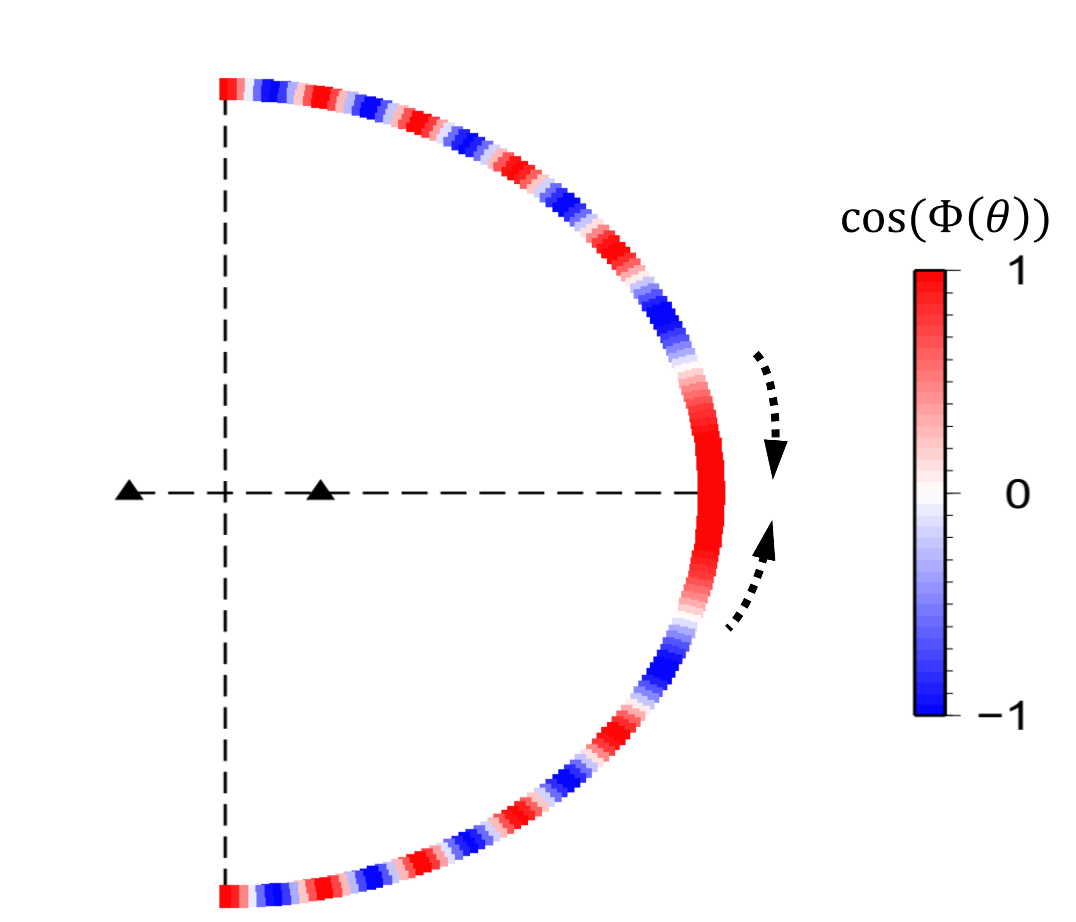

The correction of $\pi/4$ phase shift simply filters the source effects within the sensitive zone and highlight the delay time resulting from sources along station pair.

Common measurement → two-station method

3. Hybrid peak time matching method

Demonstrating how the true delay time is estimated in the proposed method by using a synthetic NCF ($r = 200$ km) .
Using the peak delay time evaluated for period 46 sec ($^{r}/_{\lambda} = 1.08$) as an example, in the following we show the procedural to access the true delay time.

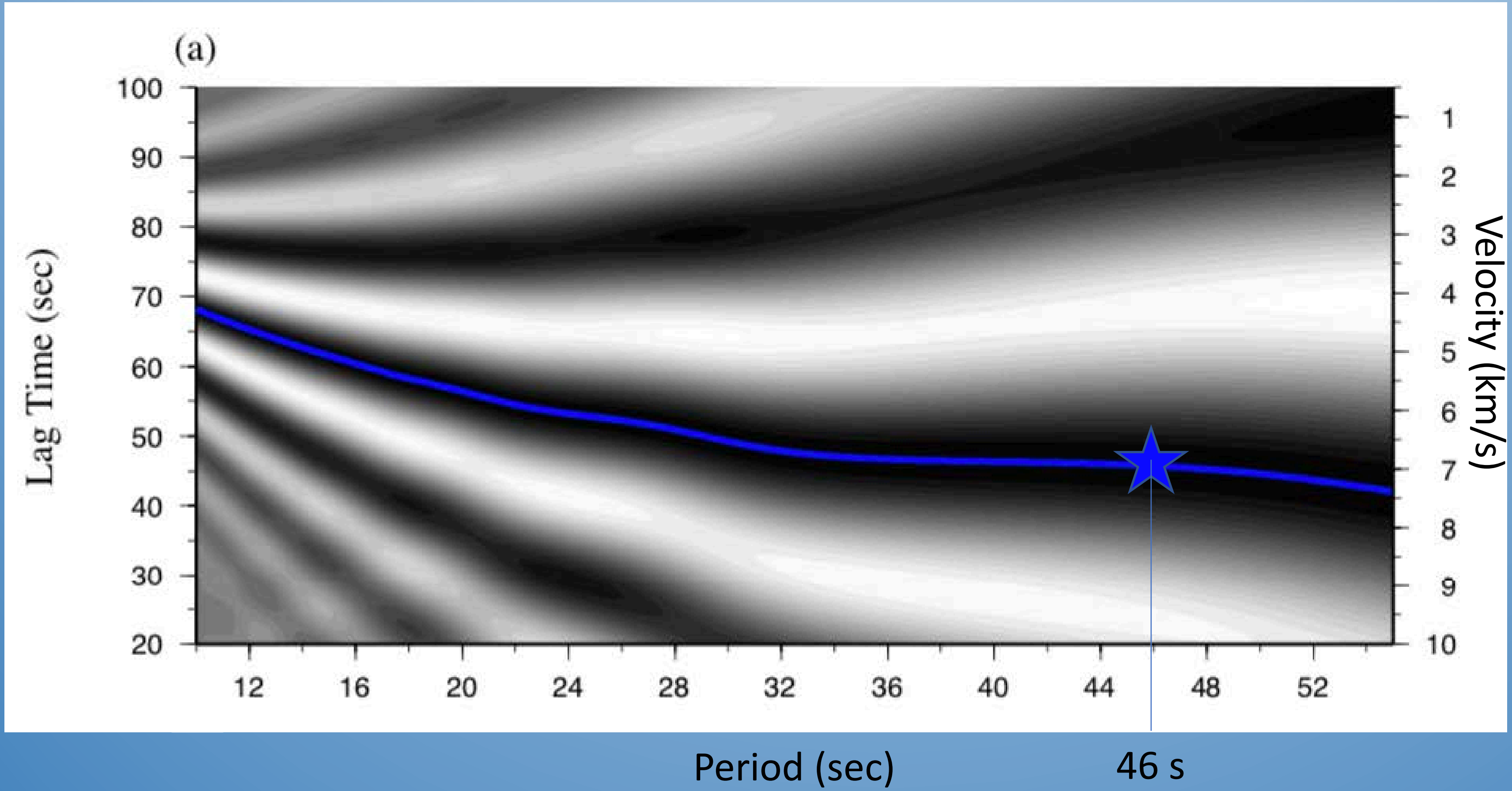

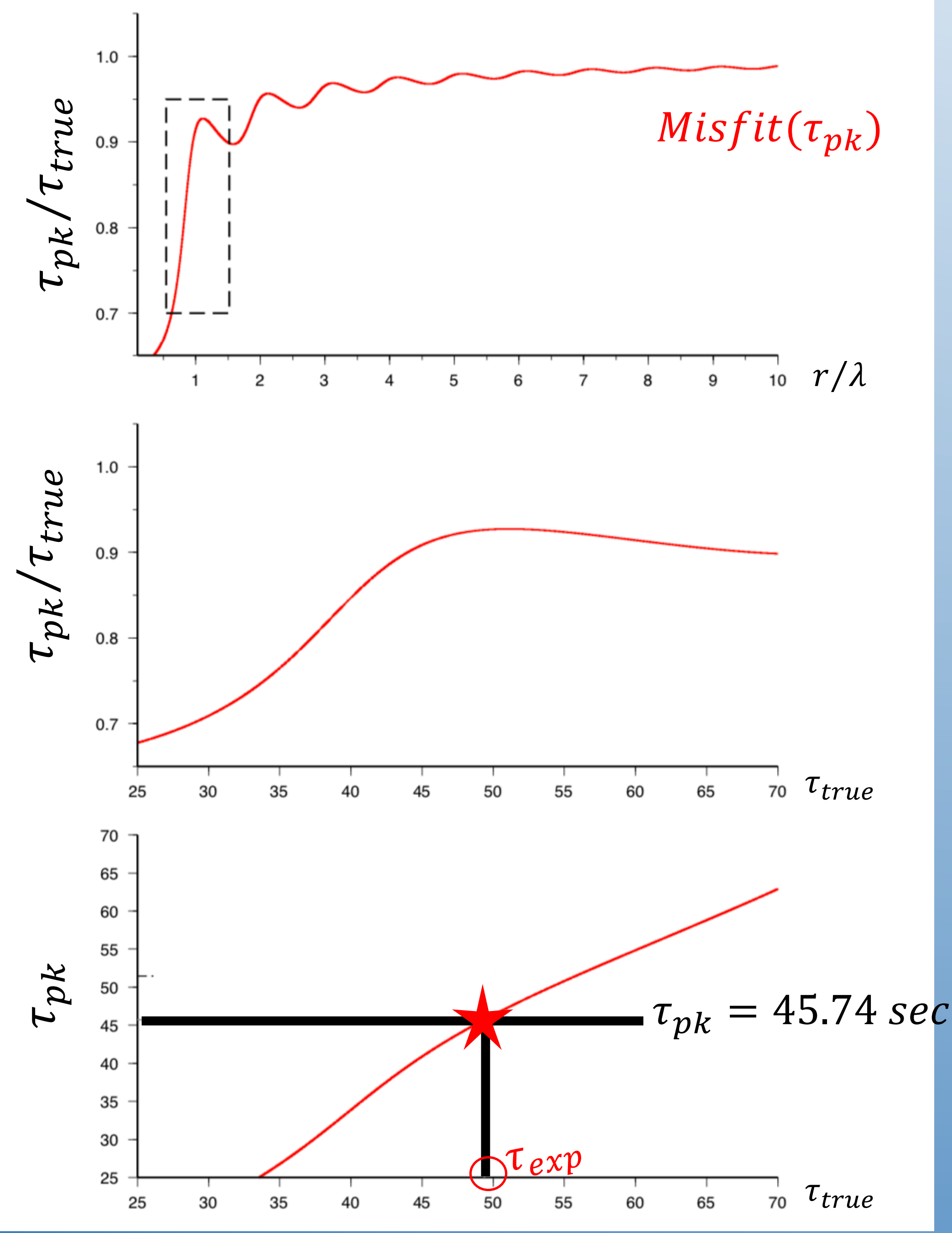

$$\boxed{\omega\tau_{pk}(\omega) + 2N\pi = \phi\left[J_0\left(\frac{r\omega}{c}\right) - iH_0\left(\frac{r\omega}{c}\right)\right]}$$

Step 1.
Given the target period (46 sec), the x-axis is replaced with the true delay time.

$$\frac{r}{\lambda} = \frac{r}{c * T} = \frac{\tau_{true}}{T}$$

Step 2. With the true delay time (x-axis), the y-axis can be replaced with the observed delay time.

$\tau_{pk} = 45.74\ sec$
$\tau_{exp} = 49.37$ sec
$\tau_{true} = 49.726$ sec

$error \equiv |1 - \frac{\tau}{\tau_{true}}|$
error(τ_{pk})~8%
error(τ_{exp})~0.6%

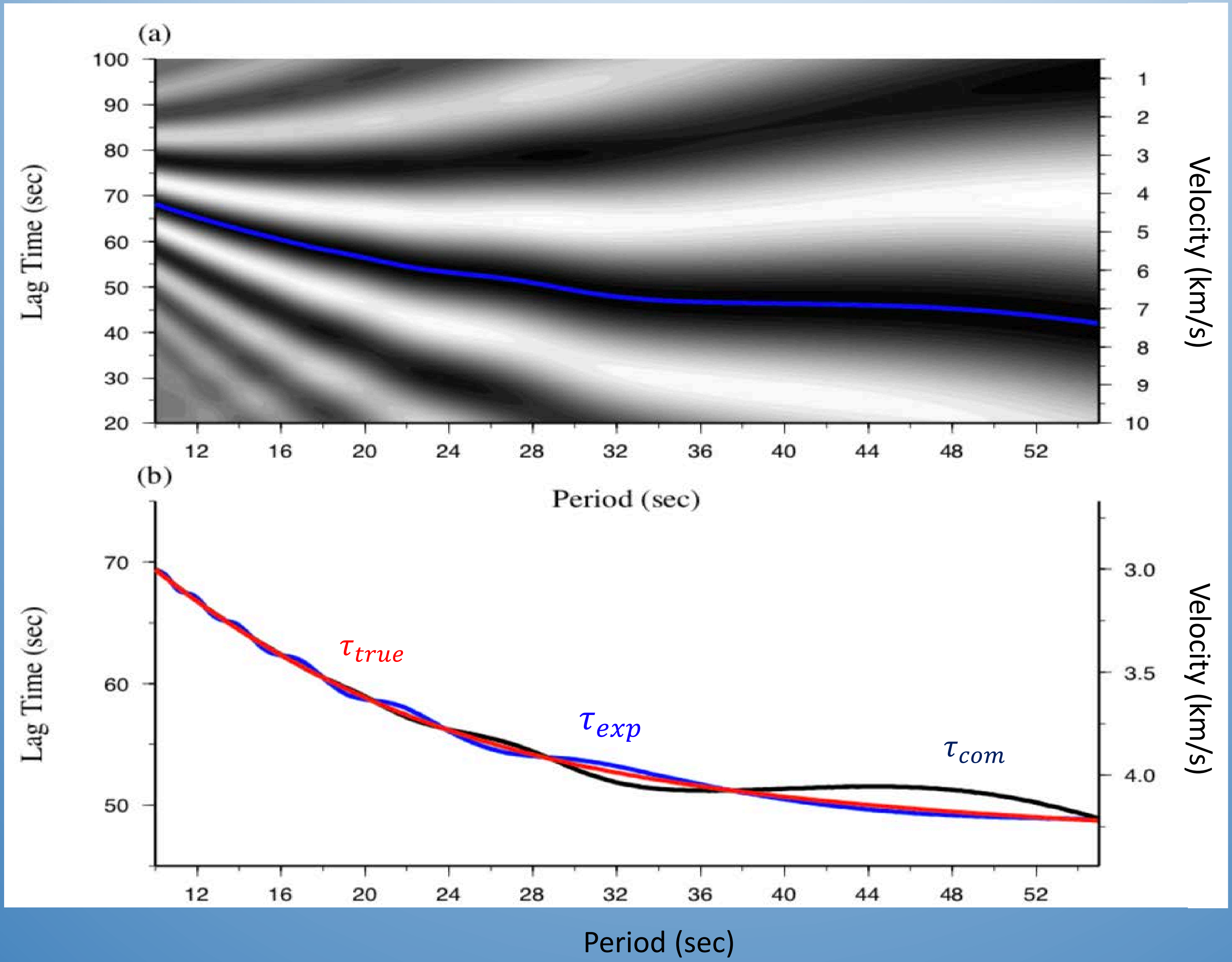

(a)
Lag Time (sec)
100
90
80
70
60
50
40
30
20
12
16
20
24
28
32
36
40
44
48
52
1
2
3
4
5
6
7
8
9
10
Period (sec)
(b)
Lag Time (sec)
70
60
50
3.0
3.5
4.0
τ_{true}
τ_{exp}
τ_{com}
Velocity (km/s)
Velocity (km/s)
Period (sec)

Single frequency measurement

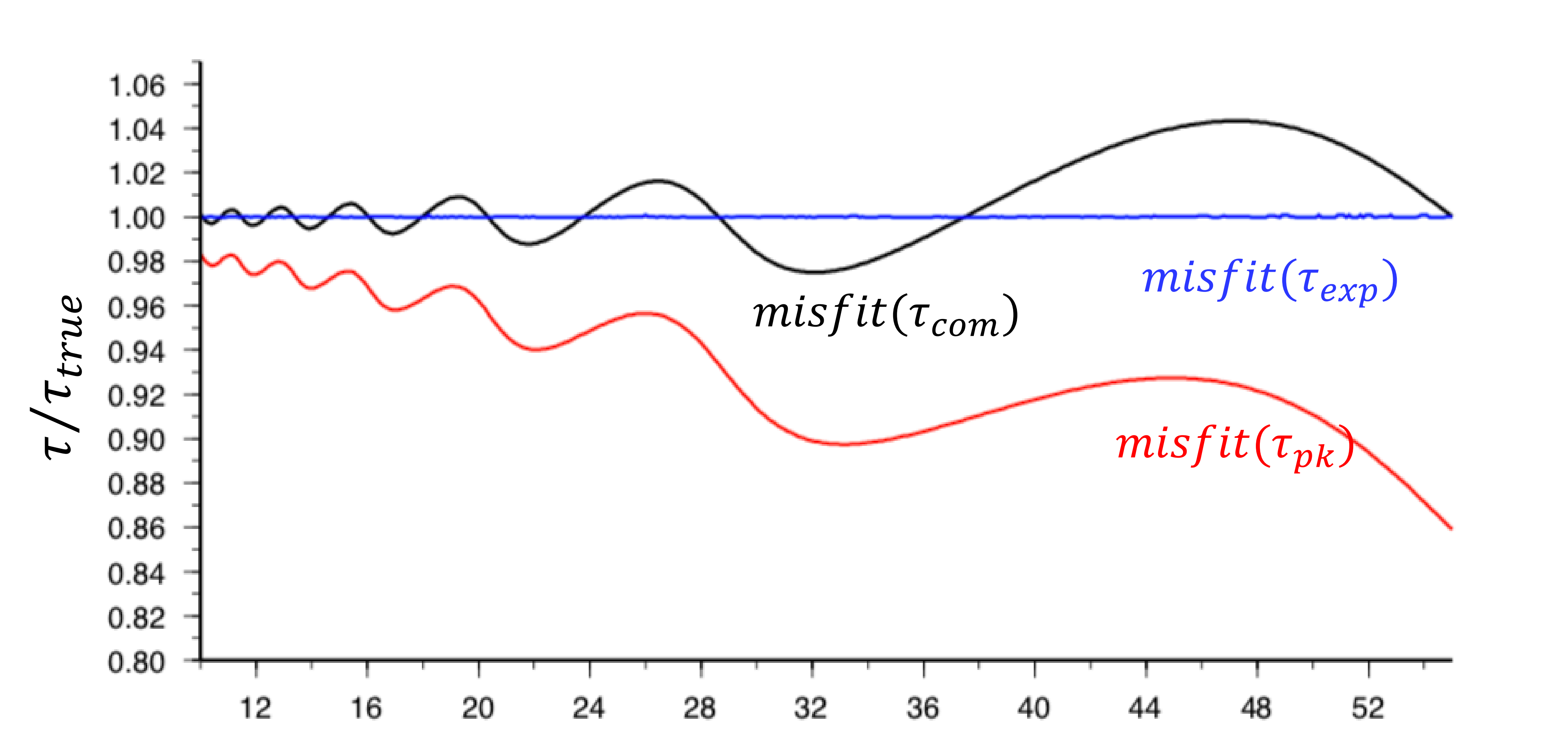

Period (sec)

4. Advantages of the new method

1. The determined dispersion curves is greatly extended to include longer periods.

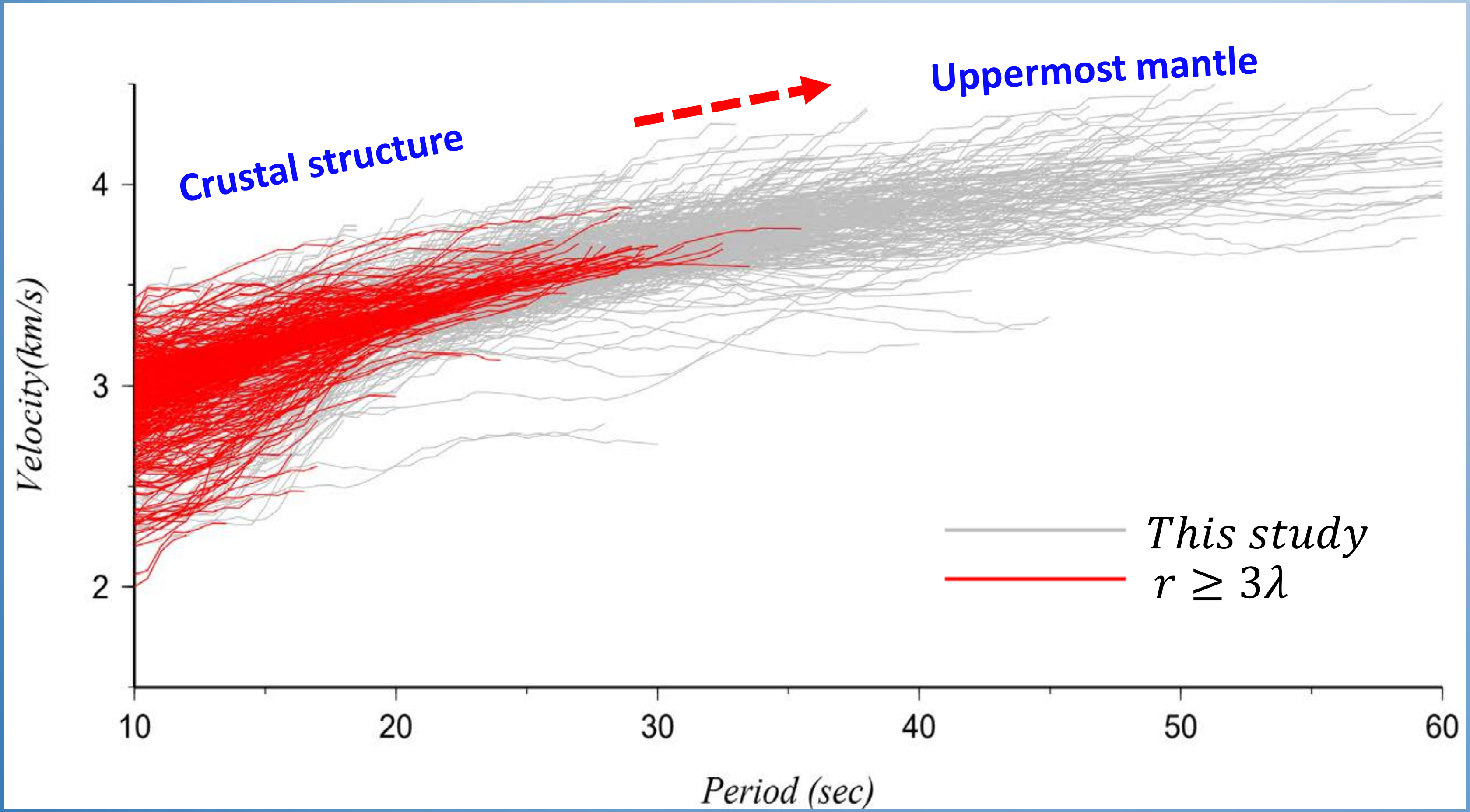

Sensitivity Kernel

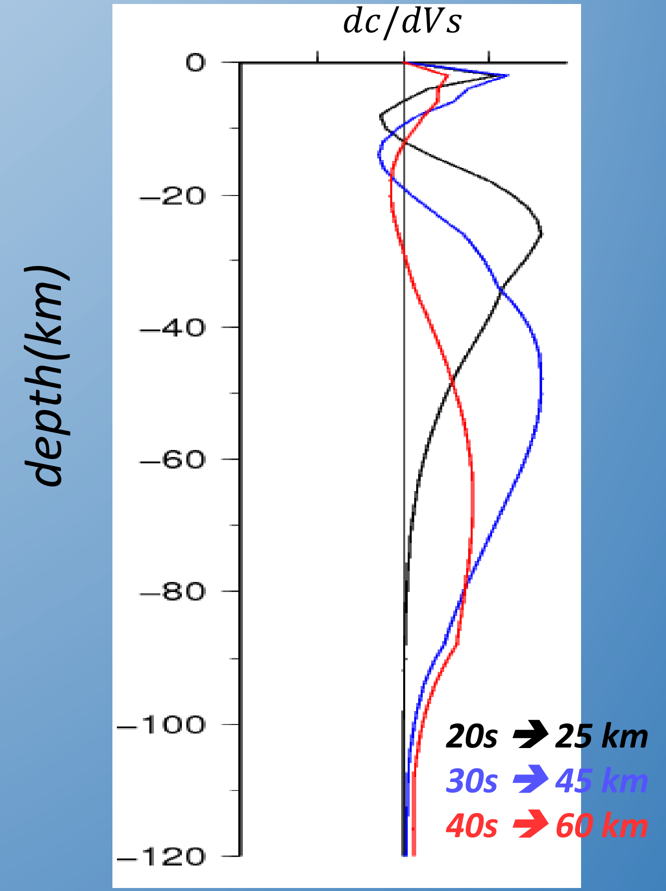

2. Enriching the azimuthal coverage for anisotropic tomography studies.

$r \geq 3\lambda$

This study

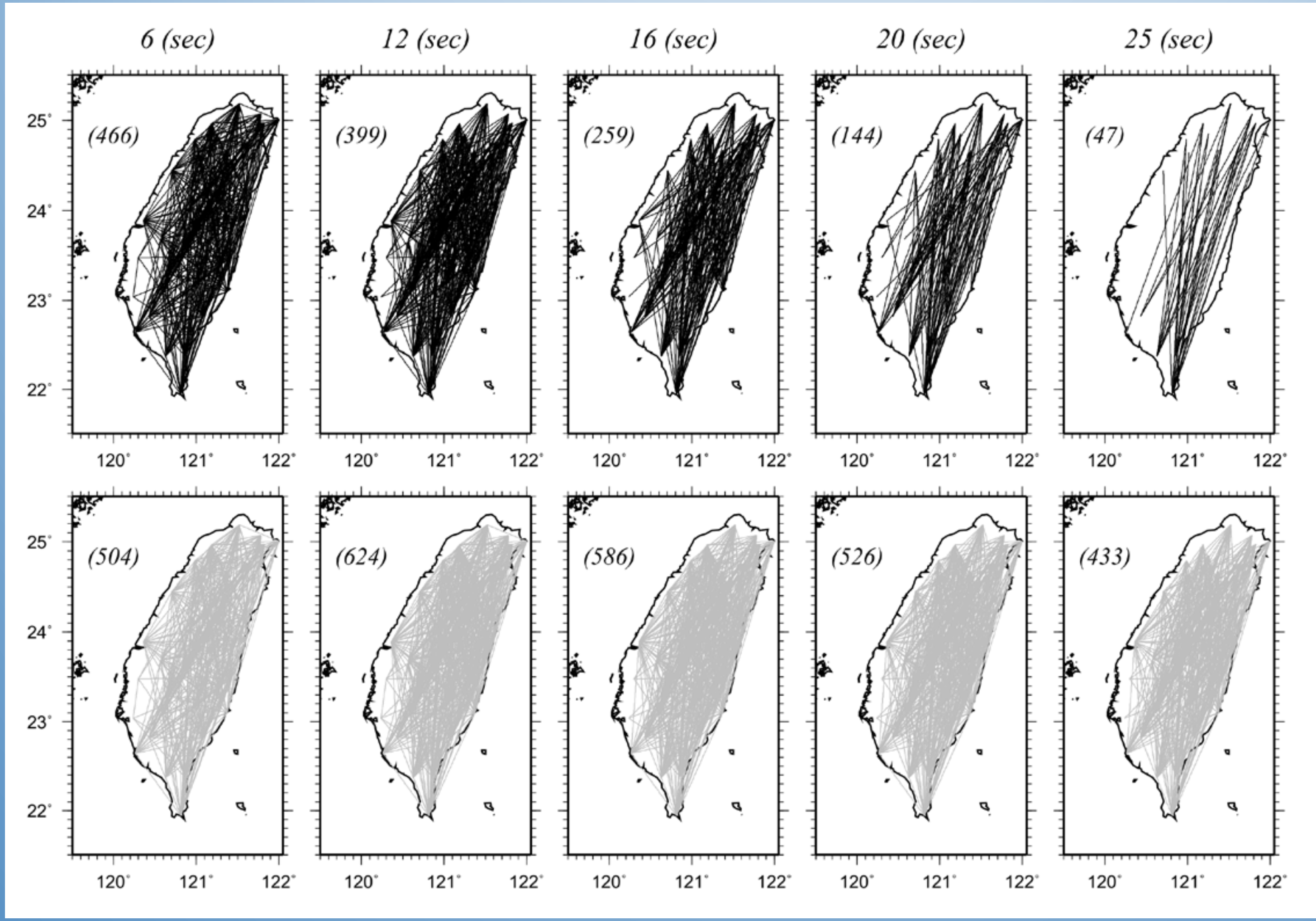

A comparison of path coverages at 5 selected periods obtained by applying two different approaches. In the upper panel, the black lines are the available path distributions that fit the 3-wavelength criterion; the gray lines shown in the lower panels are the paths obtained from the approach proposed in this study. The number of available paths is shown in parentheses at the top-left of each graph.

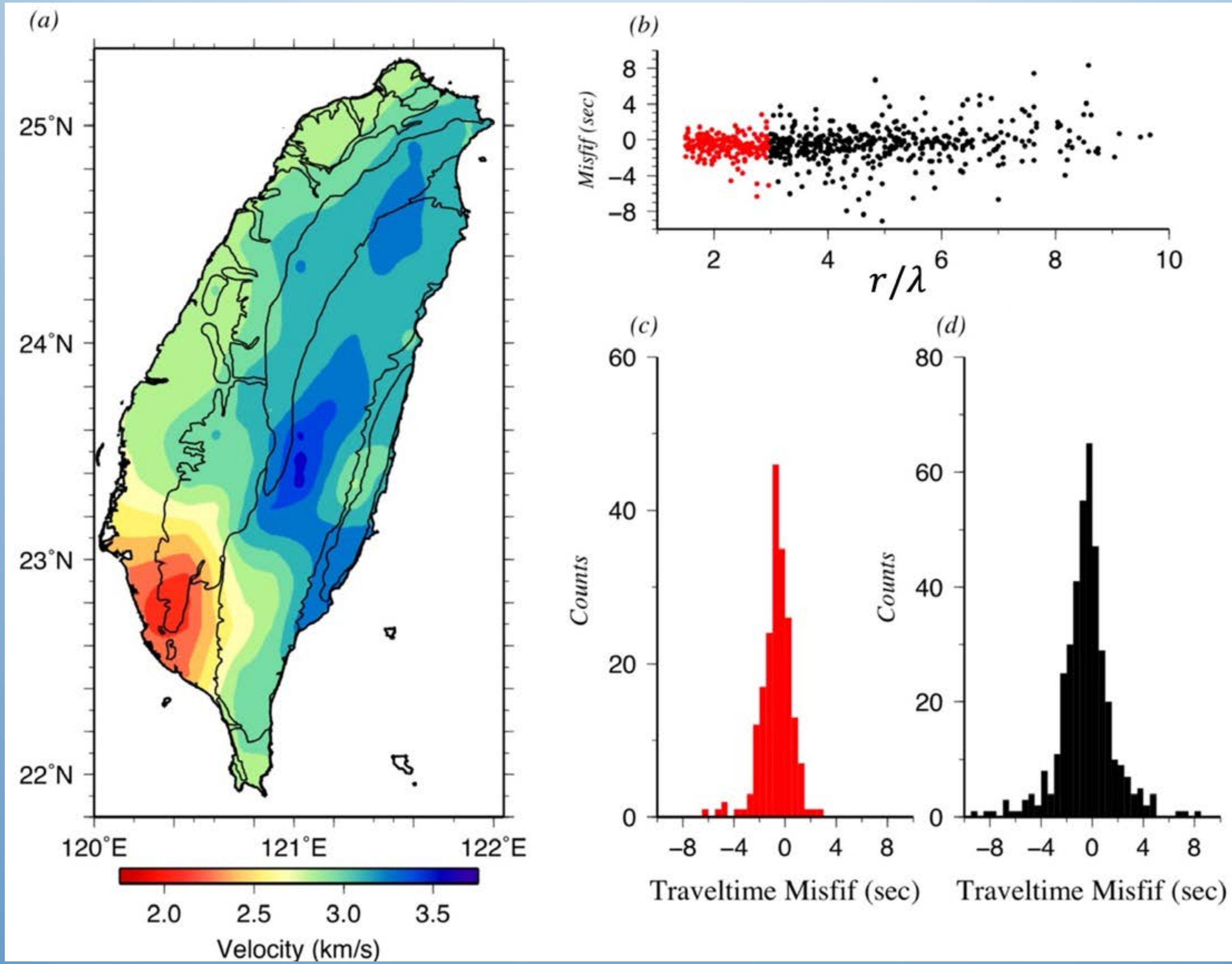

(a) 2D phase velocity map for 12 s Rayleigh waves derived from 399 long-distance ($r \geq 3\lambda$) data from a traditional measurement. (b) Travel time misfits between the observations and predictions evaluated from the velocity model. The misfits of the short-distance data ($1.5\lambda \leq r < 3\lambda$) and the long-distance data are denoted by red and black dots, respectively. (c) Distribution of the misfits for the short-distance data. (d) Distribution of the misfits for the long-distance data.

Summary

1. We present a new method based on hybrid peak delay time matching to estimate the phase velocities at much lower frequencies of the noise cross-correlation function.

2. Using this method, the dispersion measurement can be extended to much longer periods, allowing the probing of deeper structures with the same noise cross-correlation function dataset.

Amplitude Asymmetry indicates the source asymmetry in ambient noise.

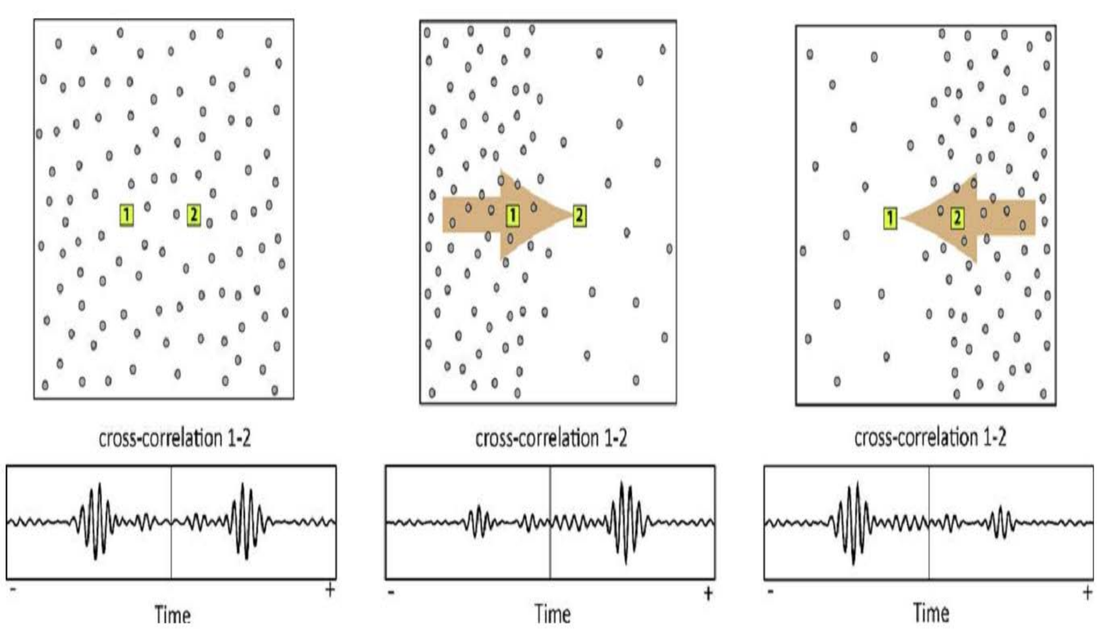

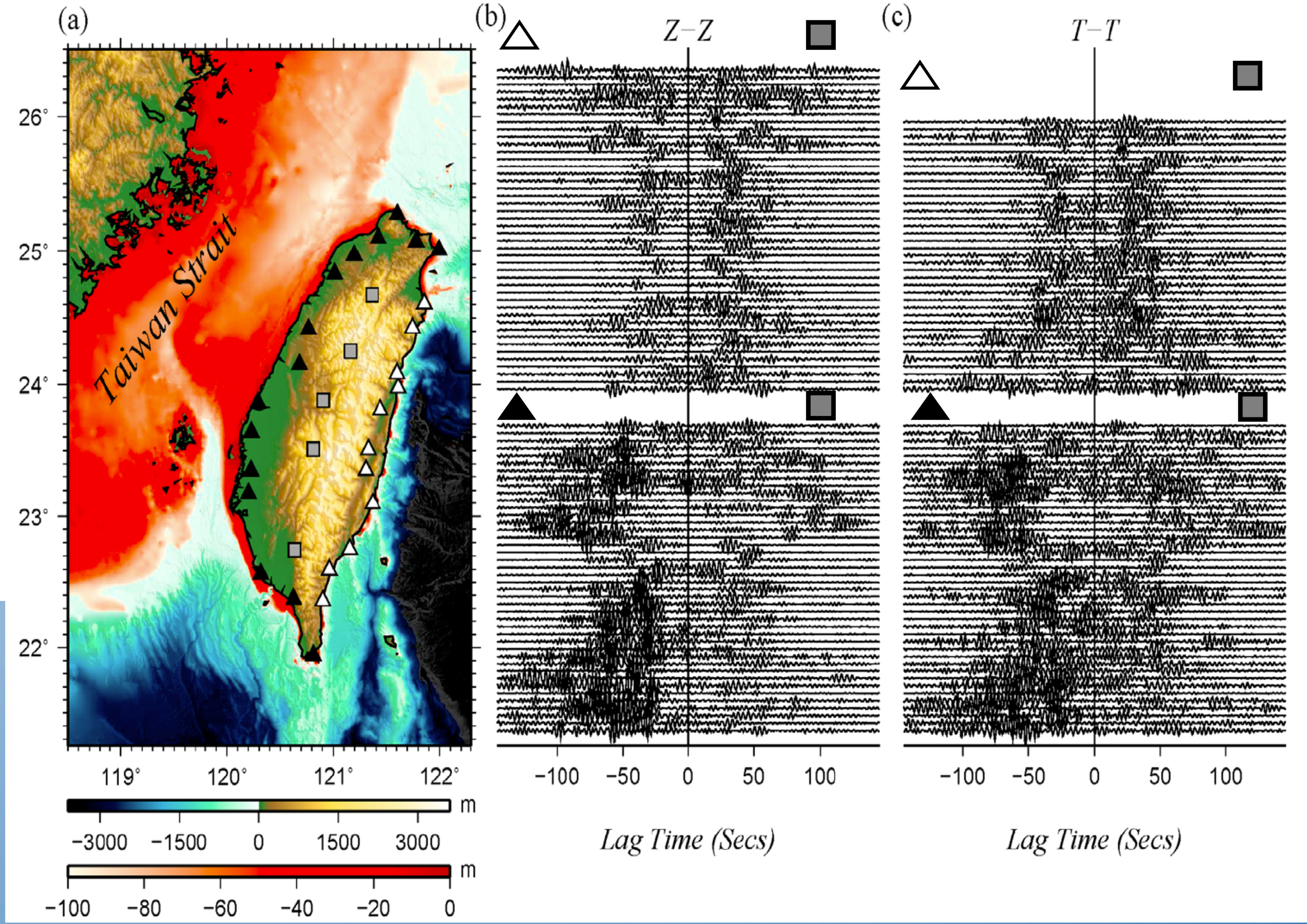

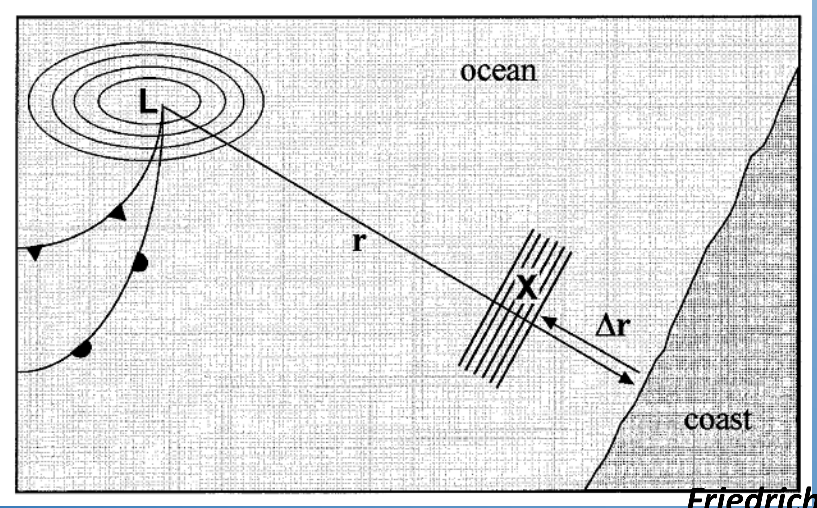

Friedrich at el. (1998)

Shallow water --> Excitation Strength

Complex coastline : more noise sources

2. Using the "*noise*" of noise cross-correlation *(A New field in noise study)*

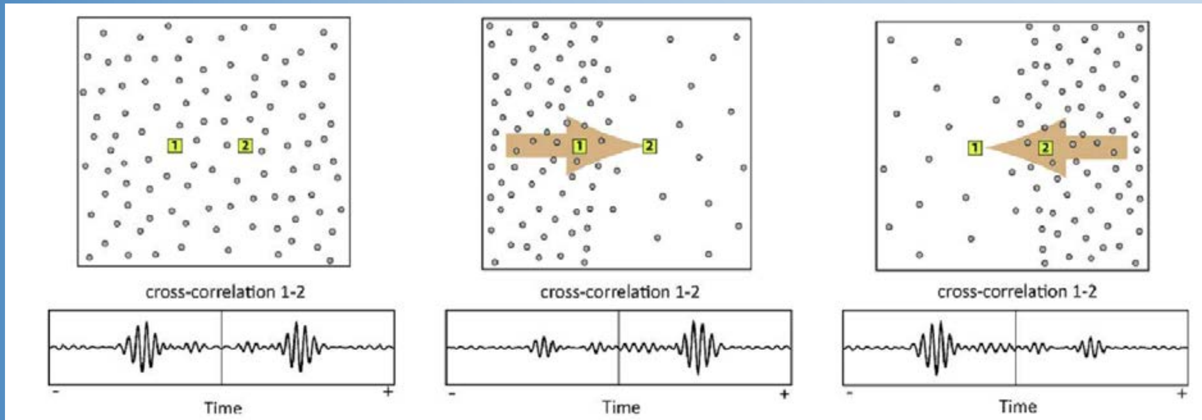

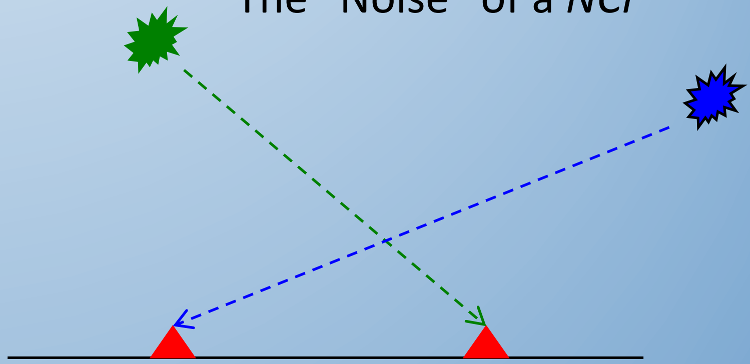

Two points:

- ***Intrinsic noise level of NCF***

  -- (Time window) Chen et al., 2017

- ***Intrinsic Uncertainty of NCF***

  -- (Arbitrary lag time)

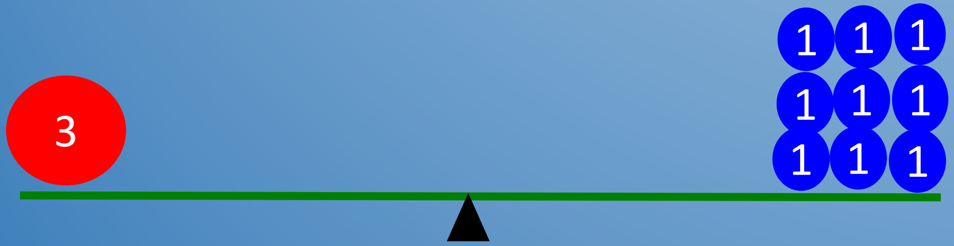

Physics Idea : Random walk (Brownian motion)

Theoretical background

Considering a case with *N* independent noise sources

$$U_j(x,t,\omega) = \sum_{s=1}^{N} A_s(\omega)\cos\left[\omega\left(t - \frac{r_{sx}}{c(\omega)}\right) + \phi_{sj}\right]$$

$$NCF_j(\omega,\tau) = \boxed{\sum_{s=1}^{N} {A_s}^2(\omega)\cos[\omega(\tau - \Delta t_s)]}$$

$$+ \underbrace{\sum_{k=1}^{N-1}\sum_{\substack{l=1\\ l\neq k}}^{N} A_k(\omega)A_l(\omega)\cos(\omega\tau + \phi_{klj}) = N\overline{A_x^2}\cos(\omega\tau + \phi_j^{avg})}_{N(N-1))\ \ elements}$$

$$\overline{A_x^2} = \frac{1}{N(N-1)}\sum A_k A_l$$

$$\Delta t_s = \frac{r_{sx} - r_{sy}}{c(\omega)}$$

$$\phi_{klj} = \frac{\omega(r_{kx} - r_{ly})}{c(\omega)} + (\phi_{kj} - \phi_{lj})$$

The "Signal" of a *NCF*

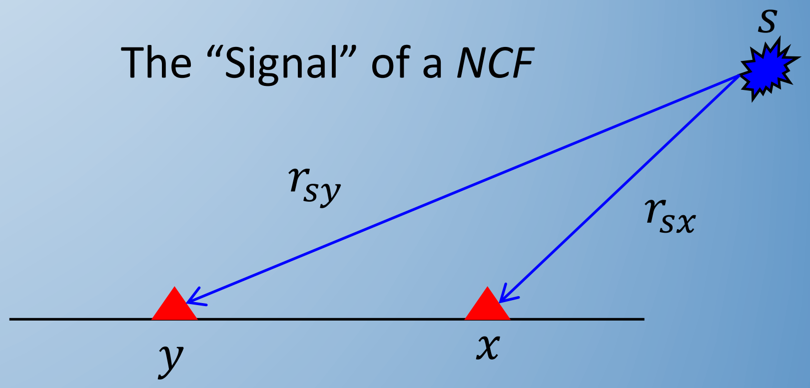

The "Noise" of a *NCF*

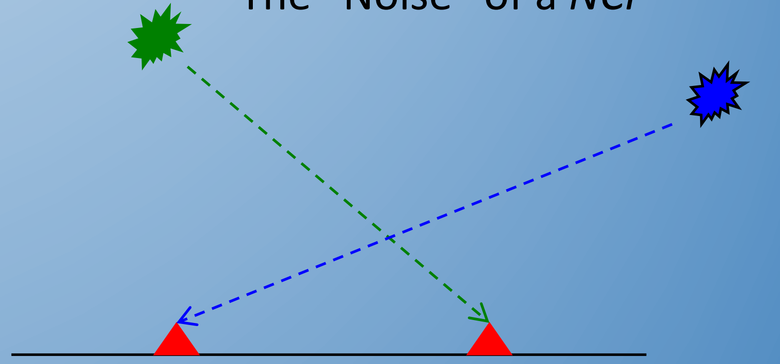

Using the coherency form:

$$NCF_j(\omega,\tau) = \frac{1}{\overline{\overline{A^2(\omega)}}}\sum A_s^2(\omega)\cos[\omega(\tau\text{-}\Delta t_s)] + N(\omega)\frac{\overline{A_x^2(\omega)}}{\overline{\overline{A^2(\omega)}}}\cos(\omega\tau + \phi_j^{avg})$$

$$\overline{NCF^{M}}(\omega,\tau) \sim \frac{\overline{As^2(\omega)}}{\overline{\overline{A^2(\omega)}}}G'(\omega,\tau) + \left(\frac{INL(\omega)}{\sqrt{M}}\right)\cos(\omega\tau + \phi_M^{avg})$$

Intrinsic noise level

$$\boxed{INL(\omega) \equiv N(\omega)\frac{\overline{A_x^2(\omega)}}{\overline{\overline{A^2(\omega)}}}}$$

2. Using the "*noise*" of noise cross-correlation

Topic One : Intrinsic noise level of NCF (Chen et al., 2017)

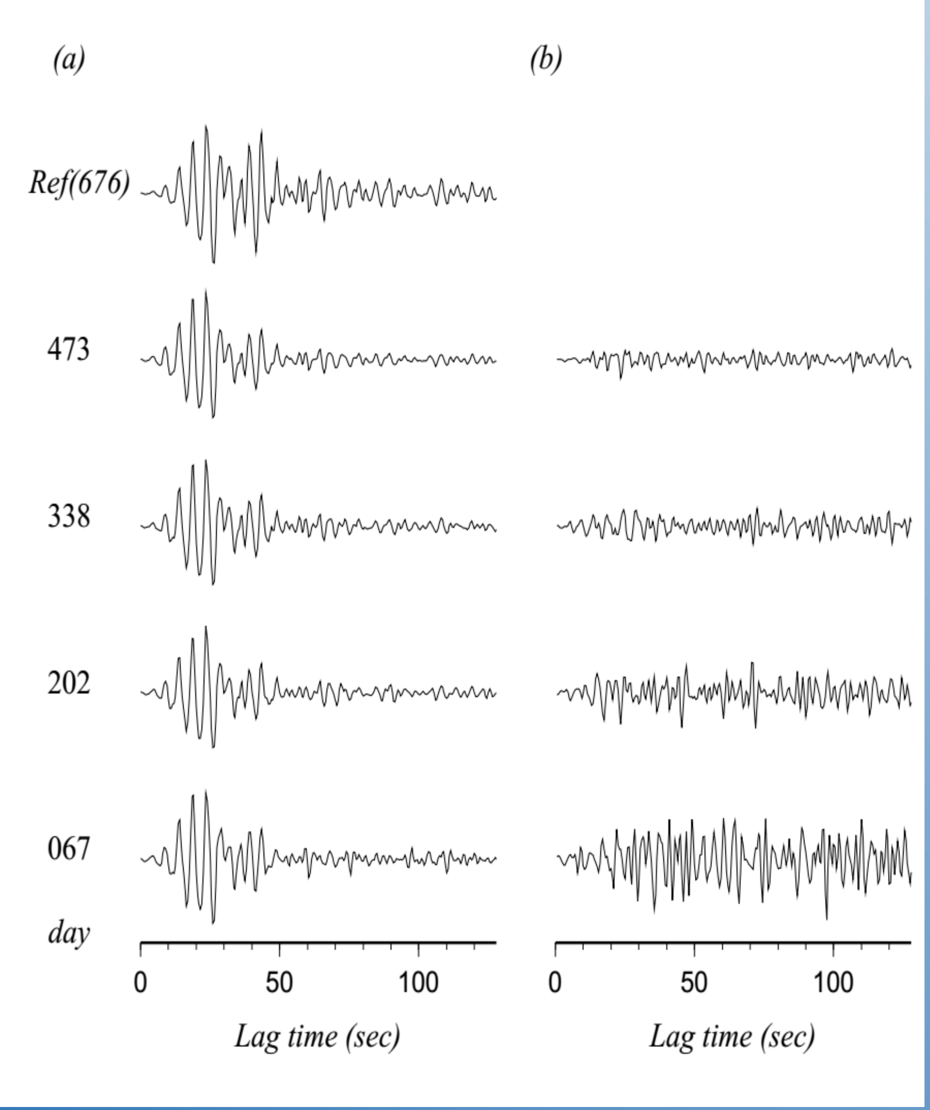

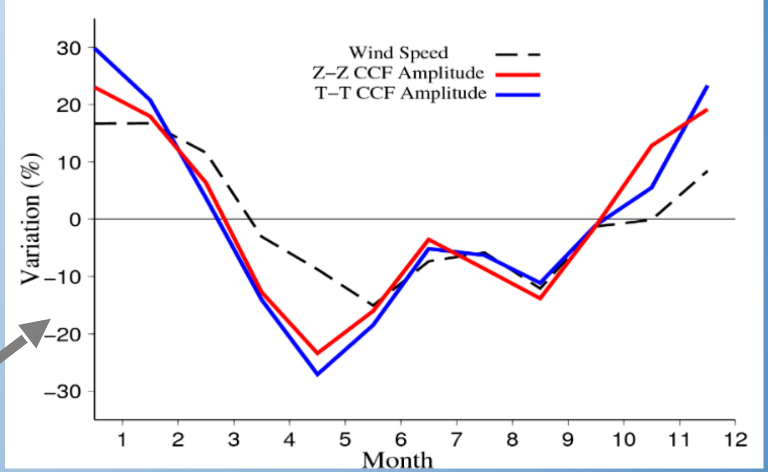

Slope : Intrinsic noise level (INL)

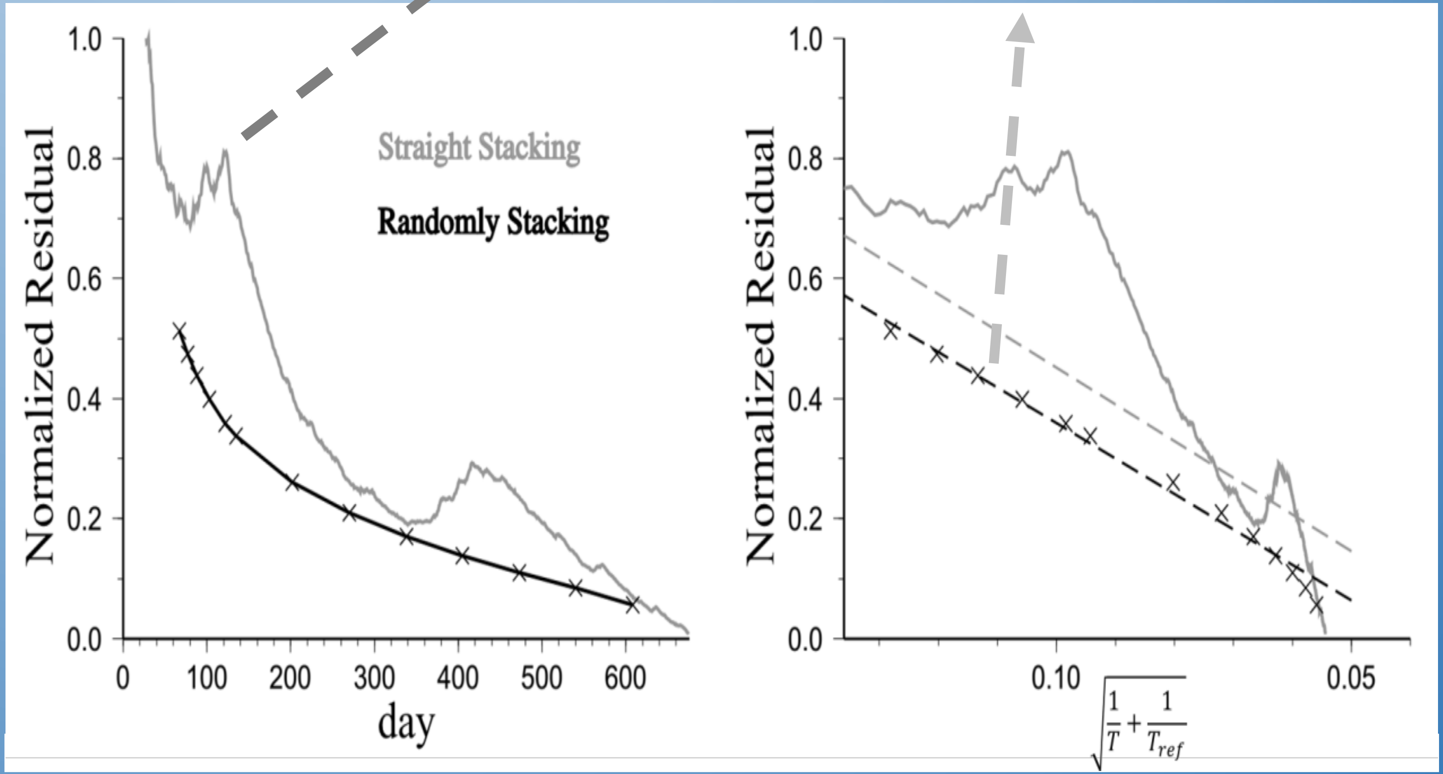

Comparison of INL derived from model with inhomogeneous source excitation strength.

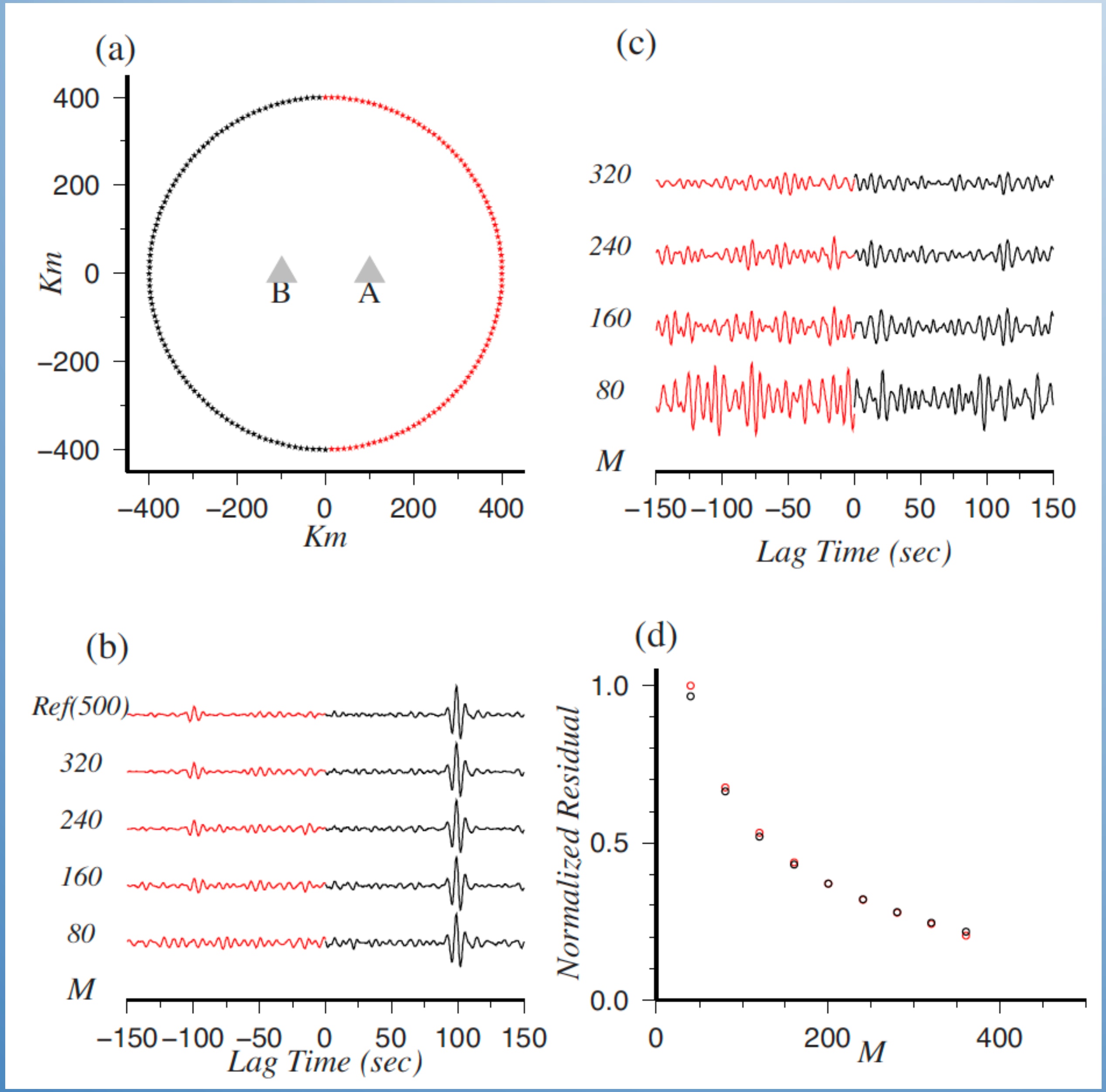

INL → source population

Applications:

(1) Recovering Primary Microseism Signature

INL → Dominant ocean wave / primary microseism

Primary Microseism: { ***High Population***, ***Weak Excitation*** }

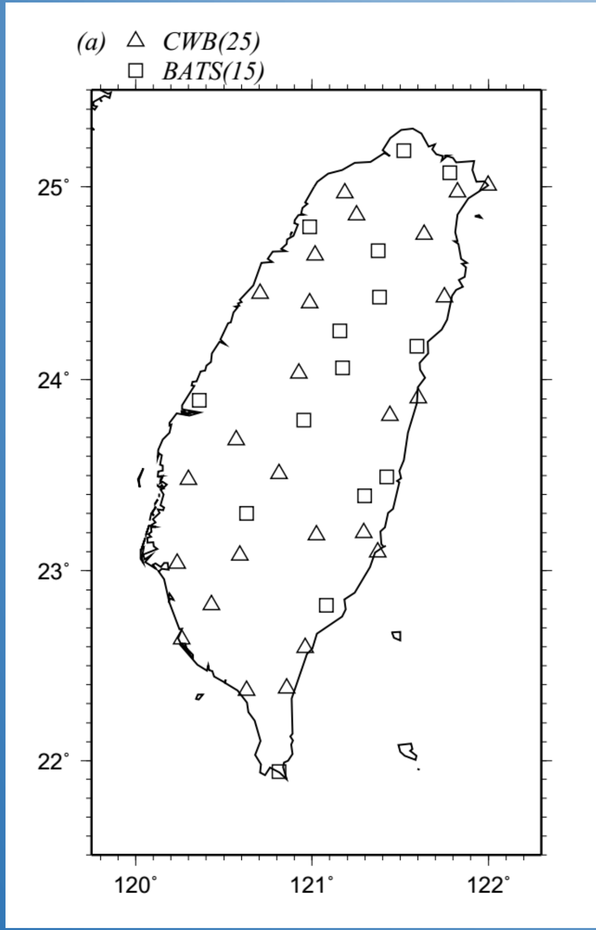

***Background noise level & Ocean wave** (Ts)*

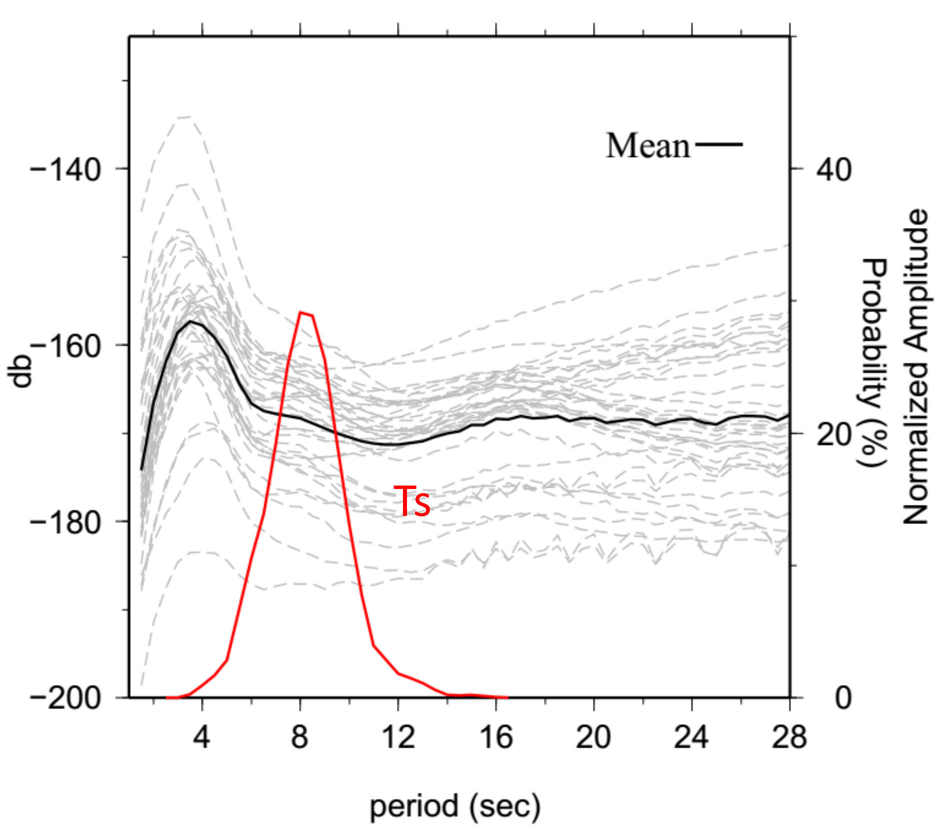

INL ←→ source population

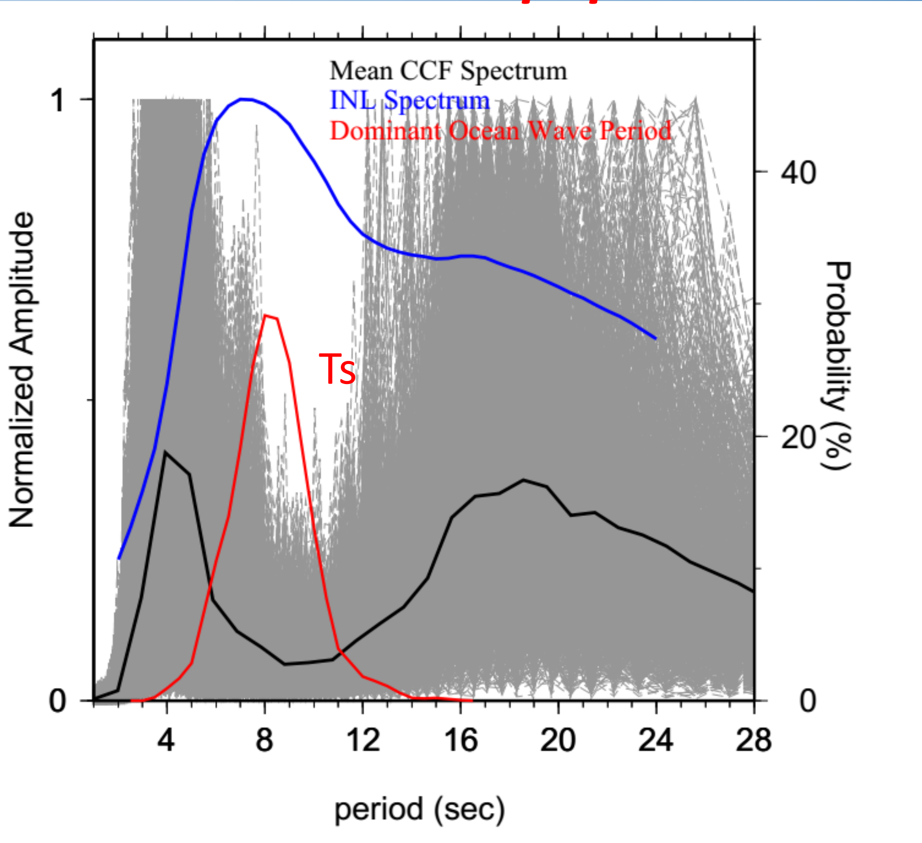

(2) Coastline Effect @ Primary microseism

NCF amplitudes → source population & source excitation

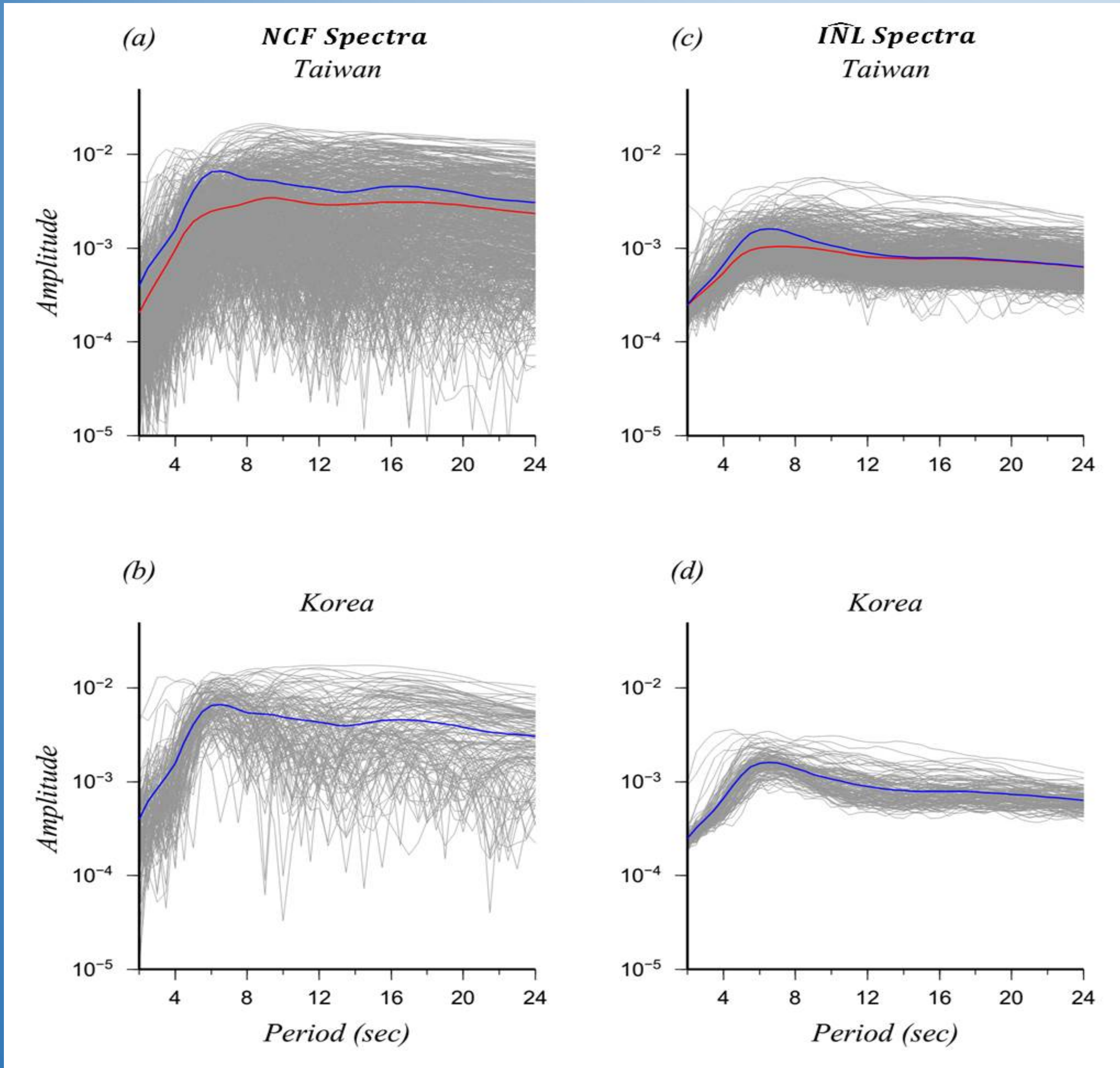

Primary microseism ≈ 7sec

INL (Korea) > INL (Taiwan) => coastline effect

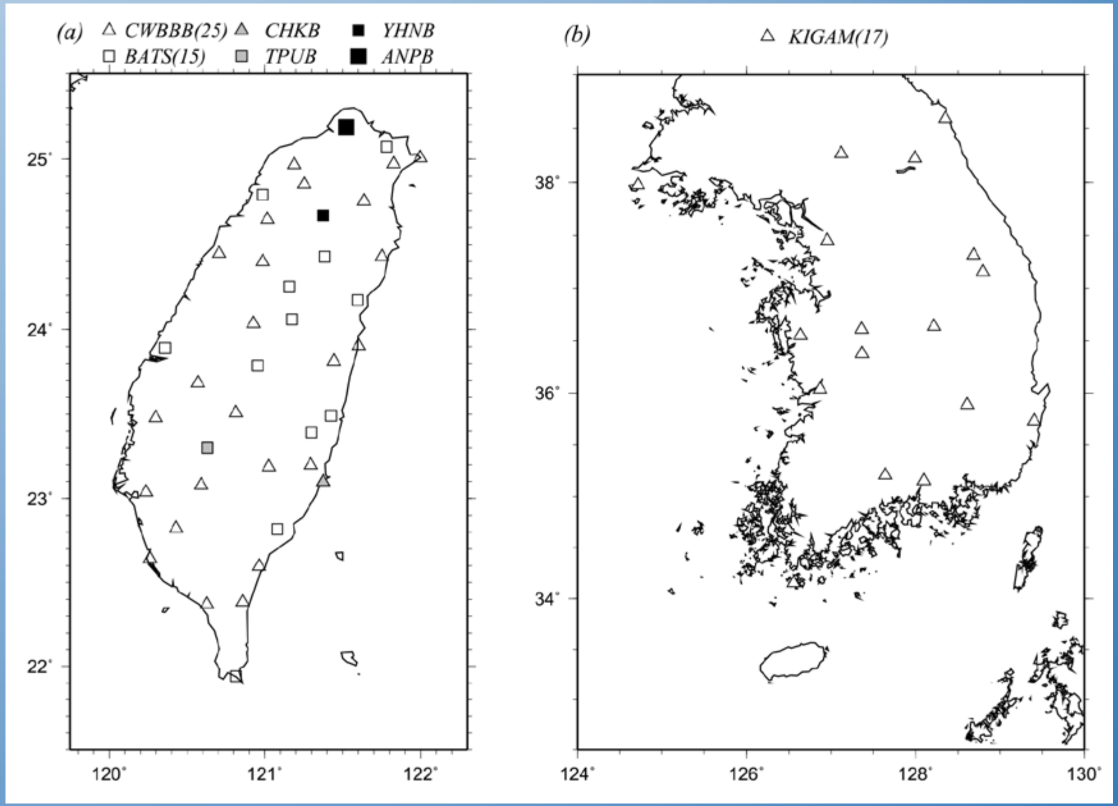

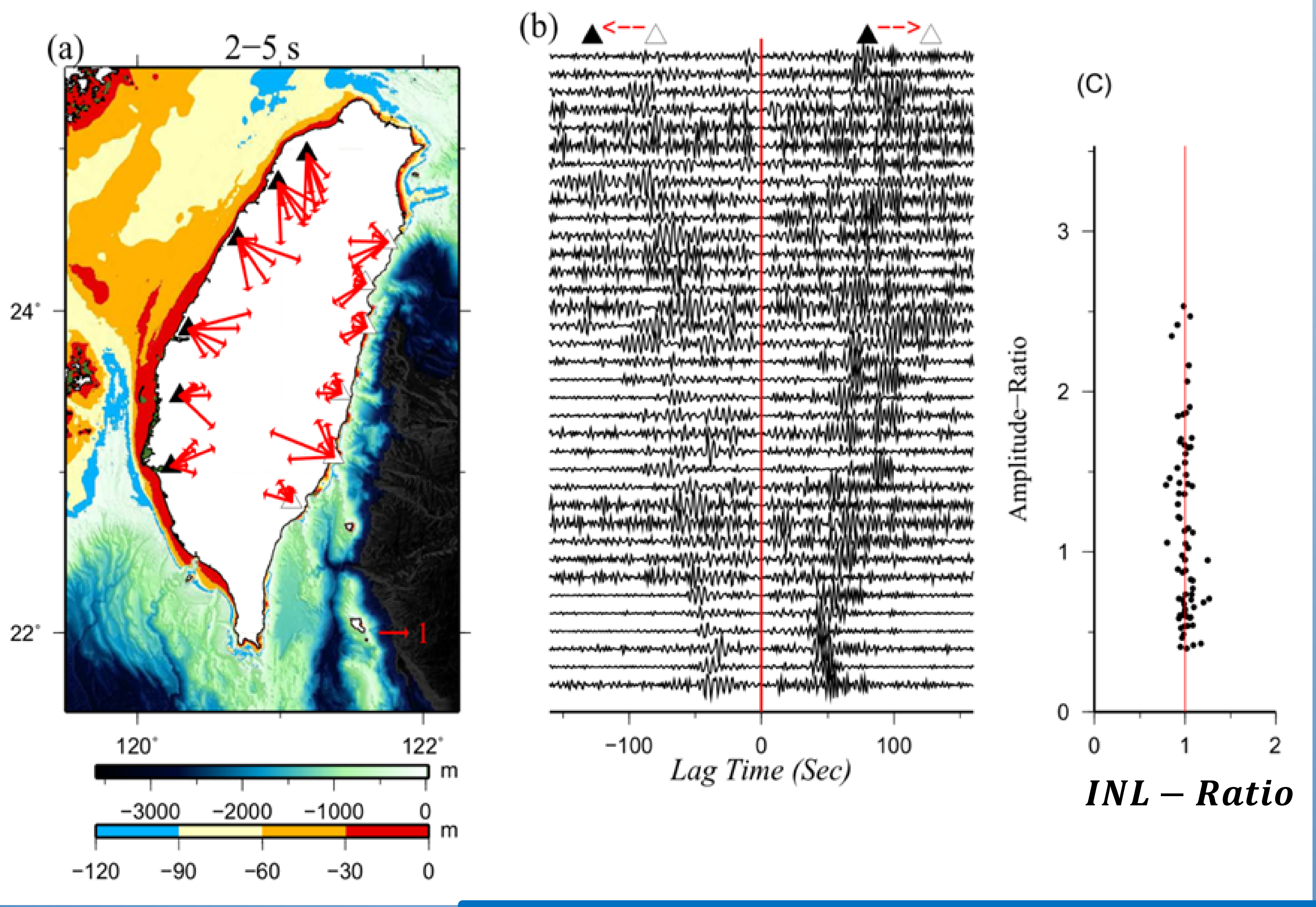

Shallow water --> Excitation Strength (V)

Complex coastline : more SPSM excitation (X)

Applications:

(2)Evaluating the exact noise level of NCF

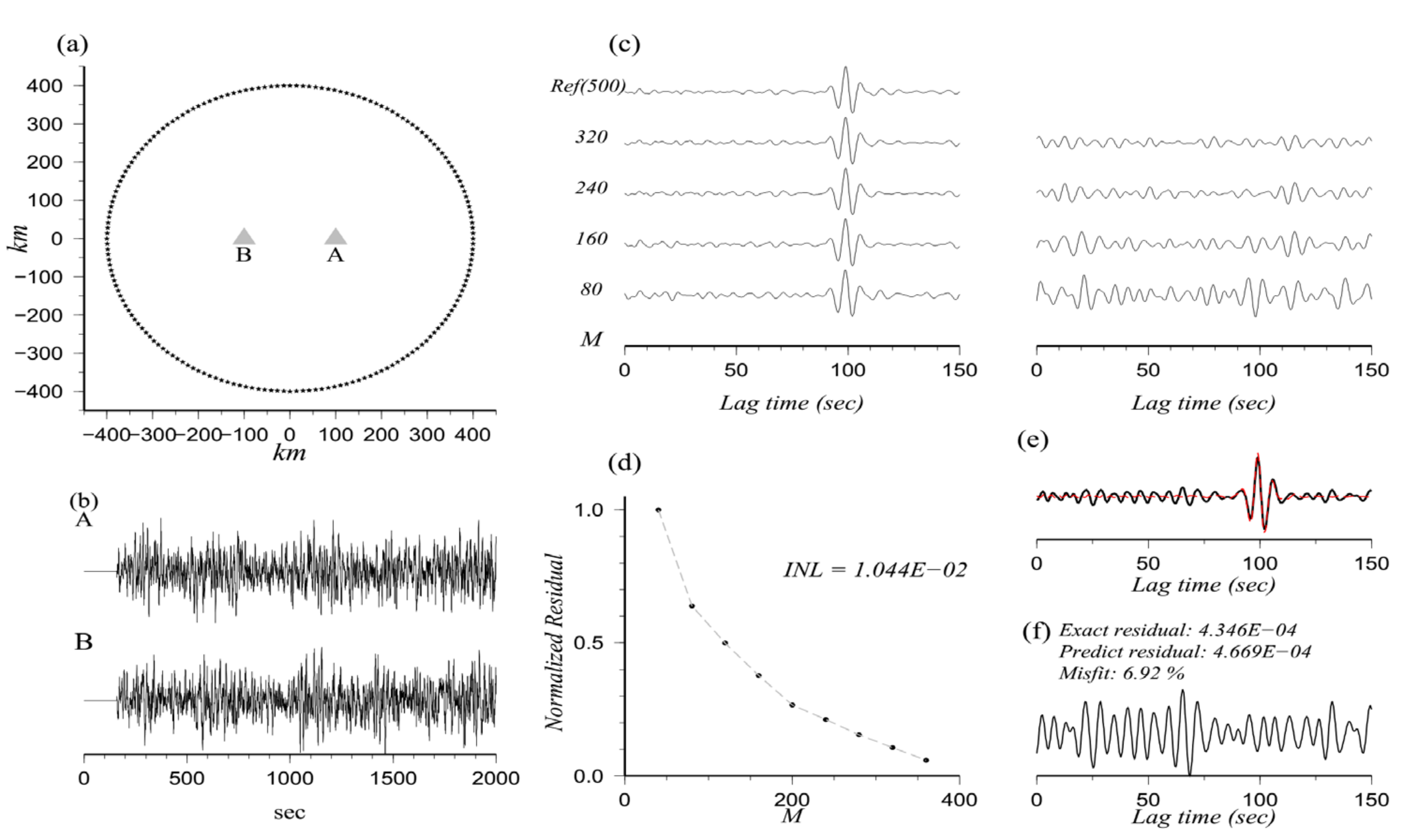

Evaluation of INL at different lag time window of NCFs

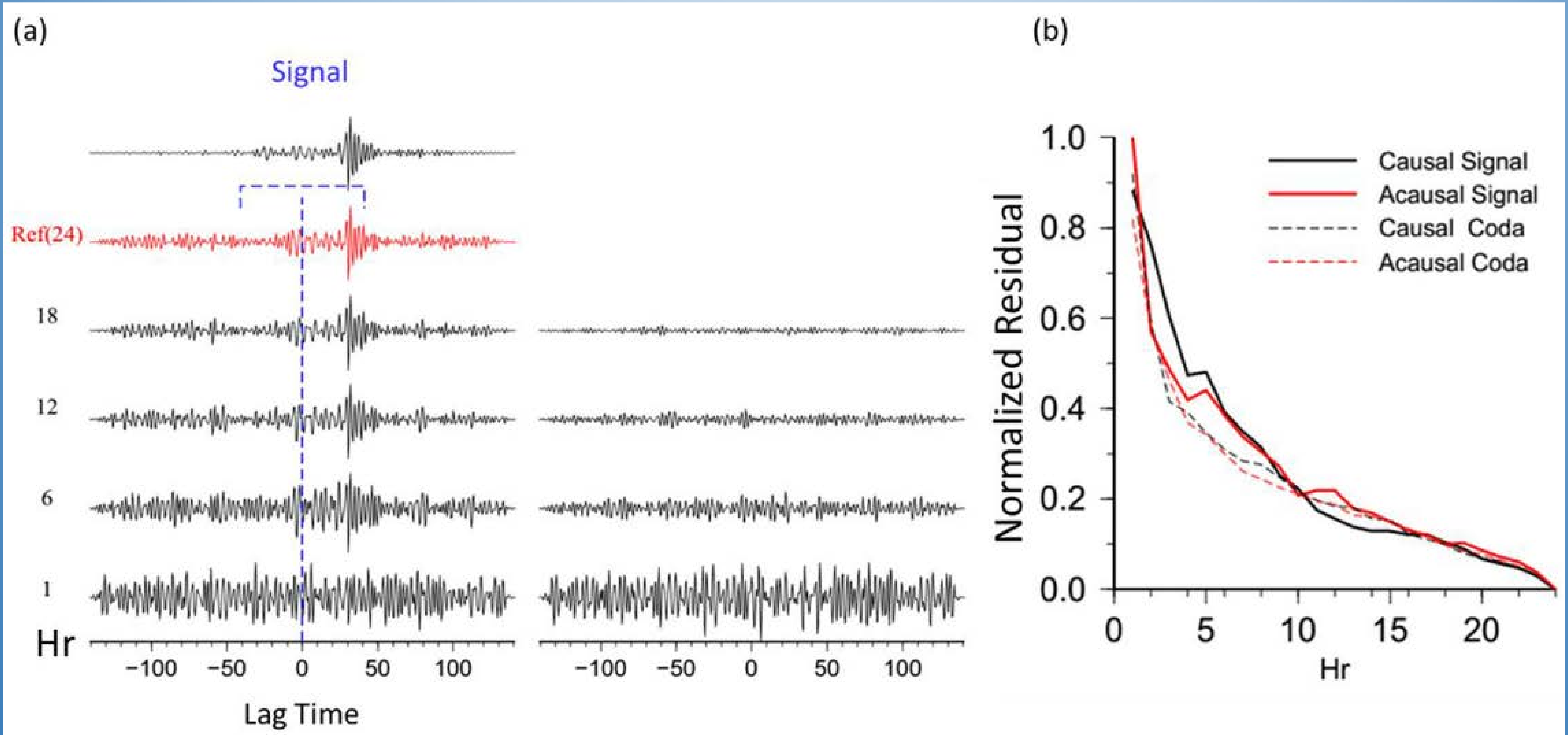

Questions:

(1) Fluctuations of an arbitrary lag time of NCF

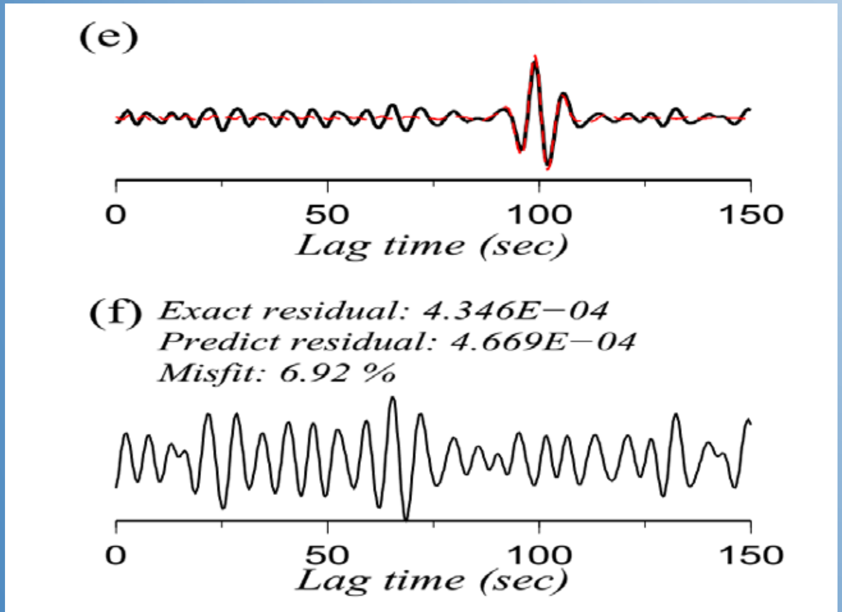

(2) The population of microseisms

A brief introduction to the theory

Fluctuation : Unrelated source pair

$$F_j(t,\omega) = \sum_{k=1}^{N} \sum_{\substack{l=1 \\ l\neq k}}^{N} A_k(\omega) A_l(\omega) * \cos[\omega(t - \boldsymbol{\Delta\tau_{kl}}) + \Delta\phi_{klj}(\omega)] \qquad (1)$$

The population of unrelated source pair: $\boldsymbol{N(\tau,\omega) = \sum_{k=1}^{N} \sum_{\substack{l=1 \\ l\neq k}}^{N} \delta(t - \Delta\tau_{kl})}$.

The mean amplitude density of unrelated source pair: $\boldsymbol{\bar{\rho}(\tau,\omega)}$

$$F_j(t,\omega) = \int_{-T}^{T} N(\tau,\omega) * \bar{\rho}(\tau,\omega) * \cos[\omega(t-\tau) + \phi_j^{avg}(\tau,\omega)] d\tau \qquad (2)$$

############ ***Random walk of*** $\boldsymbol{N(\tau,\omega)}$ ***steps → moving*** $\boldsymbol{\sqrt{N(\tau,\omega)}}$ ***units.*** #################

$$F_j(t,\omega) = \int_{-T}^{T} \underbrace{\sqrt{N(\tau,\omega)}}_{\text{Source density}} * \underbrace{\bar{\rho}(\tau,\omega) * \cos[\omega(t-\tau) + \phi_j^{avg}(\tau,\omega)]}_{\text{Source excitation}} d\tau \qquad (3)$$

3. Using the "*noise*" of noise cross-correlation

Topic two: Intrinsic Uncertainty of NCF

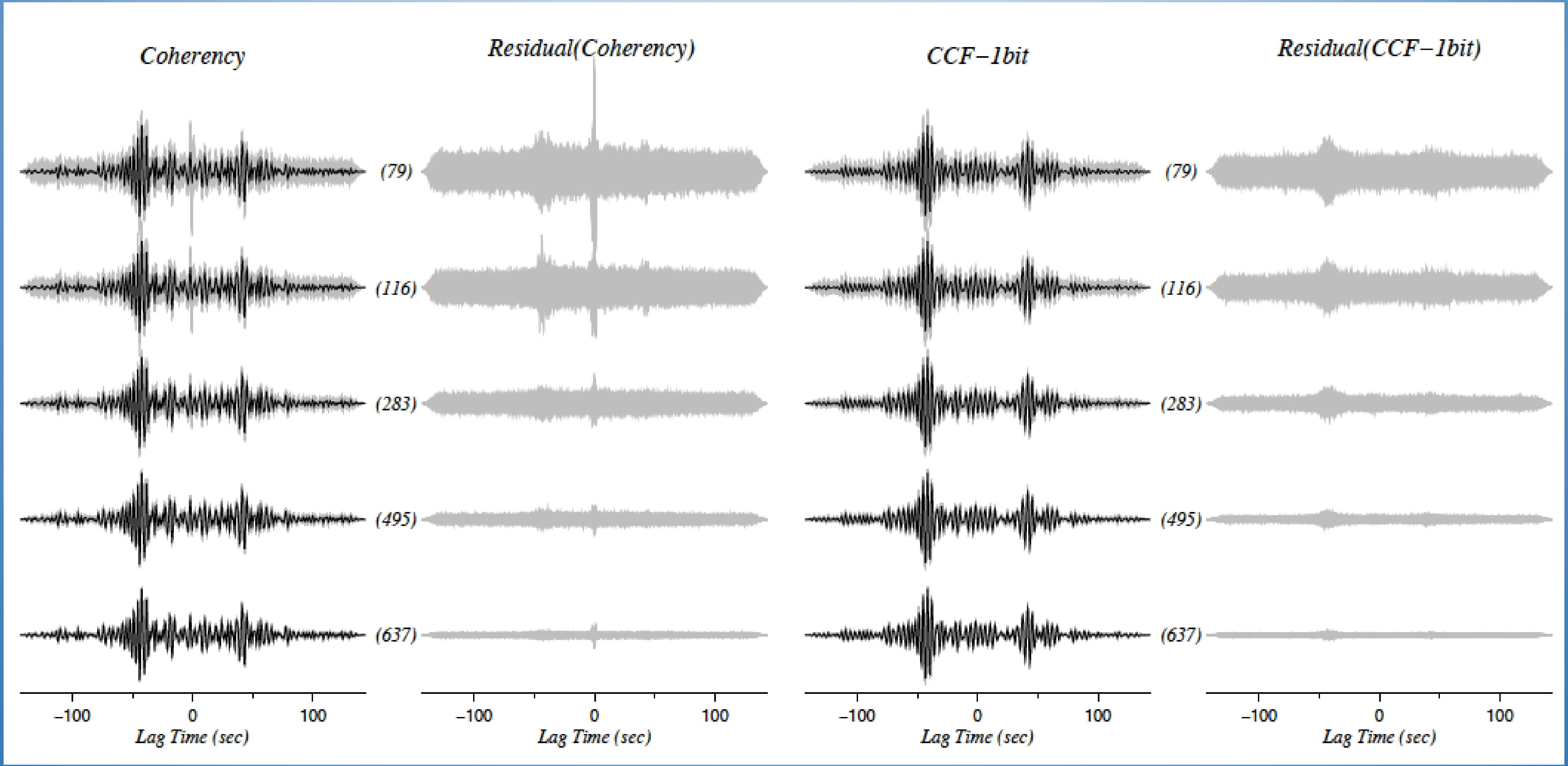

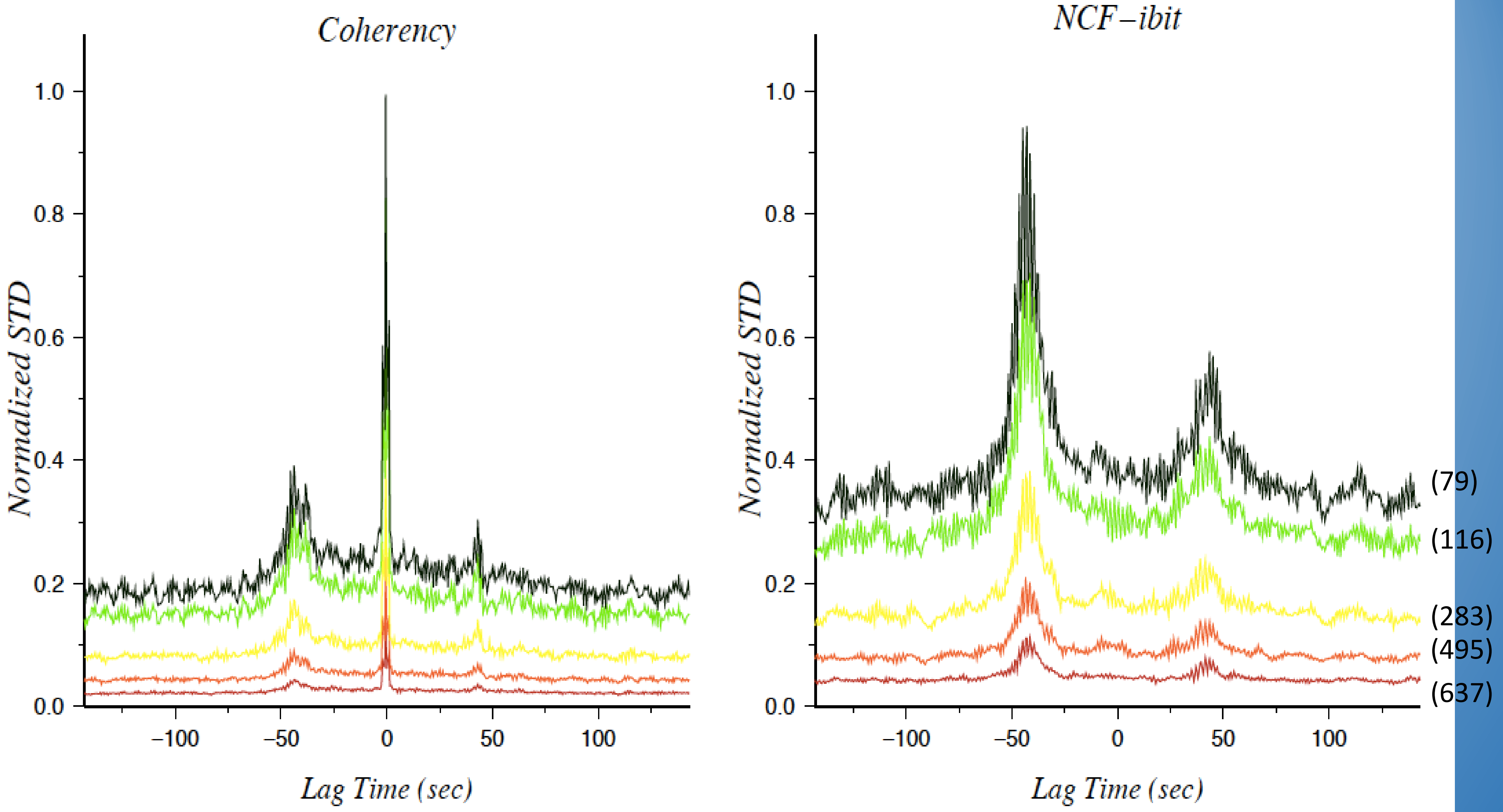

Coherency
NCF−ibit
Normalized STD
Lag Time (sec)
1.0
0.8
0.6
0.4
0.2
0.0
−100
−50
0
50
100
(79)
(116)
(283)
(495)
(637)

Slope : Intrinsic uncertainty (IU)

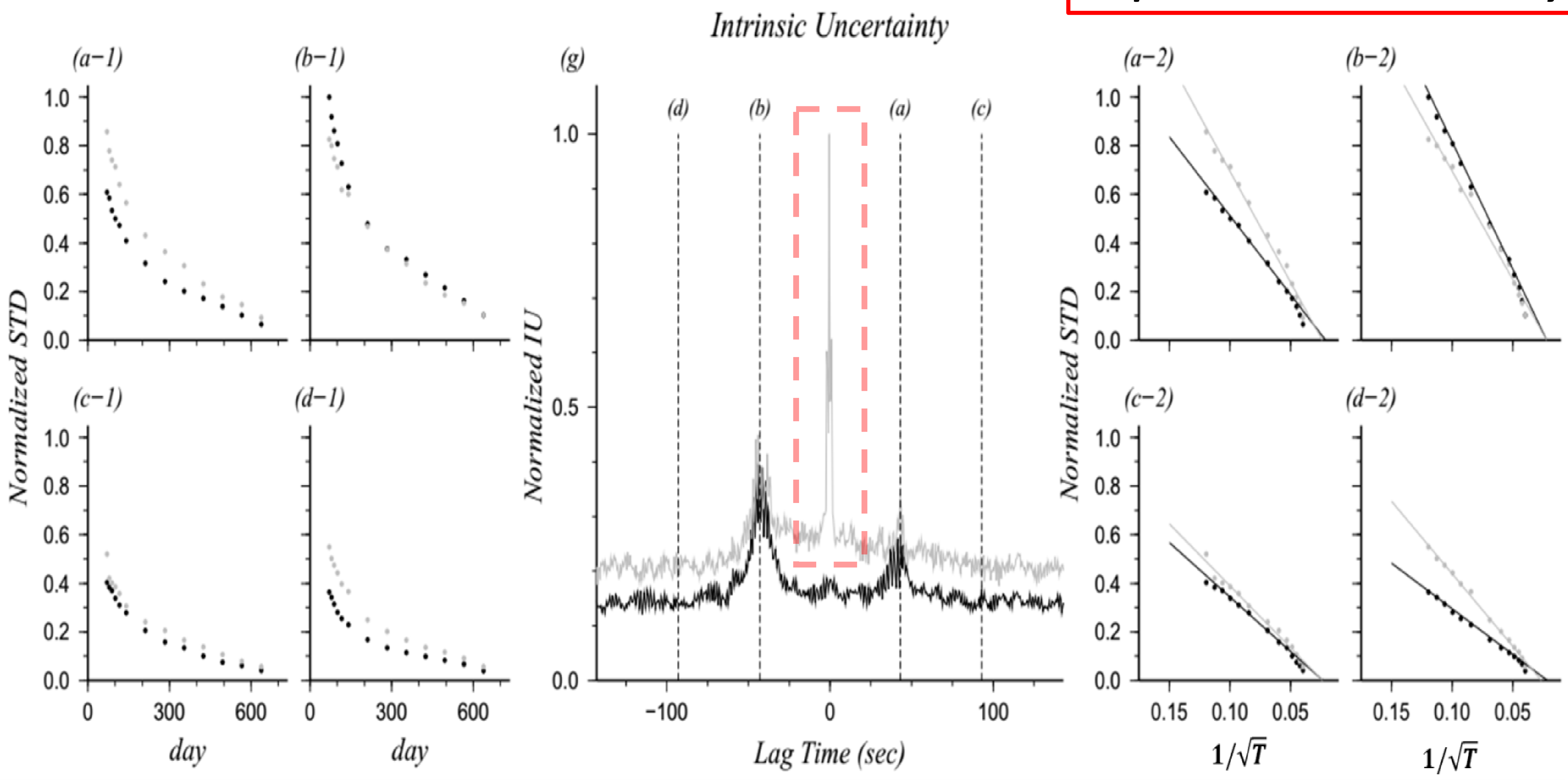

$$F_j(t,\omega) = \int_{-T}^{T} \sqrt{N(\tau,\omega)} * \bar{\rho}(\tau,\omega) * \cos[\omega(t-\tau) + \phi_j^{avg}(\tau,\omega)]d\tau \qquad (3)$$

$$\mathbf{W}(\boldsymbol{t},\boldsymbol{n}) = \mathbf{0.5} * [\mathbf{1} + \boldsymbol{cos}\left(\frac{\mathbf{2}\boldsymbol{\pi}(\boldsymbol{t}-\boldsymbol{\tau})}{\boldsymbol{T^n}}\right)]$$

$$\boldsymbol{T^n} = n * period$$
$$\boldsymbol{\tau}: [-\boldsymbol{T^n}/2, \boldsymbol{T^n}/2]$$

Synthetic test *(period=10 sec)*

$\boldsymbol{W(t, n = 2)}$ $\boldsymbol{W(t, n = 4)}$

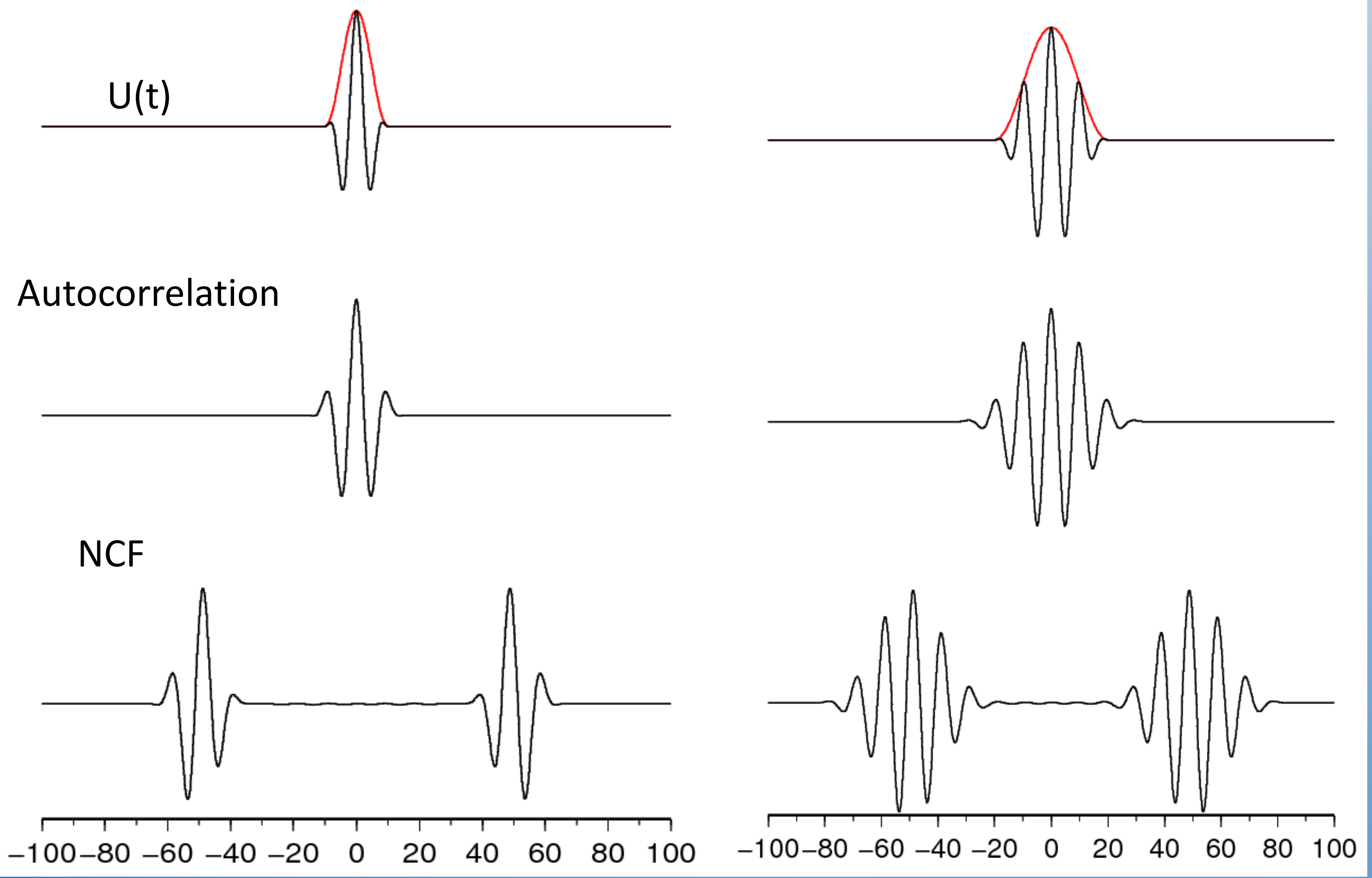

$\boldsymbol{W(t, n = 6)}$

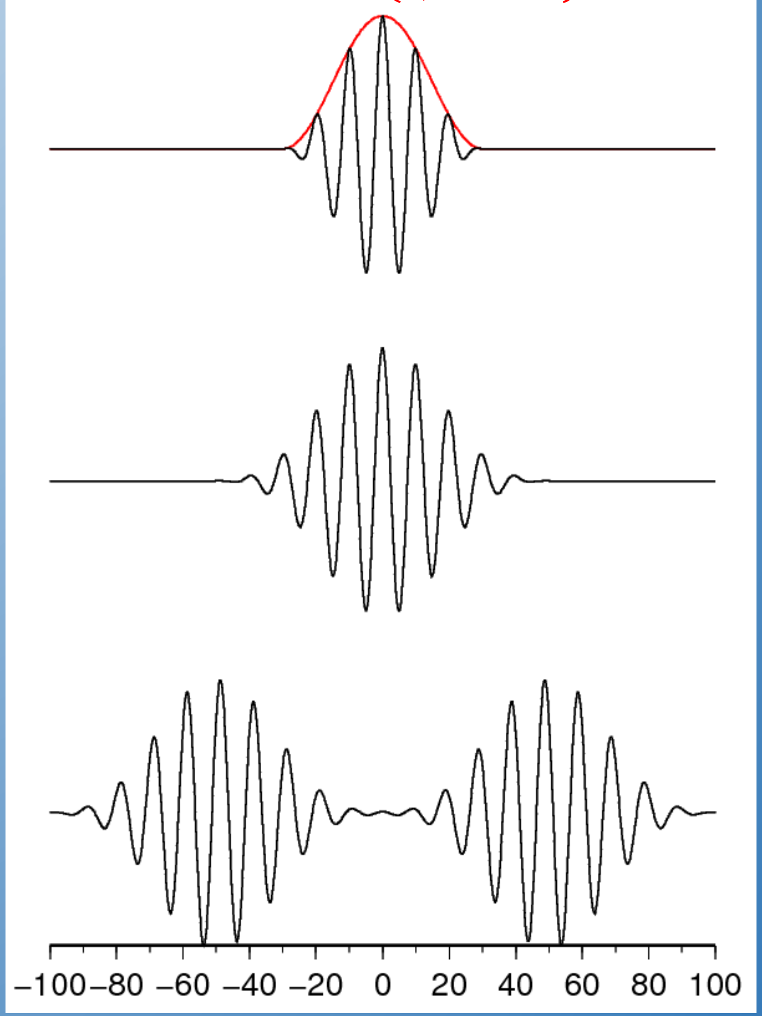

Applications: (1)Evaluating fluctuations of NCF

Predicted uncertainty: $IU/\sqrt{T}$

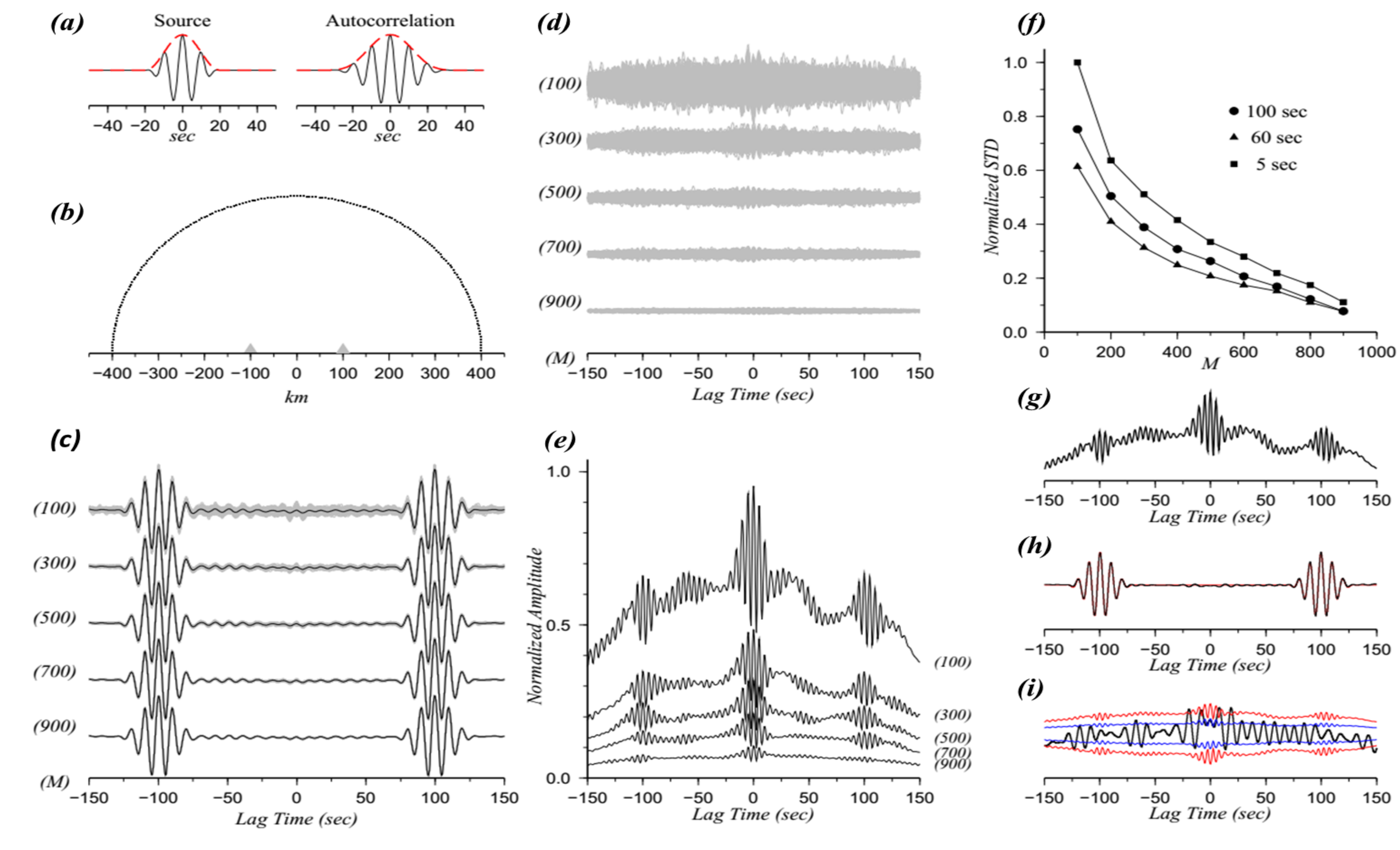

$IU(t)/\sqrt{T}$ 68%

$2 * IU(t)/\sqrt{T}$ 95%

Giving a quantitative description on the NCF coda quality!

Monitoring Temporal changes of seismic velocity

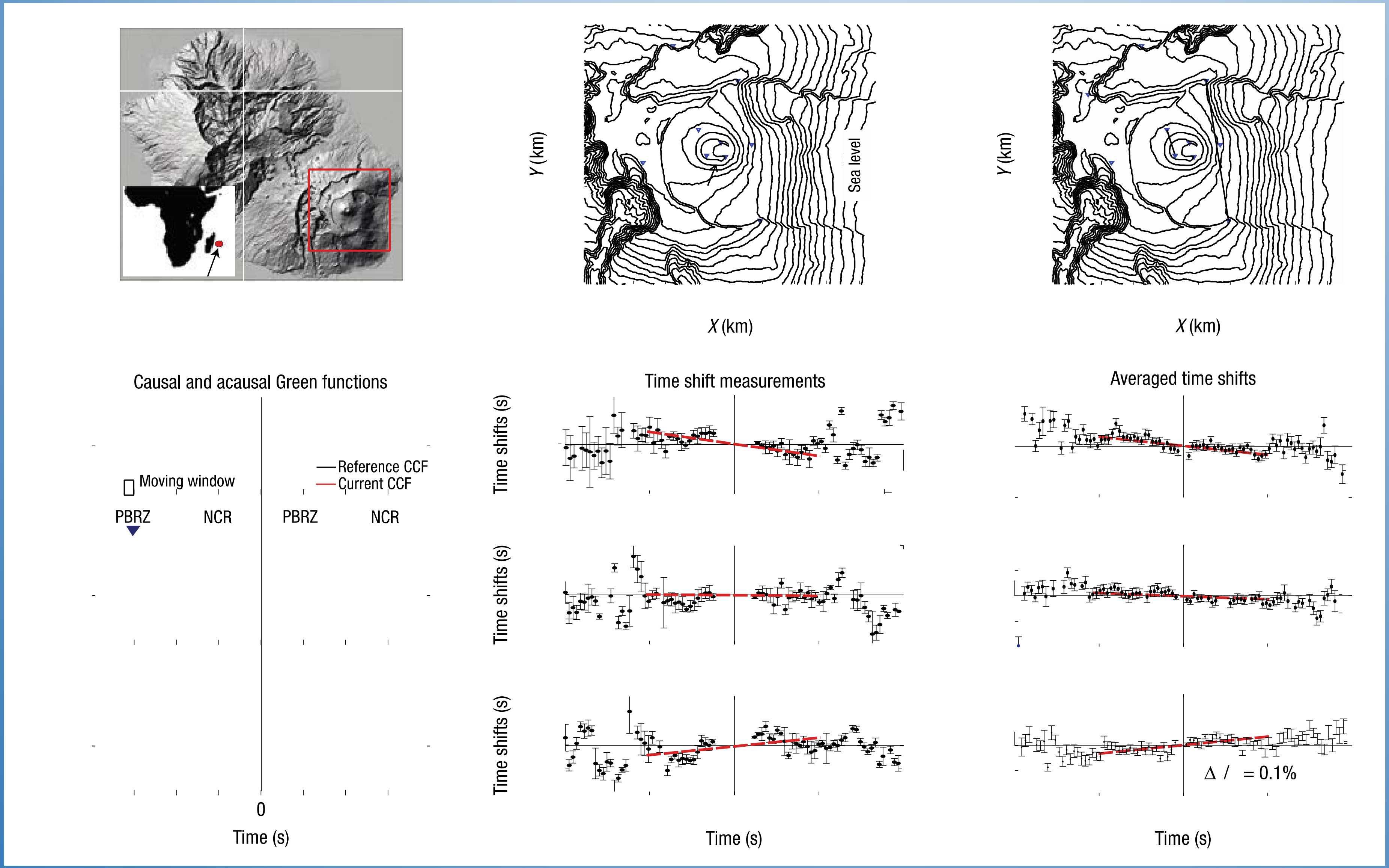

Brenguier et al., 2008

(2)Probing noise source properties

Intrinsic Uncertainty → **Distribution of noise source**

Intrinsic Uncertainty → **Excitation of noise source**

On going work :

On the relationship between PM excitation and coastline geometry

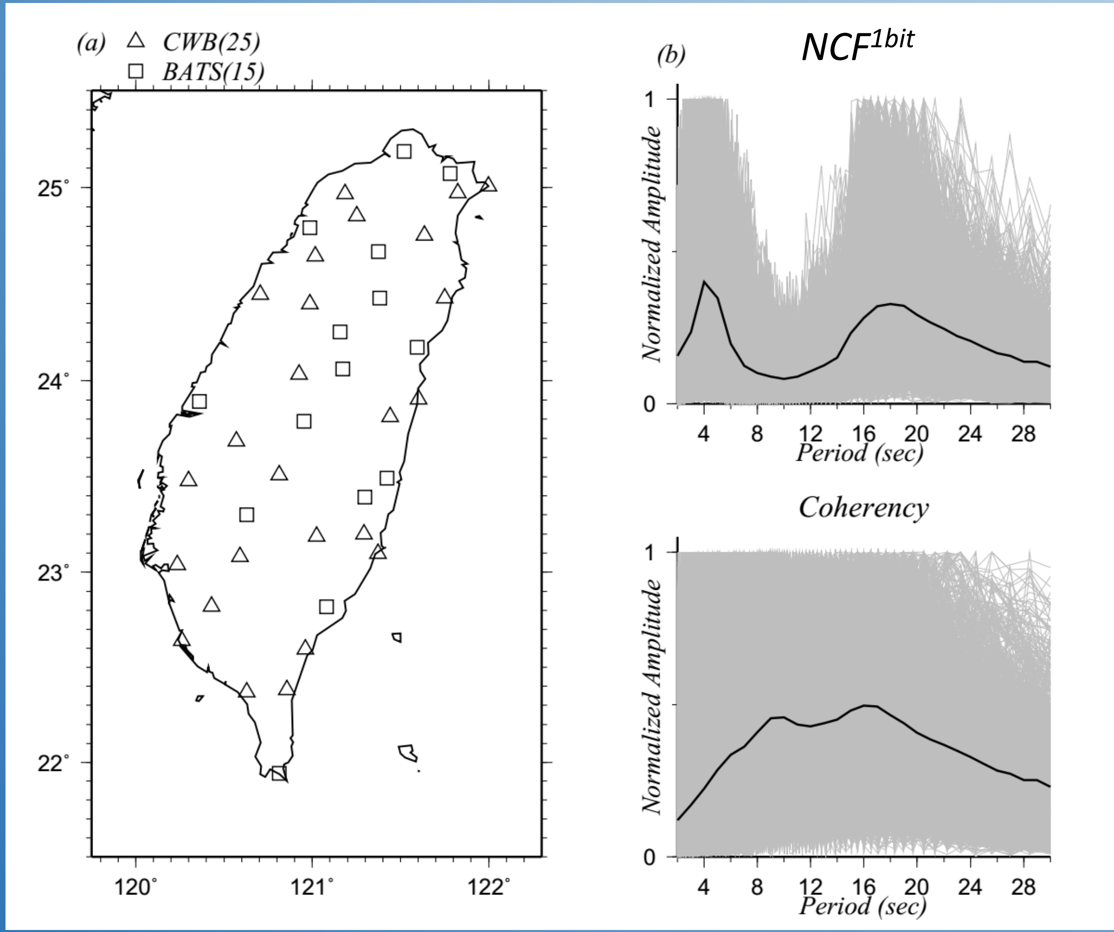

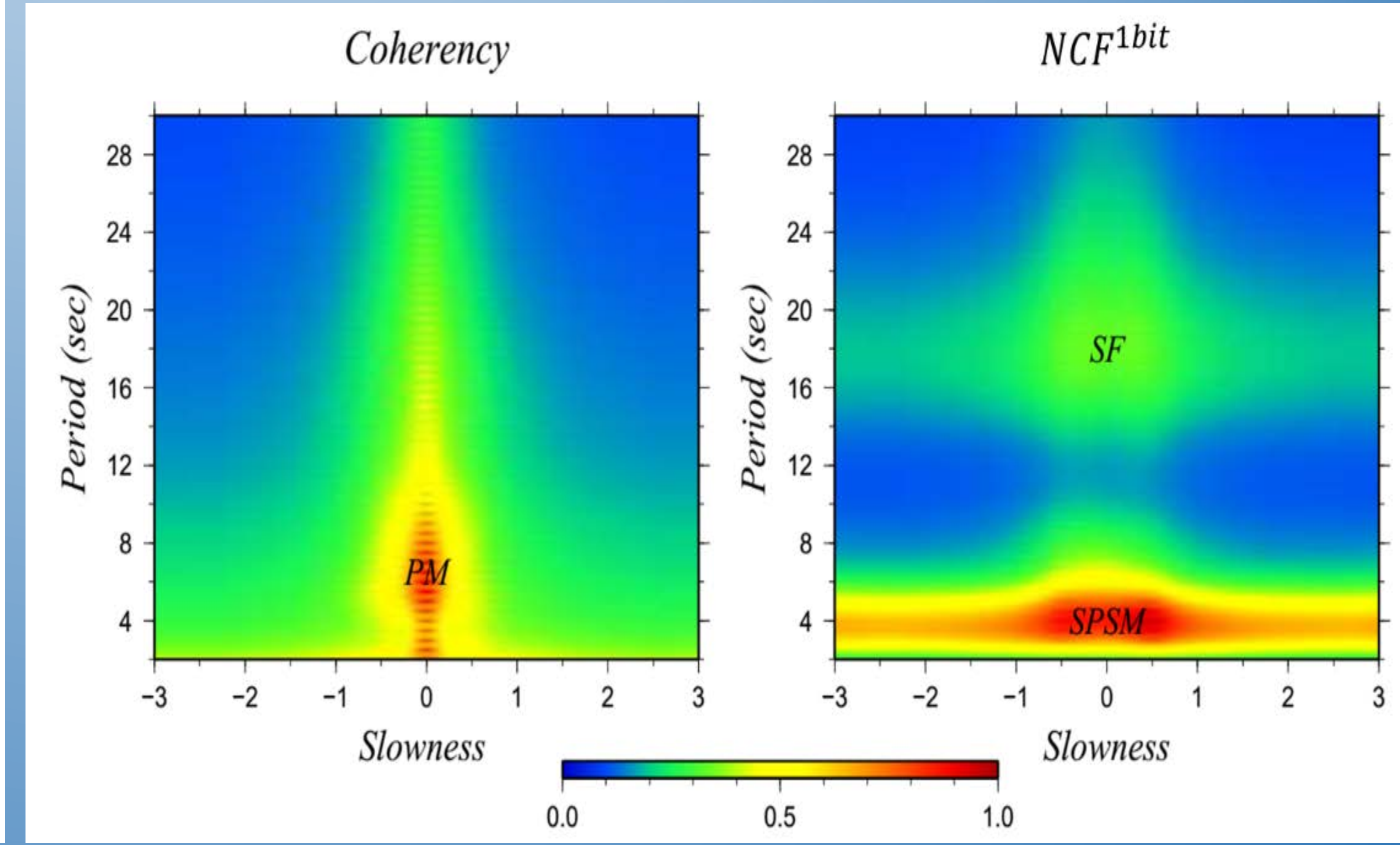

Probing spatiotemporal property of solar seismic source using *NCF*

(Source : Convection turbulence)

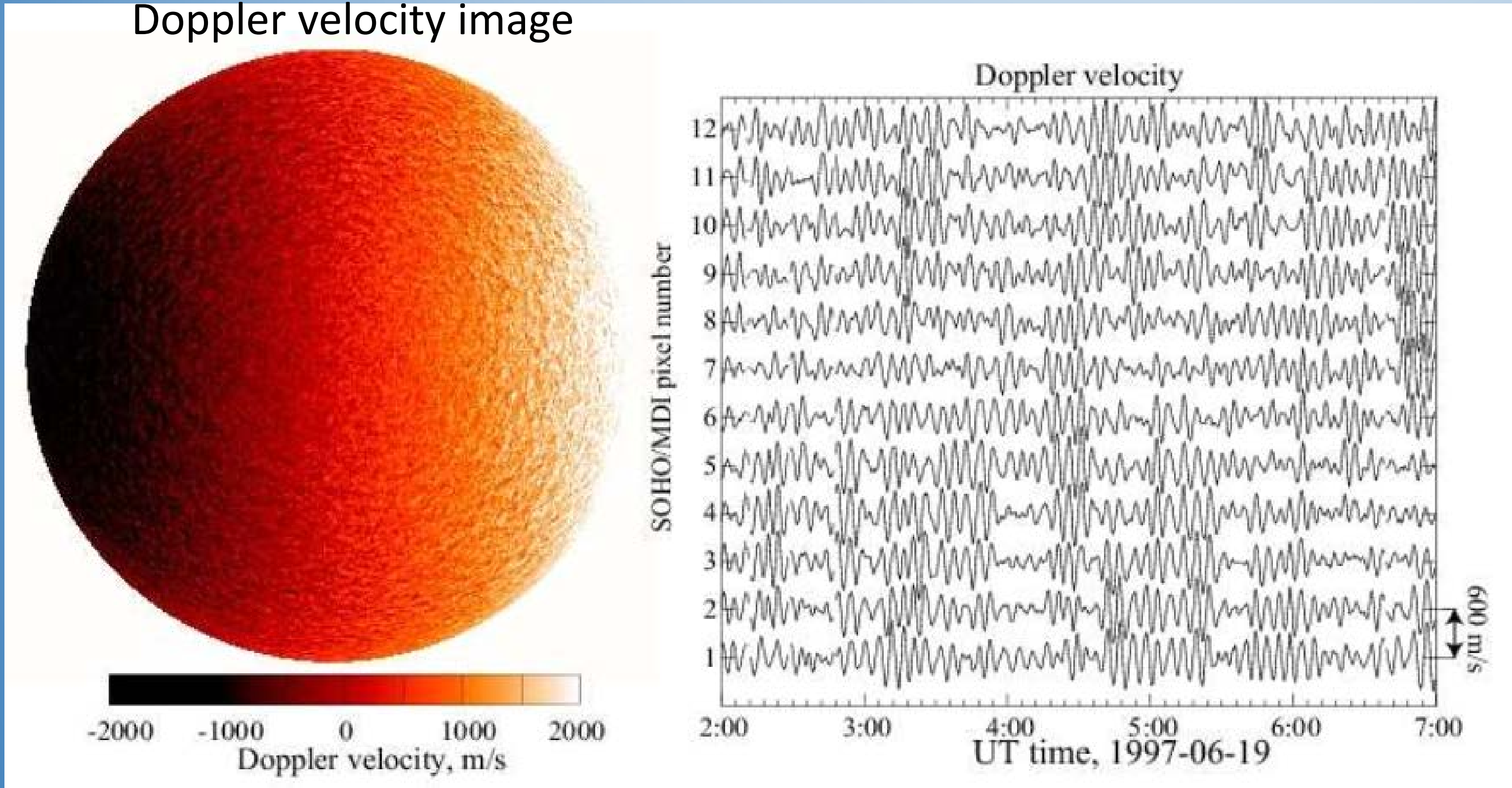

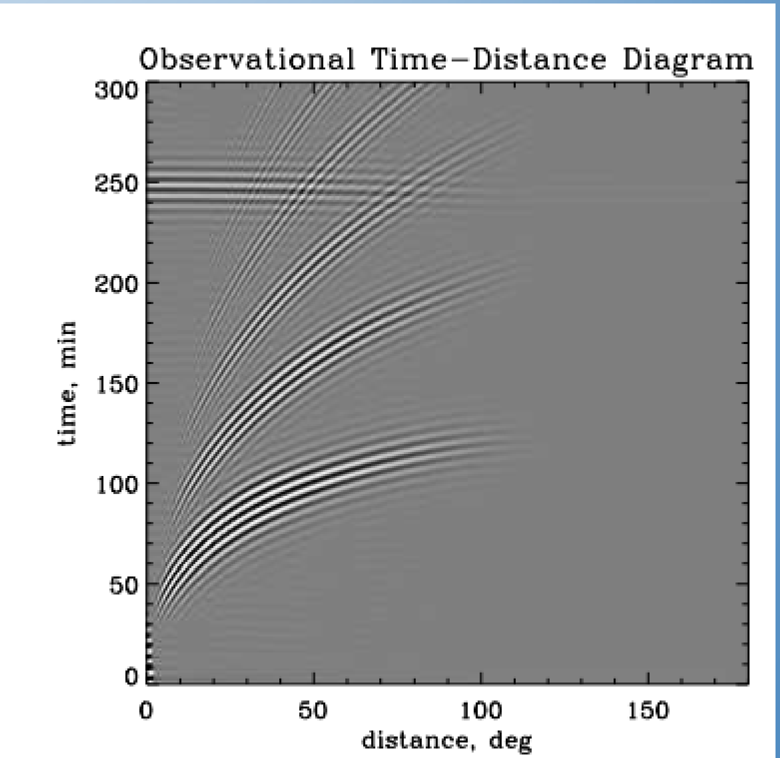

Kosovichev and Alexander G. (2011)

Working with Prof. Dean-Yi Chou (NTHU)
(Taiwan Oscillation Network)

Active Sun

Large scale convection event

Increasing small convection events

3. Investigating microseism PKIKP generated around Hawaii.

@Excitation property of body wave microseism- case study in Turkey

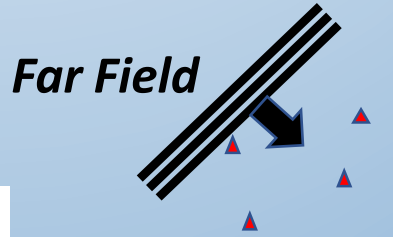

PKP phase excitation

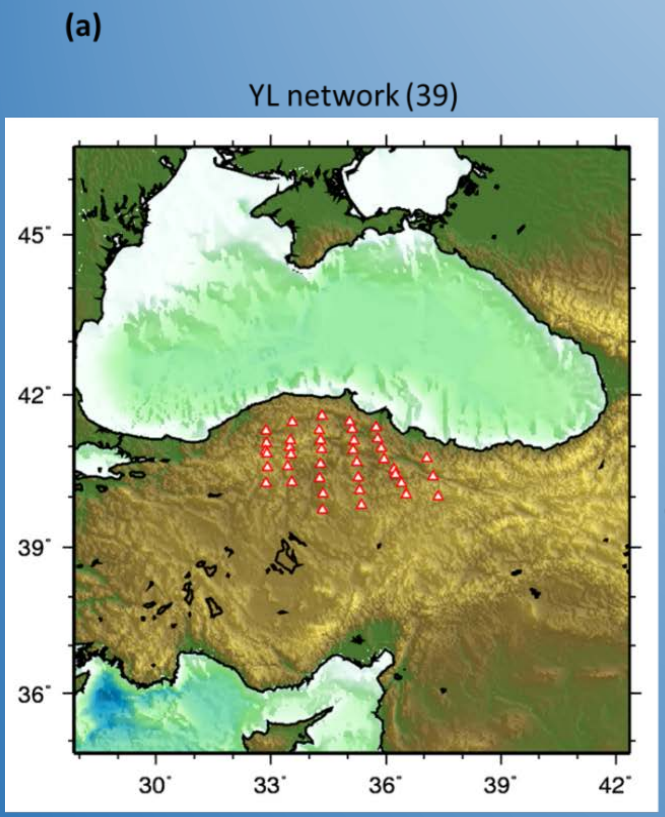

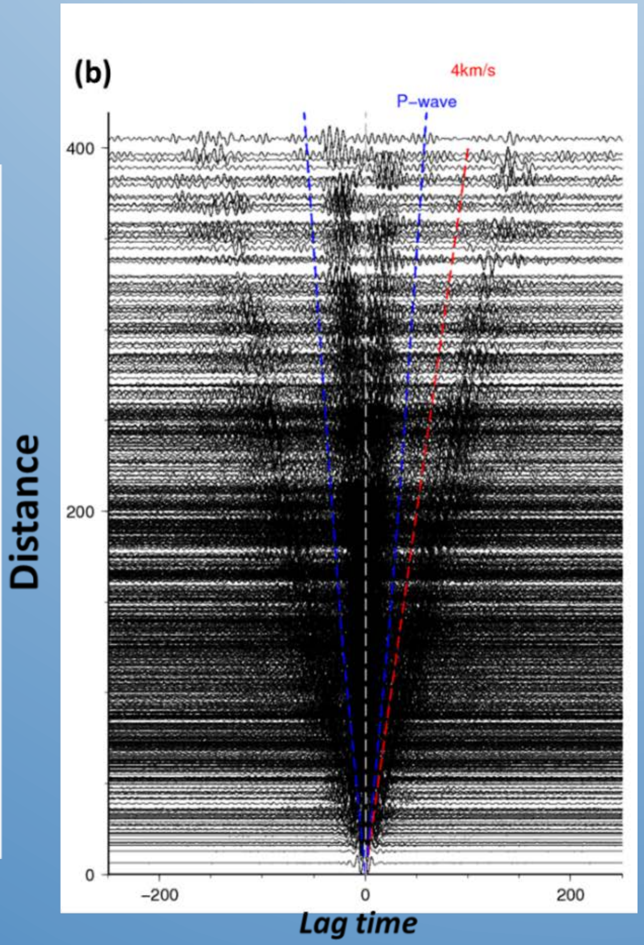

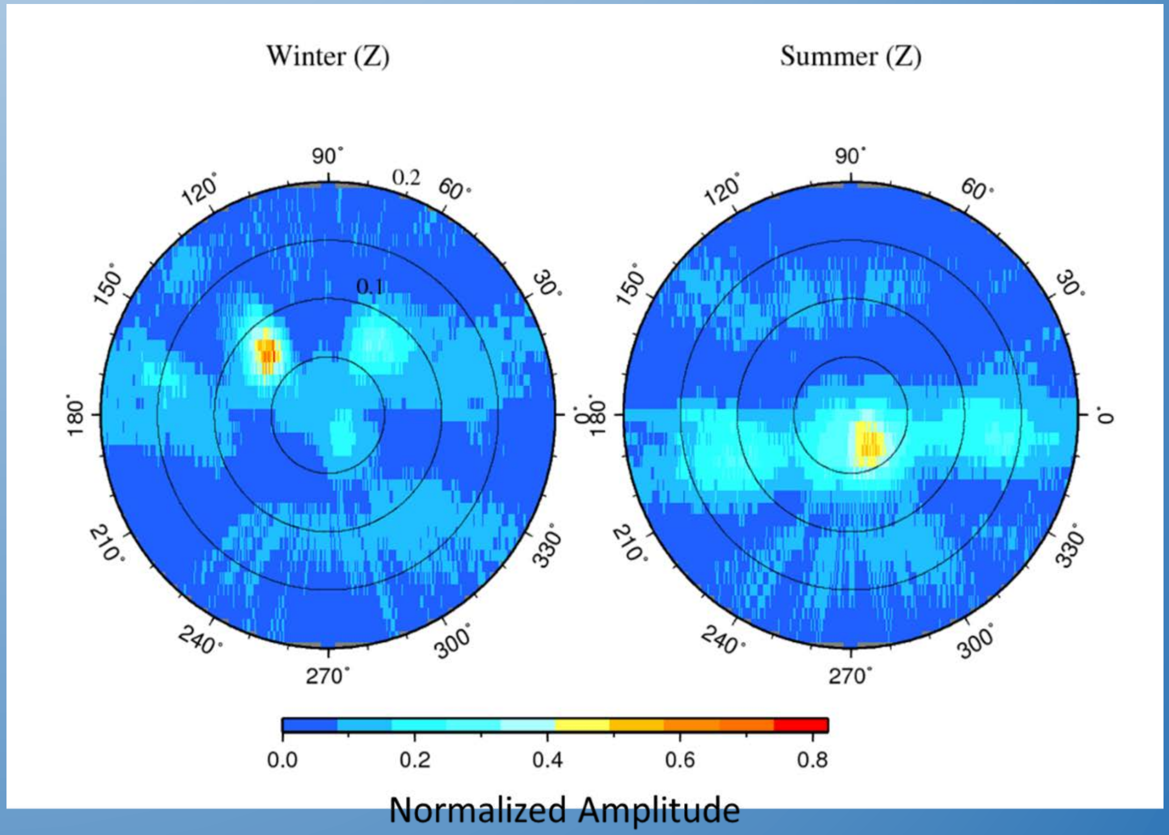

Global Microseism Catcher Network

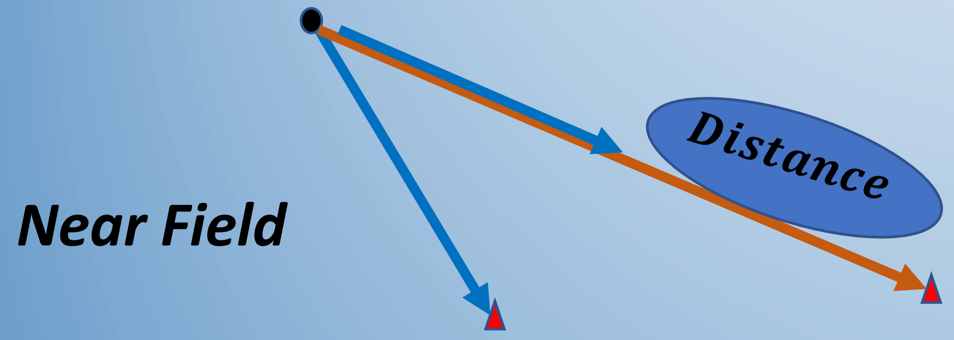

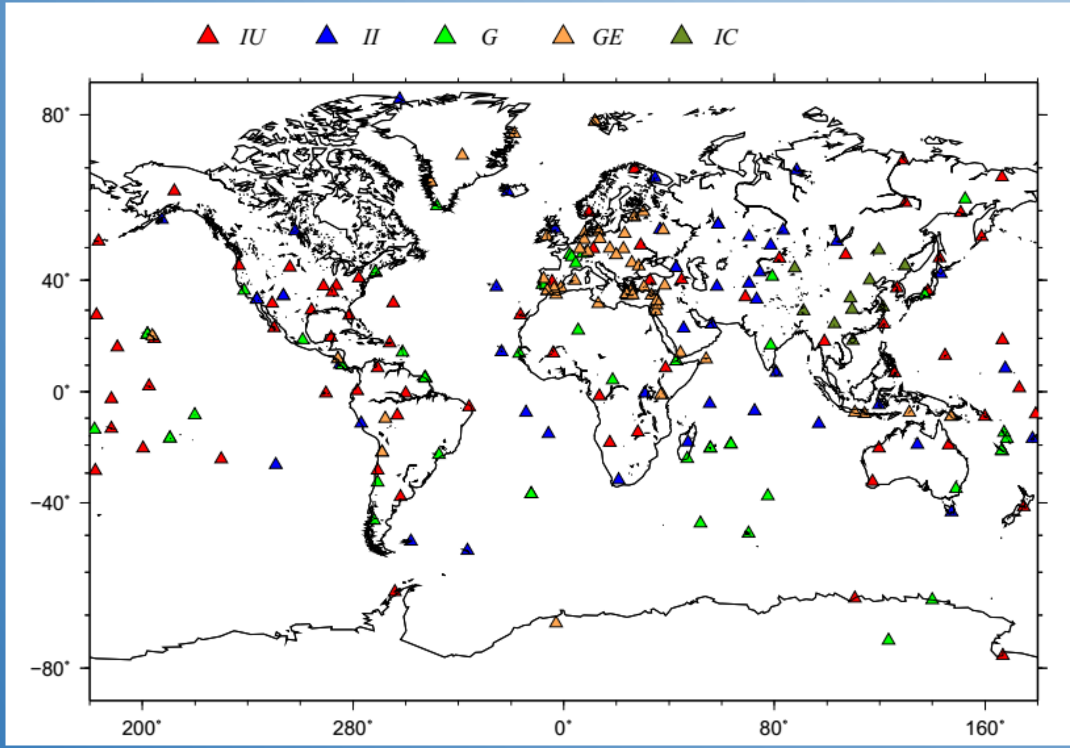

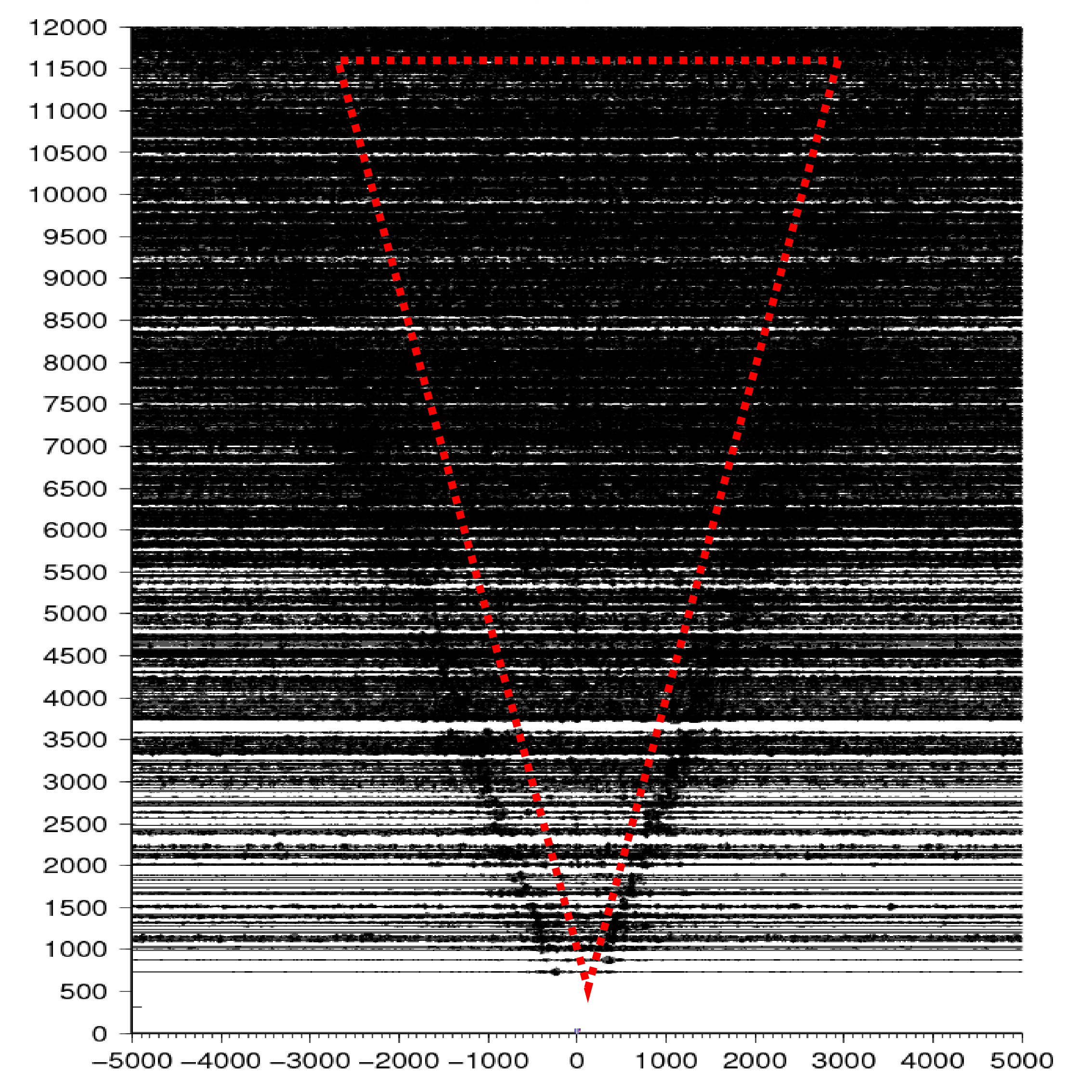

PKIKP excitation around Hawaii

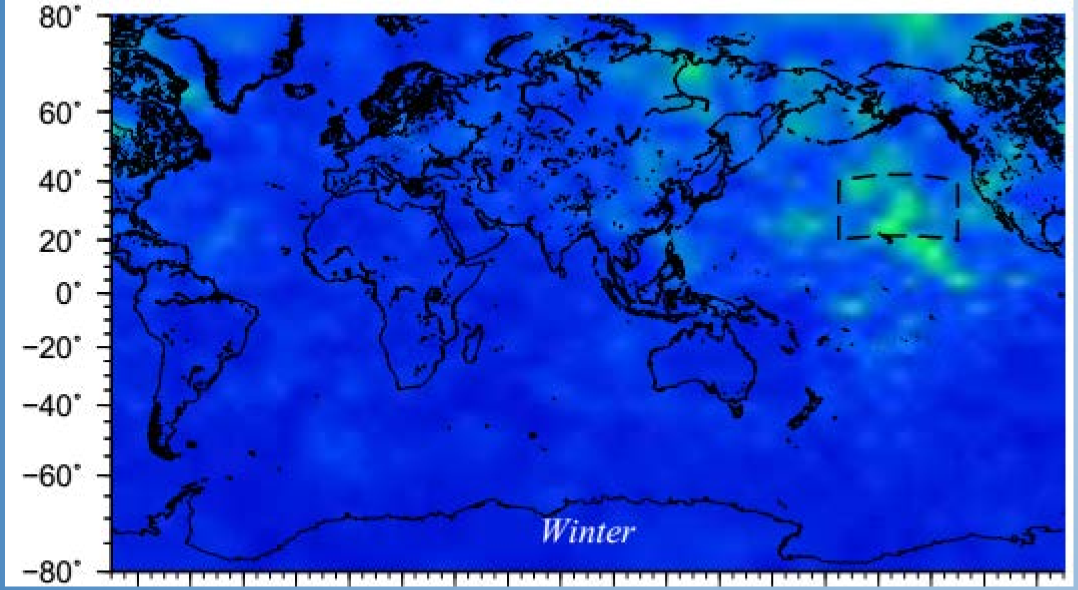

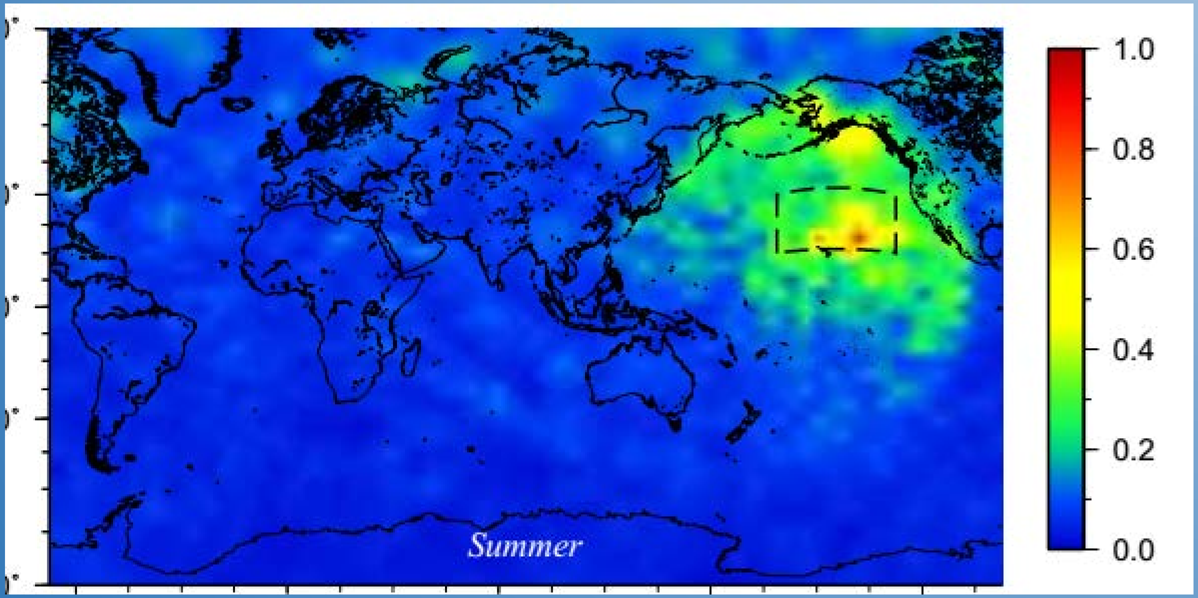

Wind stress curl (1999-2007)

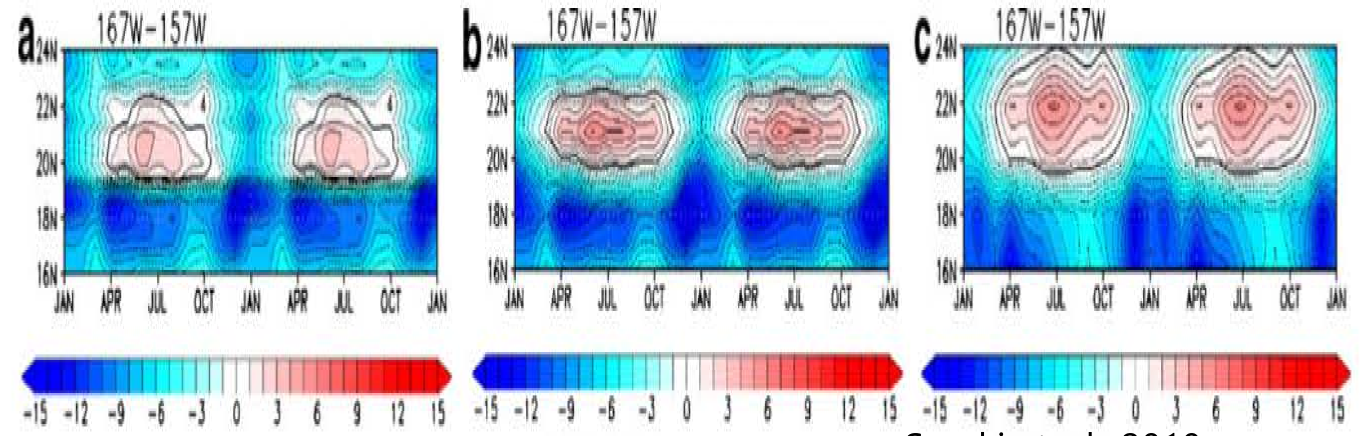

Sasaki et. al., 2010

@ microseisms → **deep oceans !**

→ **mesoscale weather phenomenon**
(Pacific Decadal Oscillation: El Niño & La Niña)

@ PKIKP → **Inner core structure**

Thank You